IMPROVING QUALITY AND PRODUCTIVITY OF CASTING PROCESS BY USING ADVANCED SIMULATION AND RAPID PROTOTYPING TECHNOLOGY

BY

AL-YOUSEF, ABDEL-HADI ABDULLAH M.

A Thesis Presented to the
DEANSHIP OF GRADUATE STUDIES

KING FAHD UNIVERSITY OF PETROLEUM & MINERALS

DHAHRAN, SAUDI ARABIA

In Partial Fulfillment of the
Requirements for the Degree of

MASTER OF SCIENCE

In

MECHANICAL ENGINEERING

(MATERIALS AND MANUFACTURING)

KING FAHD UNIVERSITY OF PETROLEUM AND MINERALS

DHAHRAN, SAUDI ARABIA

DEANSHIP OF GRADUATE STUDIES

This thesis, written by Abdul-Hadi Abdullah M. Al-Yousef (ID.19-983092-0) under the direction of his thesis advisor and approved by his thesis committee, has been presented to and accepted by the Dean of Graduate Studies, in partial fulfillment of the requirements for the degree of MASTER OF SCIENCE IN MECHANICAL ENGINEERING – MATERIALS AND MANUFACTURING.

Thesis Committee

Anwar Khalil Sheikh

Thesis Advisor
Dr. Anwar Khalil Sheikh

Department Chairman
Dr. Amro Al-Qutub

Member
Dr. Abul-Fazal M. Arif

Dean of Graduate Studies
Dr. Salam A. Zummo

Member
Dr. Yagoub N. Al-Nassar

January 2012

ACKNOWLEDGMENT

The author of this thesis would like to acknowledge the support provided by King Abdulaziz City for Science and Technology (KACST) through the Science & Technology Unit at King Fahd University of Petroleum & Minerals (KFUPM) for funding this work through NSTIP project #08-ADV71-4 as part of the National Science, Technology and Innovation Plan. Acknowledgment is also due to the King Fahd University of Petroleum & Minerals for supporting the research in terms of providing excellent lab facilities and human resources of Rapid Prototyping and Reverse Engineering Lab in the ME department.

I wish to express my appreciation to Professor Anwar Khalil Sheikh who served as my major thesis advisor. I also wish to thank the other members of my thesis committee Dr. Abul-Fazal Arif and Dr. Yagoub Al-Nassar. Special thanks and appreciation are given to Mr. Hasan Iqbal from Rapid Prototyping and Reverse Engineering Lab for his sustained assistance and outstanding support throughout the period of my thesis. I am also thankful to Dr Bilal Shaer of MASABIK in providing practical insight to the casting industry.

TABLE OF CONTENTS

LIST OF TABLES

LIST OF FIGURES

THESIS ABSTRACT

AL-YOUSEF, ABDULHADI ABDULLAH M.

IMPROVING QUALITY AND PRODUCTIVITY OF CASTING PROCESS BY USING ADVANCED SIMULATION AND RAPID PROTOTYPING TECHNOLOGY.

MECHANICAL ENGINEERING - MATERIALS AND MANUFACTURING.

January 2012

Metal casting is one of the basic manufacturing processes. Simulating the casting process accurately is very useful to predict the possible design defects of a mold and help in making better mold design, product quality improvement, defects reduction, yield improvement, cost reduction and minimize mold development time. In this research, advanced casting process simulation tools and relevant Rapid Prototyping technology, such as FDM, is used in order to improve the quality of a cast product by producing accurate patterns and near optimized molds. An extensive study of producing a moderately complex casting of a pump impeller is done. Mold design is calculated, simulated and modified to develop an optimized mold in order to avoid expensive hit and trial strategy of streamlining the mold as it is currently being practiced in the industry. Then, pattern making is facilitated by FDM, a modern RP technology. The casting results were validated by testing for dimensional accuracy and integrity of the cast product. The results of this study shows a positive impact on improving the quality and productivity of the casting products ,and demonstrate the effectiveness of computerized simulation on optimized mold design in the metal casting industry and its role in improving the quality and dimensional accuracy of the cast product.

ملخص الرسالة

الاسم: عبدالهادي عبدالله محمد اليوسف

عنوان الرسالة: تحسين نوعية و إنتاجية عملية الصب عبر استخدام المحاكاة المتطورة و تكنولوجيا "النمذجة السريعة"

التخصص: هندسة ميكانيكية

تاريخ التخرج: يناير 2012 م

صب المعادن هي واحدة من عمليات التصنيع الأساسية. محاكاة عملية الصب وبدقة مفيدة جدا للتنبؤ بعيوب التصميم ويساعد في صنع أفضل تصميم للقالب ، وتحسين الانتاجية و جودة المنتج ، و الحد من عيوب التصنيع وخفض التكاليف وتقليل الوقت اللازم لتطوير القالب. في رسالة البحث هذه ، تم استخدام برامج متقدمة في محاكاة عملية الصب والتكنولوجيا ذات الصلة بـ "النمذجة السريعة" Rapid Prototyping ، مثل (FDM) ، من أجل تحسين نوعية المنتج و نمط انتاج "القوالب الرئيسية" Master Pattern . و تم إجراء دراسة مستفيضه على انتاج "دفاعة مضخة" شبه معقدة الشكل، و حسابات تصميم القالب ، و المحاكاة وتعديلها لوضع القالب الأمثل لتفادي العملية المكلفة من التجربة التكرارية لكل تصميم مرة تلو المرة حتى الوصول للتصميم الشبه مثالي ،و كما هو ممارس حاليا في هذه الصناعة . و من ثم ، تم تجهيز "نمط القالب" عن طريق تقنية FDM . و جرى استعراض نتائج الصب واختباراتها الفيزيائية و التركيبيه للتأكد من دقتها و مطابقتها لنتائج المحاكاة . و نتائج هذه الدراسة اظهرت تأثير إيجابي على تحسين الجودة والإنتاجية لمنتجات الصب التي تدل على ان استخدام نظام المحاكاة بالحاسوب لدراسة تصميم القالب الأمثل في عمليات التصنيع تعمل على تحسين الجودة و الانتاجية و دقة المنتج.

CHAPTER 1

INTRODUCTION

In today's world, the rapid change and shorter lifecycle in product design has increased the need of such solutions which help to reduce product development time, cost and improve productivity. During the last two decades computerized simulation programs/software have been introduced and applied by many industries worldwide which have improved the quality and productivity of their products to meet demands in a shorter time frame.

Conventional pattern development involves the tedious task of designing, redesigning and complex machining of patterns in addition to a series of test castings to achieve an optimized design. The use of Rapid Prototyping (RP) processes, such as FDM, and a number of simulation tools have optimized the total product development cycle in terms of cost, time and quality.

The optimization of the casting parameters, such as design of gating, choke, sprue, feeder, riser and pouring basin, can by accurately done through a series of simulations prior to physical realization of mold and production of quality castings.

The significance of the RP and casting process simulation represent an area of research and development for many engineers and scientists. As a test case, the pattern design and process simulation of a moderately complex geometry of one part were carried out in this research. The initial mold was designed by the standard methodology design of gating,

choke, sprue, feeder, riser, pouring basin and other molding conditions, and the initial design was optimized by simulation using MAGMASOFT® software. The powerful features of this software, which includes the X-Ray and slicing views, helped us to optimize the mold design by the elimination of porosity, hot spots, real time effects of pressure, velocity, temperature, flow pattern of molten metal, heat gradient and cooling rate during the pouring and solidification phase.Figure1.1 shows the cycle of manufacturing processes, and the position of casting process among these processes.

1.1 METAL CASTING

The metal casting process is an important manufacturing process in the overall strategy in production. It is essentially pouring of the molten metal in a mold with certain design in order to produce a cast product with the designed shape. The process apparently looks simple, but it takes into consideration a number of factors which control and influence the quality of required product. Recently, the casting simulation by computerized systems has been introduced for the last few years to technically and practically assist in modeling and processing casting in a virtual domain prior to casting in real mode. As a consequence, researchers and engineers can determine the most effective process design of casting.

There are different kind of casting processes depending on the requirement of the product quality, shape, material and cost. Some metal casting fundamentals are discussed briefly.

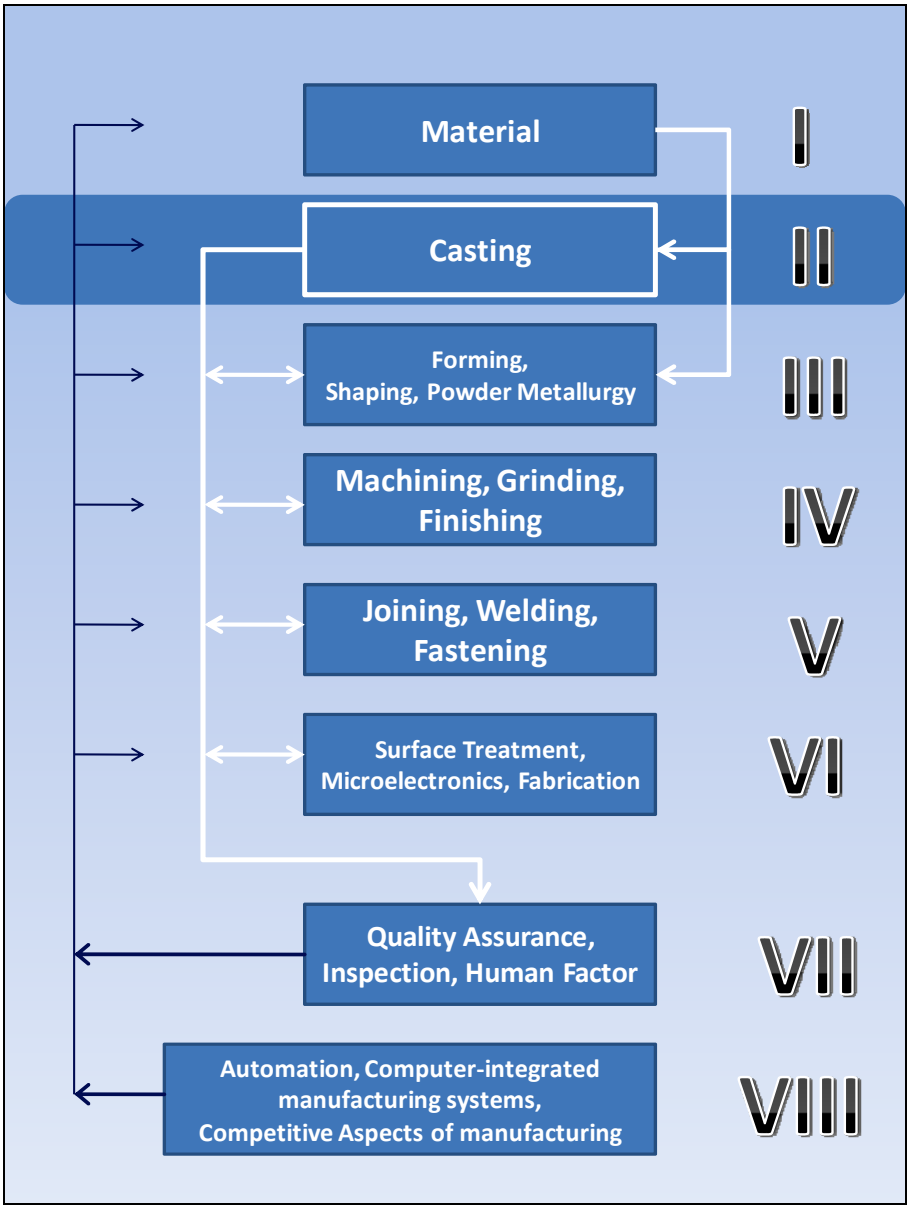

Figure 1.1 Manufacturing processes strategic diagram (Kalpakjian and Schmid 2008)

1.2 CASTING PROCESS

The casting process basically involves pouring molten metal into a mold patterned after the part to be manufactured, allowing it to cool, and then removing the metal from the mold. As with all other manufacturing processes, certain fundamental relationships are essential to the production of good quality and economical castings. Knowledge of these relationships assists in establishing proper techniques for mold design and casting practice. The main purpose is to produce castings that are free from defects and meet specific requirements such as strength, dimensional accuracy, and surface finish.

The flow of molten metal into the mold cavity, heat transfer during solidification and cooling of the metal in the mold, influence of the type of the mold material, and solidification of the metal from its molten state are considered to be the important factors in casting process [1].

1.2.1 SOLIDIFICATION OF METALS IN CASTING

The phase change from liquids state to solidus state is called solidification. During solidification, metal undergoes different phases which influence the overall material properties. Pure metals has already a defined melting and freezing points, on the other hand, alloys start solidifying when the temperature drops below the *liquidus* (T_L), and becomes a complete solid when it reaches the *solidus* (T_S) [1].

The cooling rate of solidification has an effect on the microstructure development of the castings. The structure developed and grains size has an impact on the casting properties.

The smaller grain size increases the strength and ductility and decreases the micro-porosity, and decreases the tendency to crack during solidification as well [2].

1.2.2 FLUID FLOW AND HEAT TRANSFER

Because the molten steel is poured into the mold through pouring basin, then it flows through gating system (sprue, runners and gates) into the mold cavity, the flow characteristics are of considerable significance.

In gating design, *Bernoulli's* equation and the law of *Mass Continuity* are two basic concepts which are considered about fluid flow. *Bernoulli's* equation in fluid mechanics is about conservation of energy, and expressed by equation (1.1).

$$h + \frac{p}{\rho g} + \frac{v^2}{2g} = const. \tag{1.1}$$

Where h is the elevation above certain reference plane, p is the pressure at the elevation, v is the velocity of liquid at the elevation, ρ is the density of the fluid, and g is the gravitational constant [1].

Continuity conditions apply for compressible fluids and impermeable walls.

$$Q = A_1 v_1 = A_2 v_2 \tag{1.2}$$

Where Q is the rate of flow, A is the cross sectional area of the stream and v is the velocity of liquid at that cross section area. Suffix i=1, 2 … defines the different location in the flow stream.

Flow characteristics in gating system can have turbulence or laminar flow of the molten metal (fluid). This characteristic can be defined by *Reynolds* number which is presented in equation (1.3). In ordinary gating design system, the recommended Re range is from

2,000 to 20,000. Re below 2,000 represent *laminar* flow and is undesirable, however, Re above 20,000 represent severe *turbulence* which also has negative impact on gating systems and is undesirable [1].

$$\mathrm{Re} = \frac{vD\rho}{\eta} \tag{1.3}$$

Where v is the velocity of liquid, D is the equivalent diameter of the channel and η are the density and viscosity, respectively.

Other fluid flow consideration of the molten metal is the fluidity, which describes the capability of the molten metal to fill mold cavity. It consists of two factors: (1) characteristics of molten metal, which includes: viscosity, surface tension, inclusions, and solidification pattern of the alloy, and (2) casting parameters which includes mold design, mold material and its surface characteristics, degree of superheat, rate of pouring, and heat transfer.

The heat transfer during the cycle from pouring to solidification at a cooling rate is crucial, and it is dependent on many factors of the casting material, the mold and process parameters.

Solidification time, which is an important index of completing the cycle of casting process, can be theoretically calculated using will-known Chvorinov's equation to equation (1.4),

$$\text{Solidification Time} = C\left(\frac{V}{A}\right)^2 \tag{1.4}$$

Where C is a constant which reflects the mold material, metal properties and temperature, V is the volume of the casting, and A is the surface area of the casting [1].

1.2.3 SHRINKAGE AND POROSITY

Shrinkage and porosity are important casting quality issues which can occur during the solidification in the mold. Shrinkage is a phenomenon which occurs during solidification due to thermal expansion/contraction characteristics and thermal gradient. This may cause large dimensional changes, or sometimes cracking. Shrinkage can be a result of either contraction of molten metal prior to solidification, metal during phase change, or in the casting.

Casting Defects are always a challenge in order to get the quality casting. According to "*International Committee of Foundry Technical Associations*", standardized nomenclature consisting of seven basic categories of defects which can be summarized as follows: Metallic Projections, Cavities, Discontinuities, Defective Surface, Incomplete Casting, Incorrect Dimensions or Shape, and Inclusions [3].

On the other hand, porosity can be caused by shrinkage, or gases entrapped, or sometimes both. It is common in the thicker areas of the casting, which are slower to solidify. Porosity caused by shrinkage can be reduced or eliminated by various means. This includes cast product and mold design improvement, internal or external chills in sand casting, which is the most effective means of reducing shrinkage porosity in many cases [3].

The complete handbook of Sand Casting (Ammen, 1979) discussed and summarized the casting defects and its potential occurring in different casting systems and materials. Table 1.1 presents categorized summary of most common casting defects and its occurrence.

TABLE 1.1 Summary of common casting defects (Ammen 1981)

Casting Defects	Casting Material		
	Cast Iron	Steel	Non-Ferrous *(Brass or Bronze)*
Poured Short	✓	✓	✓
Bobble	✓	✓	✓
Slag Inclusion	✓	✓	✓
Steam Gas Porosity	✓	✓	✓
Kish	✓		
Inverse Chill	✓		
Broken Casting			✓
Bleeder	✓	✓	✓
Lead Sweat			✓
Run Out	✓	✓	✓
Core Rise	✓	✓	✓
Shifts	✓	✓	✓
Swell	✓	✓	✓
Sag	✓	✓	✓
Fin	✓	✓	✓
Metal Penetration	✓	✓	✓
Rough Surface	✓	✓	✓
Blows	✓	✓	✓
Blister	✓	✓	✓
Pin Holes	✓	✓	✓
Shrink Cavity & Shrink Depression	✓	✓	✓
Cold Shot	✓	✓	✓
Blacking or Mold Wash Scab	✓	✓	✓
Sticker	✓	✓	✓
Crush	✓	✓	✓
Hot Tears	✓	✓	✓
Gas Porosity	✓	✓	✓
Zinc Tracks			✓
Drops	✓	✓	✓
Washing & Erosion	✓	✓	✓
Inclusions	✓	✓	✓

1.3 TYPES OF CASTING PROCESSES

Many parts and components are made by casting, and we use them in different applications in our daily life. A variety of casting processes have been developed over a long period of time, and every process has different characteristics and application which meet specific requirement and conditions. The challenging industrial application is the increasing trend of high quality product with close tolerances which provide high yield and reduced loss (better productivity). This section presents a principal introductory to each metal casting process, though our focus in the thesis is only on sand casting processes.

1.3.1 SAND CASTING

Sand casting is the most traditional method in casting and widely used in manufacturing facilities. A pattern, which has the shape of the required casting is designed, produced and placed in sand to create an imprint of that shape. That imprint in the sand will form the cavity in which the molten metal will fill through proper gating in order to make the casting part.

Sand casting system design consists of many components, such as sand, mold, patterns, and cores. Some of these components are essential, and others are used frequently for optimizing the castings [4]. Figure 1.2 shows a typical design of sand casting system as well as the basic components of such systems.

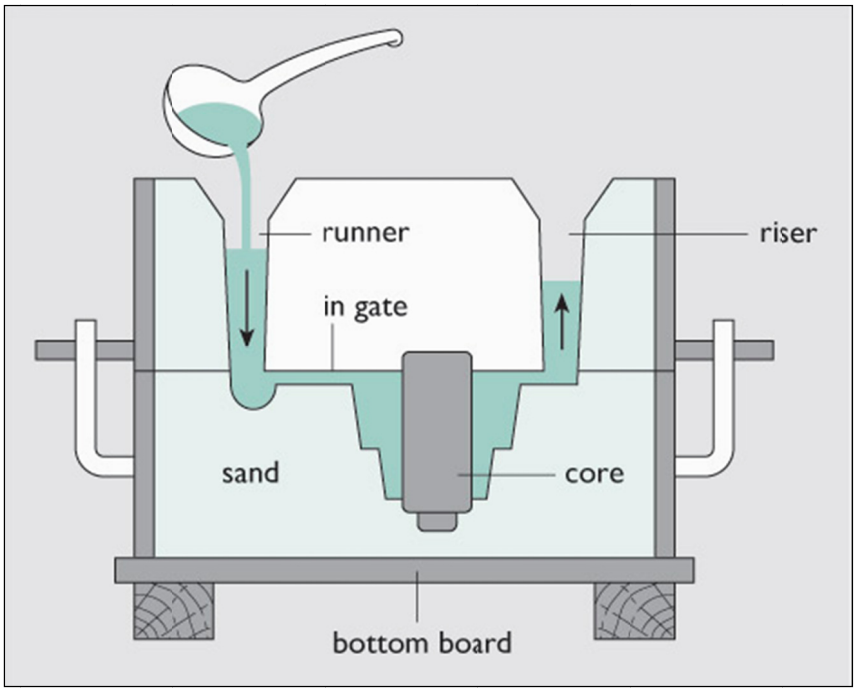

Figure 1.2 Typical design of sand casting system <www.shelmetcastings.com>

a. Sand: Several factors are important in selection of sand for mold making. Sand having fine round grains which can be closely packed and form a smooth mold surface. Generally, manufacturers in the field of sand casting use silica sand (SiO_2). However, the selection of sand involves certain conditions and changes with respect to properties.

b. Types of Sand Molds: There are different types of sand molds. Green molding sand is the most common mold material. It is a mixture of sand, clay and water. It is the least expensive method of making molds. Skin Dried method is generally used for large castings because of its high strength. This method is prepared by drying the mold surfaces by either storing the mold in the air, or drying it by torches. Cold box mold process is another method of sand molding. It uses binders (organic and in-organic)

which are blended into the sand in order to bond the grains chemically for greater strength [4].

Generally, sand molds are composed of many parts. These are:

The mold box, which combines the main pieces: cope on the top, and drag on the bottom.

1. Pouring basin.
2. Sprue.
3. Runner system.
4. Risers.
5. Cores, which are inserts made of sand.
6. Vents, which are placed in molds to carry of gases produced when the molten metal comes in contact with the sand.

c. Pattern: Pattern is a major part which is used to shape the sand mixture in the mold with the required casting design. They can be made of wood, plastic, or even metal. The criterion in which the pattern material is selected depends on the size and shape of the casting, the dimensional accuracy and the quantity of casting required. Table 1.2 explains the characteristics of different pattern materials.

TABLE 1.2 Characteristics of pattern materials (Ekey and Winter 1958)

Characteristic	Rating				
	Wood	***Aluminum***	***Steel***	***Plastic***	***Cast Iron***
Machinability	E	G	F	G	G
Wear Resistance	P	G	E	F	E
Strength	F	G	E	G	G
Weight	E	G	P	G	P
Repairability	E	P	G	F	G
Resistance to:					
Corrosion	E	E	P	E	P
Swelling	P	E	E	E	E

E: Excellent, G: Good, F: Fair, P: Poor,

Pattern can be used as single piece or split pieces. Pattern design is a crucial aspect of the total casting production. It is always taken in consideration the metal shrinkage during solidification which may cause defects or inaccurate dimensions. Also, the ease of removing the pattern from the mold is considered by the means of taper or draft.

Rapid Prototyping technology has recently used in developing mold pattern making. For example, Investment casting using the direct RP resin pattern which replaces the wax patterns. Some industries have started using other RP technologies such as LOM to produce master pattern. In this research, we will use FDM process to develop a pattern from the solid model prepared with Solid Work or other CAD software.

d. Cores: Cores are made of the sand aggregates, and placed in the mold cavity before casting to form the interior surfaces of the casting, and then they are removed by breaking from the casting part after shakeout and further processing.

1.3.2 SHELL-MOLD CASTING

Shell-mold casting has positively grown because it can produce many types of casting with close tolerances and good surface finishes at low cost. Shell-mold casting is considered more economical than the other casting processes according to different production factors. Since it gives high quality of good surface finish as well as tolerances, it will reduce the cost and time of machining and cleaning [5].

Complex casting designs can be produced with less labor and the process can be automated. Figure 1.3 shows the different component of shell-mold casting process as an example.

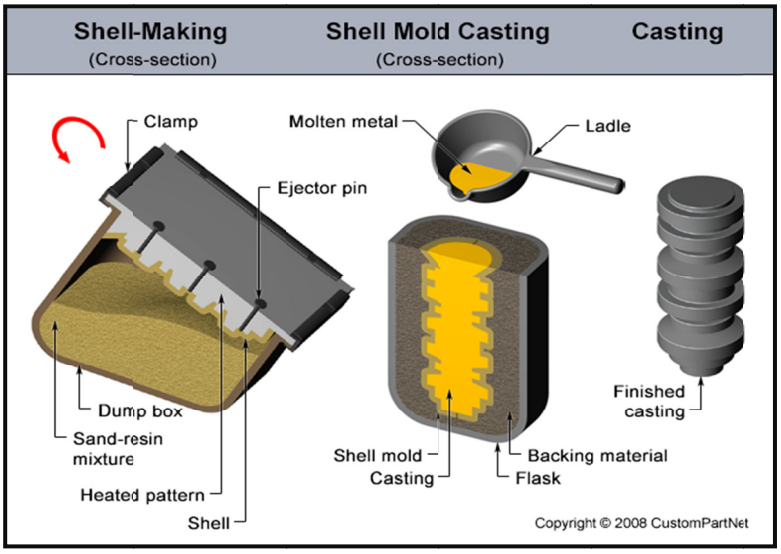

Figure 1.3: Shell-mold casting components and process <www.shelmetcastings.com>

1.3.3 INVESTMENT CASTING

The investment casting is also called Lost Wax process. In this process, the pattern is made by injecting molten wax into a metal die in the shape of pattern. Then, the pattern is dipped into slurry of refractory material. After this initial coating is dried, the pattern is coated repeatedly to increase its thickness. Those wax patterns require very careful handling because they are not strong to withstand the force involved during mold making [5].

There are other types of casting processes such as Permanent-Mold Casting and Die Casting, which more information and background can be found in literature.

1.4 DEFINITIONS/TERMINOLOGY

Definitions of the important terms and key words used in this research are given below to explain the main complex terms which are used in this thesis.

Quality: It is used for the study of the internal and the external characteristics of the cast product, such as material microstructure defects which includes porosity, inclusions and impurities as well as shrinkage and dimensional accuracy.

Productivity: It is used for the study of how fast and efficient the mold is prepared and processed in terms of time and quantity per unit time.

Casting Yield: It is used for the study of the percentage of added casting material (in form of runners, sprue, pouring basin, and risers) during casting process which needed to be removed after solidification in order to finish the product. This extra material added

during casting is considered as waste and required to be minimized for better productivity.

Sand-Cast Ratio: It is used for the study of the quantity (volume or weight) of sand used to cast a specific volume or weight of the product. It is calculated in percentage by knowing the total volume of casting cavity which needs to be filled by molten metal and the total volume of the sand which is used in the mold.

CHAPTER 2

RESEARCH METHODOLOGY

2.1 RESEARCH BACKGROUND

The study is based on the objective to get the quality product with less (near optimized) time and cost by using simulation tools and rapid prototyping technology. Six tasks were strategically established and implemented. Those tasks represent the method by which the complete development cycle of mold design was accomplished, and then these results were validated by experimental validation

2.2 RESEARCH OBJECTIVES

The research aims to find/show the benefits of simulation in casting process in order to reduce the development time and achieve the quality casting. So, the objectives are to design a mold for a semi complex part commonly used in industries by using standard best practices calculations and optimizing the mold by using the numerical simulation. The most optimum design for the mold can be achieved with less development time and better product quality. The research includes experimental validation which investigates the product quality by performing physical check and microstructure study. The results of simulation will be analyzed by studying the solidification rates and its effects on

porosity at different selected points inside the casting system and to show the impact of the cooling rate on the microstructure of the casting.

So the objectives of this research can be summarized as follows:

2.2.1 To develop a strategy of mold designing procedures of semi complex geometry by adopting industrial best practices in designing the casting system in sand casting process

2.2.2 To analyze the flow behavior and the effect of variable factors, filling time, filling pressure, filling velocity and solidification rate on quality of casting indicators such as air entrapment, hot spots, porosity or shrinkage by simulations.

2.2.3 To conduct an experimental program to validate design process plan, the reduction in mold development time and product quality issues

2.2.4 To conduct a metallurgical study of the casting in selected points and study the effect of the solidification on the grain structure and compared with simulation results

2.3 TASK 1: LITERATURE REVIEW

The first task in this research was to conduct a literature survey on casting processes, casting process parameters, mold design strategies, best industrial practices and pattern making paths. Detail review was focused on casting simulation and mold design to reduce the development time and cost of trial and errors practices in industries until one reach at a final streamlined mold. The knowledge of casting process parameters and

conditions, such as filling time, solidification, cooling rate and flow consideration are necessary to understand the solidification of a metal in a mold (Chapter 3).

In this part of the research, simulation tool of the casting process was identified. The survey of the simulation software and programs was discussed from the literature. The selection of the software was justified and the prior use of the selected software in some applications was pointed out in the literature review.

MAGMASOFT® simulation software was used in this research, which is widely used software in the foundry industries for casting process simulation. Input parameters such as: filling time, casting material physical properties, heat conductivity of material, size and number of the enmeshment, were defined which depend upon the cast design and material to be cast.

2.4 TASK 2: PRODUCT SELECTION AND INITIAL MOLD DESIGN

Pump impeller was selected as a representation value added part of moderate complexity (more detail about the part under study is presented in Chapter 4). The initial mold design was done according to metal casting theory (Chapter 1), and then the mold was modified and redesigned using current industrial best practices (Chapter 4) to reach a better design which was further improved by series of simulation leading to a final streamline design.

2.5 TASK 3: SYSTEMATIC PROCESS OF MOLD DESIGN

The third task is to present the systematic process of the optimized mold design resulted from the iterative simulation of the initial designed mold in Task 2.This is to first present an introduction to metal casting process simulation tool (MAGMASOFT®), then the whole strategy of simulation iterations of the mold design in Task 2, and finding the opportunity of improvement until a defined target of improvement is met as illustrated for the impeller mold for sand casting (Chapter 5).

2.6 TASK 4: IMPLEMENTATION OF RAPID PROTOTYPING TECHNOLOGY

In this task, new Rapid Prototyping technology was used as a promising technology in the pattern making. The FDM technology was selected to develop the pattern of the test part (product). The FDM technology will be briefly introduced and steps taken to realize the FDM pattern of the impeller are presented (Chapter 6).

2.7 TASK 5: EXPERIMENTAL VALIDATION OF SIMULATION

In this task, the validation of the optimized mold design resulted from the simulation was done by actual casting of the impeller in a physically realized sand mold. The optimized mold design was prepared and casting was made in similar condition and parameters as used in the simulation. The experimental strategy is explained in Chapter 7.

2.8 TASK 6: CONCLUSION AND RECOMMENDATIONS

In the light of the result from the tasks1 to 5, some explanatory remarks and conclusions were written highlighting the valuable results of using the simulation tool in sand casting. Moreover, the conclusion shows the advantages and benefits of using R.P. technology and FDM in making patterns. Recommendations are also presented for optimized casting process with improved quality product.

The block diagram in Figure 2.1 shows the tasks flow and explaining the process of the research from Task 3 to Task 5.

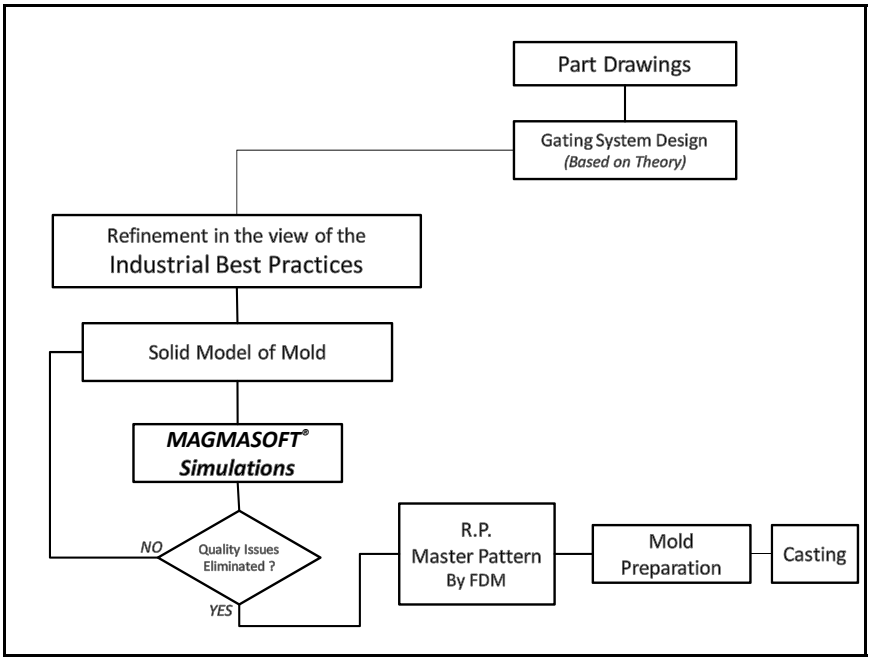

Figure 2.1 Research tasks flow diagram.

CHAPTER 3

LITERATURE REVIEW

3.1 LITERATURE SURVEY

Lately, great considerations have been brought in the manufacturing world regarding the development time and cost, and improving the product quality as well as delivering the products into the market in a relatively short time. The literature survey focused on researches of casting processes, mold designing, sand casting simulation, and the use of rapid prototyping technology in casting.

Senthilkumar, *Ponnambalamb*, and *Jawahar* (2008) investigated the most influencing factor for controlling pull-down defects in iron castings. The identified optimization factors were pouring temperature, carbon equivalent and gating system. Some of the underlying process characteristics, which affect the quality of casting such as metal filling pressure, velocity, solidification, hot spot location, stress distribution and porosity, can be predicted by the simulations. [6]

Fu-Yuan, *Jolly* and *Campbell* (2009) used a computational fluid dynamics (CFD) code, Flow-3D for the simulation to eliminate the trial and error approach in the designing of multiple-gate system. They investigated the behavior of L-junction, and gating system. [7]

Guo-fa, Xiang-yu, Kuang-fei, and Heng-zhi, (2009) used View Cast simulation tool for the optimization of valve block casting. They investigated the temperature field, flow pattern, and stress distribution. They predicted three kinds of potential defects including cold shut shrinkage and crack in the casting. They optimized the structure of the pouring system, and temperature distribution during the filling stage and eliminated the defects. Based on the simulation results, double gating system were replaced by a single-gating system. It can be concluded that the riser and chill are useful to eliminate the shrinkage defects in the casting. The position and volume of defects in casting with chill and modified riser were redesigned in order to avoid the shrinkage. Optimized mold design was achieved after the analysis of solidification by simulation. [8]

Hong-Jun, Ming-Bo, Jing and Kang (2006) used *ProCast* simulation tool for the analysis and optimization of solidification simulation process. [9]

Zhang, Luoxing and Zhu (2009) used numerical simulation for the optimization of A356 Aluminum thin-walled component with permanent mold and after optimization they found no obvious defects such as gas porosities and shrinkages in the component. The solidification process of casting was also discussed. The results indicate the numerical simulation is an efficient tool for the design of casting process. [10]

Ferguson, Chen, Bonesteel and Vosburgh (2009) concluded that "Physical simulation has developed into an extremely useful and valuable tool used to study many metallurgical processes, develop new materials, and obtain characteristics of materials in real world situations. The benefits include lower product and process development costs, rapid

trouble shooting of existing procedures and materials problems, improved materials and materials applications, development of new procedures, and reduced energy cost". [11]

Vijayaram, Sulaiman, Hamouda and Ahmad (2006) presented a paper on Numerical simulation of casting solidification in permanent metallic molds. They could identify the conditions and optimum values by simulation of solidification process with running local developed computer software for the casting process selected for investigation. By analyzing the time-temperature profile generated by the software as shown in Figure 3.1, and heat transfer coefficient values which plays a key role in the effective design of castings, they studied the defects in the cast product caused by variation of heat dissipated from the casting to the mold at the metal – mold interface. [12]

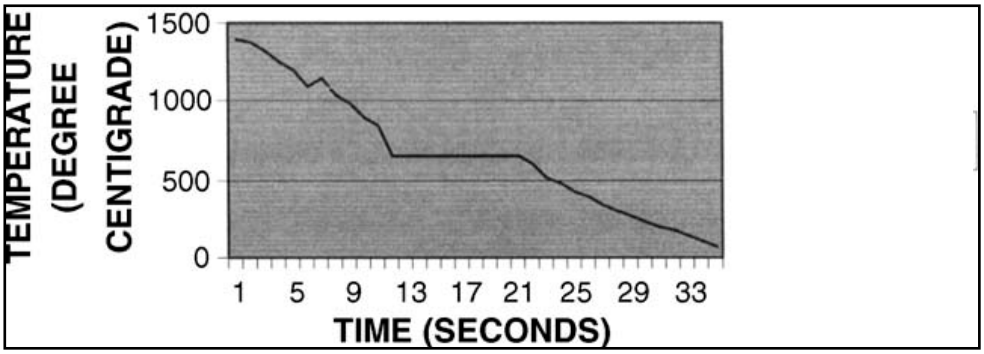

Figure 3.1 Time-temperature curve from solidification simulation. (Vijayaram 2006)

Venkatesan, Gopinath and Rajadurai (2004) presented a study on Simulation of casting solidification and its grain structure prediction using FEM. A program for finite element modeling of casting solidification was developed by C++ language and Gaussian elimination method to solve the matrices generated. This program was used to analyze the solidification of Al–6 wt% Si alloy in sand and metal mold as the cooling curve is

shown in Figure 2.2. The program was designed to perform two dimensional heat transfer analysis for non-linear transient cases. Latent heat release is incorporated in this program using enthalpy method. They have developed the equations to be used to calculate the solid–liquid interface velocity (R), solidification rate (dT/dt) and thermal gradient (G). From the simulation results, R and dT/dt could be calculated and using these values G could be found and there by the most probable grain structure could be predicted. [13]

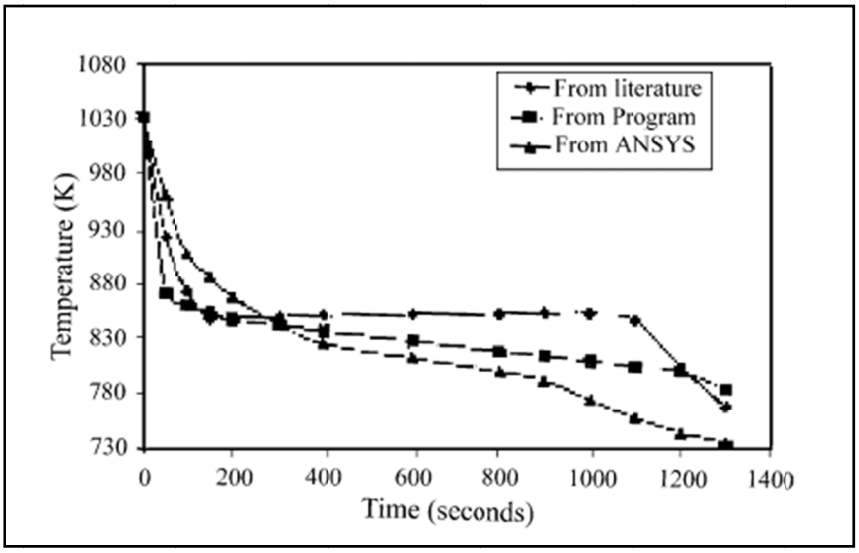

Figure 3.2 Cooling rate of Al–6 wt. percentage Si alloy by simulation. (Venkatesan 2004)

Cheah, Chua, Lee, Feng and Totong (2004) reviewed the applications of rapid tooling in investment casting. They had found results which can be summarized in terms of advantages and disadvantages. It was found based on different researches that the advantages of RP in production include: RP is not limited by part complexity, provide easy and fast evaluation of tooling design, and by integrating simulation and RP (in

investment casting) problems due to wax shrinkage or feeding/filling can be rectified before manufacturing. The disadvantages shown were mainly dimension accuracy because RP rely on CAD, as well as surface finish due to layering build up. It was also mentioned that as part of direct fabrication of investment casting pattern, the fused deposition modeling (FDM) for non-wax RP patterns, two significant advantages are identified. Firstly, the durability and strength of non-wax patterns will allow the casting of thin wall structures, which are previously difficult due to the fragility of wax structures. Secondly, the relatively tough non-wax patterns allow finishing operations to be conducted to improve surface quality, which is then transferred onto the castings. [14]

Dunne, P., Soe, S. P. and others (2004) had investigated the demands of Rapid Prototypes used as master patterns in rapid tooling for injection molding. The research had been conducted on two direct rapid tooling processes for injection molding. These are enhanced silicone molding and sand molding. Surface finish were mainly dependent on RP pattern material, but had shown more effective in sand molding. Porosity of rapid prototypes had shown effect on both processes. Dimensional accuracy also had some effects on both processes, and finishing of the rapid prototype has been shown to effect accuracy. [15]

Wu, Tinschert and others (2001) had presented a paper describes a method of making titanium dental crowns by means of integrating laser measuring, numerical simulation and rapid prototype (RP) manufacture of wax patterns for the investment casting process. They measured four real tooth crowns (FDI No. 24, 25, 26, 27) by means of 3D laser scanning. The laser digitized geometry of the crowns was processed and converted into

standard CAD models in STL format, which was used by RP systems and numerical simulation software. Commercial software (*MAGMASOFT*®) was used to simulate the casting process and optimize the runner and gating system (sprue) design. Figure 3.3 shows the shrinkage porosity in the crown simulated in casting design 3. RP crowns were printed directly on a Model Maker II 3D Plotting System. A silicone negative mold (soft tool) was made from the RP crowns. The duplicated crowns were joined to the optimized runner and gating system. All castings were examined for porosity by X-ray radiographs. By using the integrated scanning, simulation, RP pattern and casting procedure, cast crowns, the results found were crown cast products free of porosity, with excellent functional contour and a smooth surface. [16]

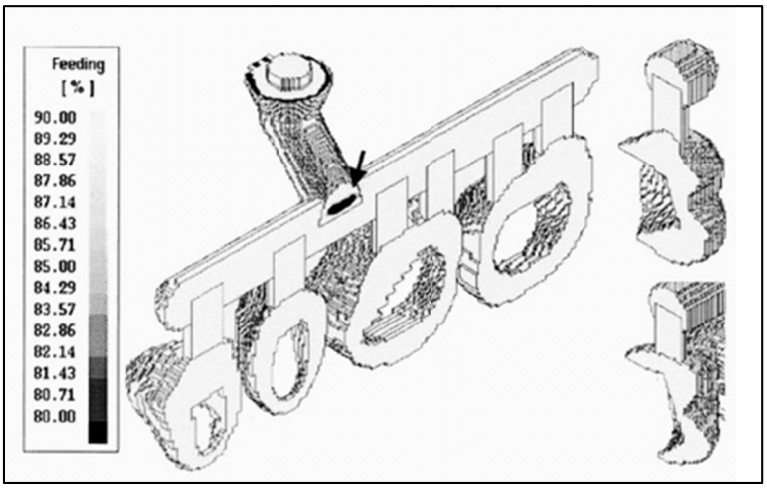

Figure 3.3 Shrinkage porosity simulated by MAGMA® using feeding criterion. (Wu 2001)

Hu, Tong, Niu and Pinwill (2000) presented a study on die casting of two types of runner and gating systems for a thin-walled magnesium telecommunication part. Numerical simulation showed that the new design they developed by simulation provided a

homogenous mold filling pattern with the last filled areas being located at the upper edge of the part, where overflows and vents were conveniently attached. Figure 3.4 shows a series of casting experiments resulting in good quality parts with sound microstructure were produced. [17]

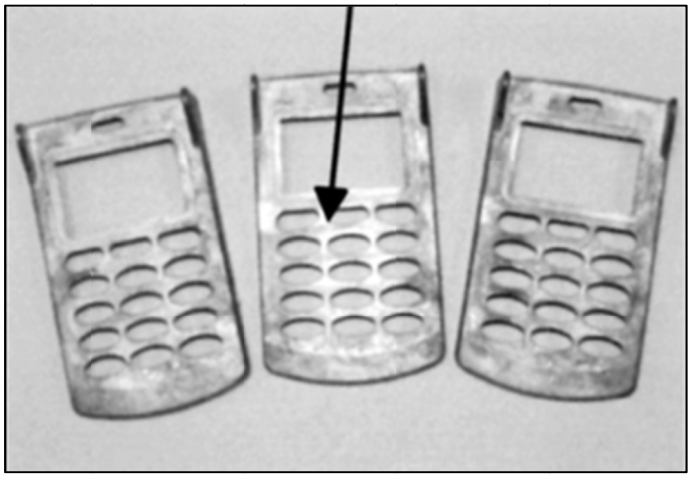

Figure 3.4 Good quality parts produced after simulation. (Hu 2000)

Fu-Yuan, Jolly and Campbell (2009) proposed by a technical research paper the L-shape junction in runner and gating systems used in Aluminum gravity casting. Two geometries of L-junction were developed by computational modeling. The change in flow direction through L-junctions can yield a high coefficient discharge C_d (equation 2.1). The main aim of that research was to reduce/eliminate the trial and error approach as designing a multiple gate system.

$$A_c = \frac{ActualFlowRate}{TheoriticalFlowRate} \tag{2.1}$$

Where Theoretical flow rate = $A_V = A\sqrt{2gh}$, and A is the cross sectional area of sprue. [18]

Talamantes-silva, Rodriguez, Valtierra, and Colas (2008) assessed the microstructure of the aluminum-copper alloy of the A206 type after melting and casting in molds by measuring the secondary dendrite arm spacing, grain size, and porosity. It was found that these parameters increase as the solidification rate decreases. The aim of work was to determine the effect of solidification kinetics and heat-treatment conditions on the mechanical properties of Al-Cu alloy. The experimental work was achieved so that the metal was poured into molds that force a thermal gradient and promote the continuous variation of the microstructure within the ingot. The cooling rate was determined by establishing the curves registered by the thermocouples inserted in the instrumented mold. [19]

It was discussed that during heat treatment, most of the copper containing particles dissolve into the grains and this is more noticeable in samples that solidified at a lower rate. The particles that do not dissolve are able to stop grain growth and explain the reasons for observing coarsening as shown by the SEM in Figure 3.5.

It was found that microstructural parameters such as DASs, grain size, and porosity engross as when the material solidifies at lower rates which produces coarser grains. [19]

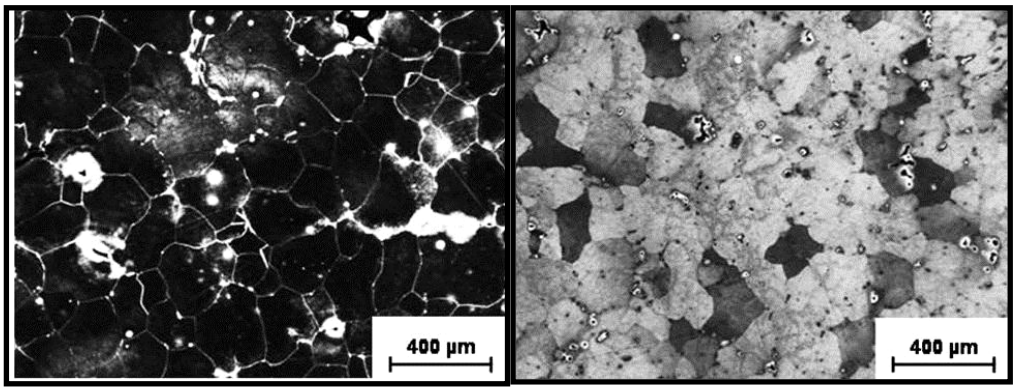

Figure 3.5 Coarsening on solidified samples at lower rate. (Talamantes-silva 2008)

Other technical papers and text books have been used to provide some basic and elaborated background information about the research subject. Reference literature reviewed above and other sources of papers are be classified into three main groups. Some of them are discussing the casting simulation using CAD and software, and its importance in optimizing the casting process and improving the metallurgical and mechanical characteristics. Other group studied the impact of Rapid tooling used in casting and its contribution to the quality of cast product, and the positive results in improving the productivities in terms of casting yield and economy. The last group of literature review has presented integrated solutions by utilizing CAD systems, advanced software for simulation, and rapid prototyping and tooling for better lead time and productivity. Some parameters and materials properties and specification are referenced from the materials books and tables.

3.2 SUMMARY OF LITERATURE SURVEY

From the literature review on the application of casting simulation and Rapid Tooling, the following can be summarized:

a. Shrinkage defect is the most common problem during and after solidification in castings particularly in the heavy sections. Gating design, dimensions or location is not positively adding value. Different parameters control the shrinkage such as casting material and heat transfer coefficients.
b. Porosity defects occur after solidification inside the casting material, or at the surface. Porosity is proportional to the shrinkage, and they may occur in the same locations. X-ray activation in similar software can show the internal porosities in the casting.
c. Gating Design, and its influence on the flow which cause turbulence. This can be a cause of the shrinkage or porosity. Pressurized gating was discussed in the previous research as a positive factor. However, no direct relation could be proven between pressurized gate design and solidification rate or internal defects. An attempt will be made to establish such relationship.
d. Variation of applications of numerical casting simulation and rapid tooling such as rapid prototyping by FDM in the investment casting, particularly in medical applications.
e. Grain structure is affected by faster cooling rate generating small grain structure, compared to slower cooling rates where larger grain structure generates.

3.3 DESIGN STANDARDS AND INDUSTRIAL BEST PRACTICES

It is very important to mention that *Rio Tinto Iron and Titanium Inc*. and *Japan International Cooperation Agency* standards (JICA) were mainly used in developing the mold design as part of the best practices in the manufacturing industries. Runners, gates, risers, and other mold components are designed according to the standards and recommendations written in JICA (1995). Some recommendations and basic principles of sand casting processes are also collected from the complete handbook of Sand Casting (Ammen, 1979), and the recommendations of *Rio Tinto* best practices (SORELMETAL®, 2000).

CHAPTER 4

MOLD DESIGN AND CALCULATIONS

The sequence of sand casting system design according to the Japan International Cooperation Agency (JICA) and other designing books [1] can be briefly described below. The same procedure was applied in this research.

a. Filling time based on the weight of the casting, gating, runners, etc.

b. Sprue Design

c. Pouring Basin

d. Runner design

e. Gate Design

f. Choke Runner

g. Sprue Runner

4.1 MOLD DESIGN BEST PRACTICES BY "JICA"

Nagoya International Cooperation Agency was established in 1974, and it is an agency for technical cooperation aimed at the transfer of technology and knowledge around the world. It is the primary Japanese governmental agency responsible for technical cooperation component of Japan's Official Development Assistance (ODA) program.

JICA best practice in foundry and casting design provide the basic and advanced notes in making the casting designs from the view point of dimensions and numbers of the castings to be produced, the shapes of the castings, and other views such as machining and finishing. Also, it provides the fundamentals of flow and the shapes and sizes of castings and their casting design.

JICA was used in the calculations for the initial mold design. The design calculation using JICA was for Pouring time, Effective sprue height, Design of sprue, runner, and gate and risers. Basic shapes and sized recommended by JICA also were considered in designing the mold system such as the shape and angles of the runners. The following provides the detail pertain the calculations.

4.1.1 FILLING (POURING) TIME

When the adequate filling time is fixed, the pouring weight is known and the flow rate of molten bath is considered. Consequently, the sizes of every part of gating system can be chosen. JICA refers the filling time as proportional to the pouring weight, as H.W. Dieter's relation [20] as calculated in section 4.4.

4.1.2 EFFECTIVE SPRUE HEIGHT

The effective sprue height (ESH) for the same castings may differ by the positions of casting molds according to the parting line. The flow velocity in this case is considered for two reasons. If the major part of the casting is in the cope, the flow velocity will

gradually reduce, and this is recommended to large castings. If the part is in the drag, the flow velocity is almost constant.

This relation can be used to calculate the ESH as follows [20]:

$$ESH = \frac{(2H \times C - P^2)}{2C} = H - \frac{P^2}{2C} \quad (4.1)$$

Where H is the height from the pouring position, C is the height of the casting, and P is the height of the upper mold half (cope).

4.1.3 DESIGN OF SPRUE, RUNNER AND GATE

Generally the sprue is designed in a parabolic taper shape if the sprue is long for large size casting. However, it can be uniform circular section without tapering.

For calculating the sectional area of the sprue, the following was proposed by JICA:

$$Sprue\ Area = \frac{W}{T} \times \frac{C}{\sqrt{ESH}} \times 7.160 \quad (4.2)$$

Where W is the pouring weight, T is the filling time, ESH is the effective sprue height as explained earlier, and C is a constant. The constant C can be set to 0.286 for choked runner [20].

During filling, some slag or sand particles flow into the runners, so that it is necessary to remove them in the runner, or to stop them before. So in order to collect these impurities, trapping basin at the runner extension is added in the design.

It is also recommended that the total sectional area of the runner to be three times as large as the runner choke. In order to make the molten metal flow uniform through the gating system, the runners' dimensions need to be increased to increase the pressure at the gates.

It is also recommended that the height of runner is generally four times higher as of gate in order to give the flow pressure to the gate extension. [20]

For the gate, the cross-sectional area of one gate must be calculated according to the thickness of casting. The following was also recommended by JICA:

$$Total\ Sectional\ Area\ of\ Gates = \frac{W}{V.d.T} \tag{4.3}$$

Where W is the pouring weight, d is the density of metal, T is the filling time, and V is the mass flow of the molten metal in cm/sec, and it can be calculated by the following relation:

$$V = \sqrt{2\ g\ H} \tag{4.4}$$

Where g is the gravity acceleration and H is the height.

The following considerations are recommended by JICA and it was implemented in this research during mold designing [20]:

a. The gates were set at locations apart from the sprue and runners extension.
b. The gates were set in opposite direction as that of bath flow.
c. The length of the gates is set no larger than the width of runner.

4.2 SELECTED PART FOR THE RESEARCH

A component was selected to illustrate the systematic process of virtual sand casting mold design. The component (an impeller) was selected based on the following criteria:

a. It belongs to most commonly used components in industry.
b. It is mostly sand casted due to its moderate complex geometry.

c. It possesses difficulty to machine using conventional machining setup due to its complex shape.

d. It contains both thin and thick section to analyze the effect of variable factors such as, filling time, filling pressure filling velocity and cooling rate.

According to this criterion, the CAD model of the impeller shown in Figure 4.1 was selected.

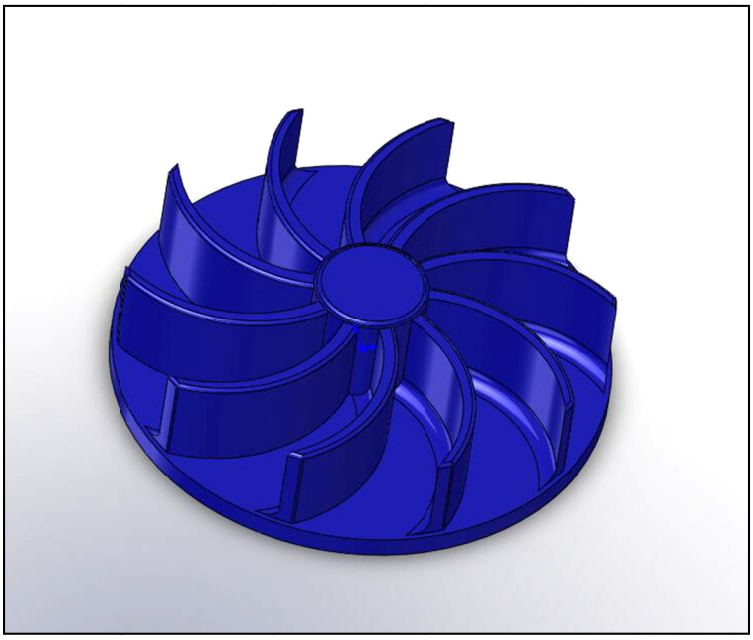

Figure 4.1 Physical model/geometry of the selected product – A pump impeller.

4.3 INITIAL MOLD SYSTEM DESIGN

In this chapter, detail information, geometry and preprocessing of simulation for the tested part under consideration provided and discussed. The design process was started with basic assumptions from theory and the industrial best practices. Then, the designing

process was followed by the simulation with MAGMASOFT® program. Details of software and simulation conditions are also presented and discussed in details in Chapter 5.

4.3.1 GEOMETRY AND CASTING PROPERTIES

The selected impeller geometry is shown in Figure 4.2. Table 4.1 shows the detail information of the pump impeller. Table 4.2 shows the material properties of Aluminum alloy that is used in the impeller casting [21].

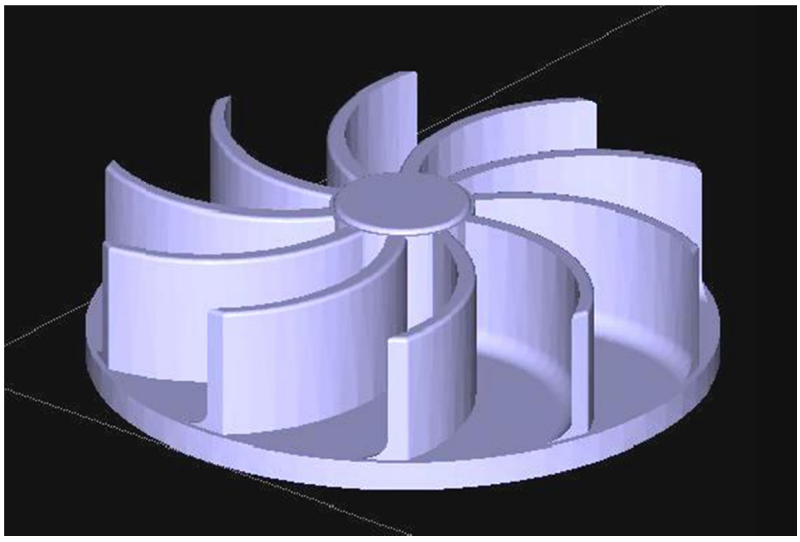

Figure 4.2 Moderately complex geometry of cast product – A pump impeller.

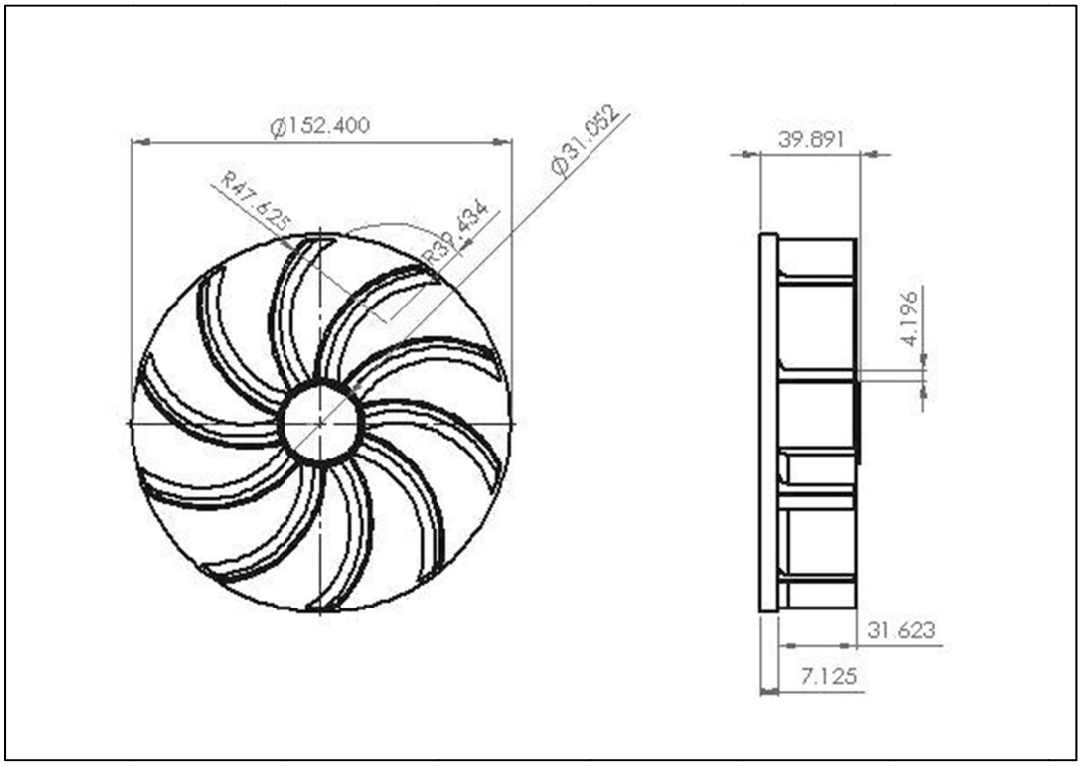

Figure 4.3 Selected (pattern) pump impeller drawings.

TABLE 4.1 Cast product material information – Pump impeller

Material	Dimension (Dia.) mm	Total Volume cm^3	Total Weight kg	Density g/mm^3	Shrinkage Allowances
Aluminum $AlSi_6Cu_4$	102	294.85	0.830	8.8	1.05 - 1.06 Factor from total volume

TABLE 4.2 Material Property of $AlSi_6Cu_4$ (Kaufman 2009)

Material Property	Value
Density (kg/m^3)	$2.81 * 10^3$
Viscosity (η/mPa s) – above 700 ºC	1.298
Specific Heat (J/kg.K)	963
Thermal Conductivity (W/m.K)	121
Latent Heat (J/kg)	$3.89 * 10^5$
Modulus of Elasticity (GPa)	71
Shear Modulus (GPa)	26
Liquidus Temperature (ºC)	638
Solidus Temperature (ºC)	593
Poisson's Ratio	0.33

4.3.2 CALCULATIONS OF INITIAL MOLD SYSTEM

The initial mold system design was based on the JICA standards and best practices. It was assumed that the complete cast product is in the drag (or cope) of the mold. The filling time was calculated and found to be four seconds according to H.W. Dieterts (JICA, 1995):

$$T = S\sqrt{W} \tag{4.5}$$

Where S is a coefficient depends on the thickness of the casting, and W is the total pouring material weight.

Area of the choke was calculated according to the formula [22]:

$$A_c = \frac{V_D}{t.f_r\sqrt{2g.H}} \tag{4.6}$$

Where V_D is the total volume of the castings, H is the *ferrostatic* head in the sprue, and f_r is the friction factor which is in this case 0.2 (SORELMETAL®, 2000)

Friction is involved because that the potential energy of liquid at the top of the sprue may not be completely converted to mechanical energy at casting cavity.

Two gating system is introduced as shown in Figure 3.2 which is considered as one of the best practices in literature, which represent:

$$A_c = A_1 + A_2 \tag{4.7}$$

Where, A_1 and A_2 are the cross-sectional area of the first and second gates respectively.

Choke and sprue design and calculations are carried out according to JICA, and summarized in Figure 4.3. Gate runner design is calculated according to the chock cross-sectional area A_C:

So, that is:

$$3A_C = A_R \tag{4.8}$$

And

$$a_r = \sqrt{\frac{A_R}{2}} \tag{4.9}$$

Where A_R is the cross-sectional area of the runner, and a_r is the side length of the cross-sectional area of the bottom of the runner, which found to be 1.50 cm [20].

In our case, the part is small and the mold size is limited. So the relation (4.1) was not applied and the sprue was designed to the maximum cope height which is 8 cm.

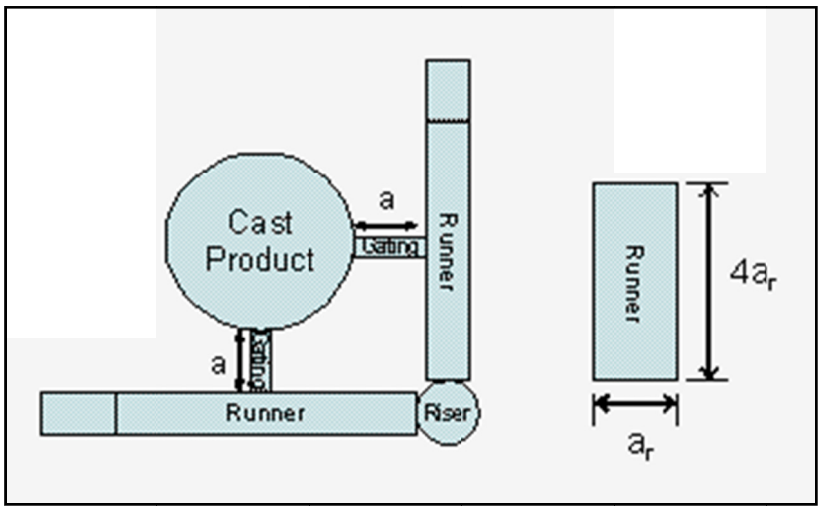

Figure 4.4 Casting system for impeller and runner dimensions.

Table 4.3 shows the summary of calculated mold design. A_c represents the cross-sectional area of choke, A_1 and A_2 represent the areas of first and second gates respectively, a_r is the side length of the cross-sectional area of the bottom of the runner, H is the total height of the sprue and basin, h is the basin height, A_s represents the cross-sectional area of the sprue, A_T is the cross-sectional area of the sprue at the top, and A_B is the cross-sectional area of the sprue at the bottom, as illustrated in Figure 4.4.

TABLE 4.3 Summary of casting system dimensions by calculations –units in cm

A_C	$A_1 = A_2$	a_r	H	h	A_S	A_T	A_B
2.94	1.47	0.61	8.0	2.0	5.89	5.89	2.00

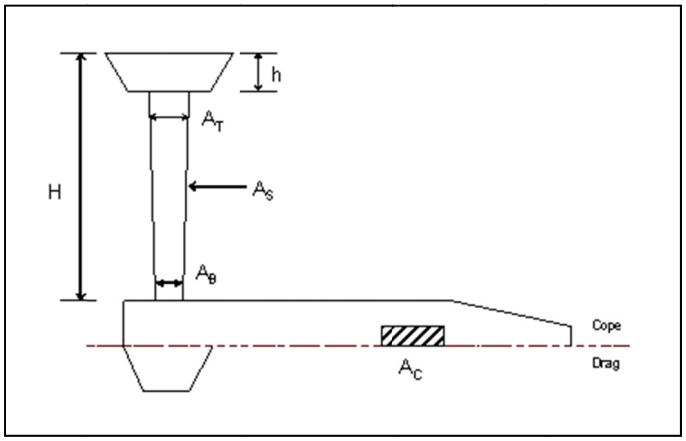

Figure 4.5 Gating components design.

The pouring basin and sprue well design with dimension ratios were calculated based on the best practices of JICA, and as also recommended in the literature [23].

The final design detail drawings are shown in Appendix A1.1 and A1.2.

CHAPTER 5

THE SYSTEMATIC PROCESS OF VIRTUAL SAND CASTING

With the development of computer technology, numerical simulation has been more and more widely used in many applications. Simulation techniques not only play very important roles in scientific study, but also occupy very important places in education, military, entertainment and almost any fields that we can imagine. In this chapter, illustration of the systematic process of sand casting simulation is presented, discussed and results are shown on a component of moderate complexity i.e. an impeller casting in sand mold.

5.1 INTRODUCTION

The numerical modeling solution in this research was conducted by one of the most powerful software available. The basic mathematical and physical analysis performed by this software is simply reliable combination of theoretical calculations and experimental measurements. The core part of the analysis is the calculation, and generally the calculations related to the numerical simulation of any casting processes contains of three major parts: fluid flow, solidification and stress strain analysis. Stress analysis will not be covered in this thesis.

The importance of modeling and simulation in production technology is increasing due to the steady reduction in development time. This is motivated by the need of optimization of the production processes, the enhancement of product quality and a reduction of costs. The application of numerical modeling is especially recommended in the development of new production methods and in use of new materials. The traditional approach of making casting compared with numerical simulation tools can be demonstrated as in Figure 5.1.

Besides all advantages and disadvantages of traditional casting and mold design, the following characteristics cannot be easily determined through traditional casting design.

a. Metal flow pattern
b. High pressure area
c. Metal velocity distribution
d. Heat transfer behavior
e. Stress distribution
f. Hot spot areas
g. Air entrapment
h. Porosity concentration

The predetermined information about above mentioned areas can help to produce better quality casting.

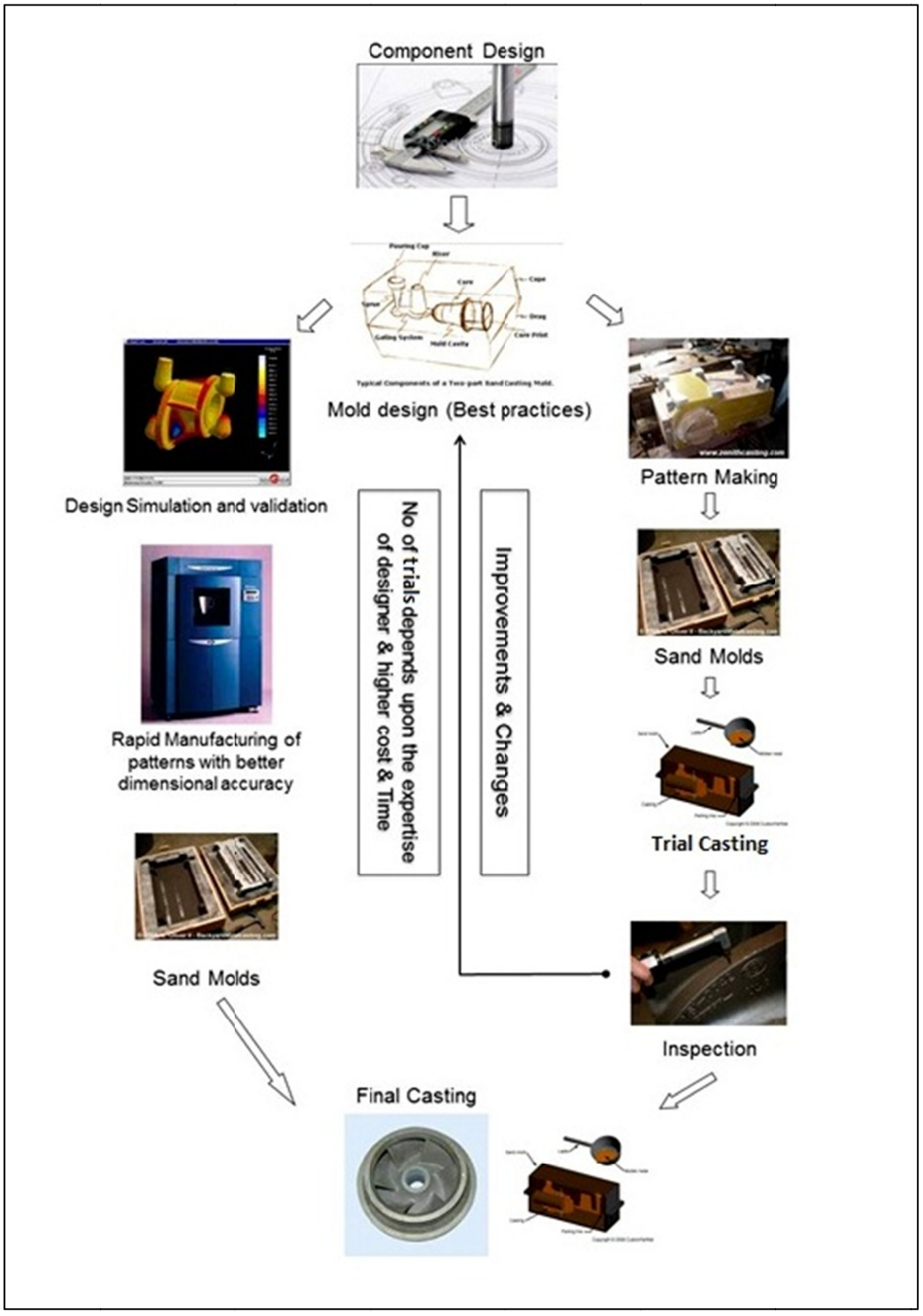

Figure 5.1 Traditional casting processes versus simulation approach.

5.2 THE GOALS OF SIMULATION

The first and most important is to make sure that the process being simulated is the same as that being carried out in the foundry. Pouring temperature, filling time, mold material and alloy composition are the parameters which must be checked

The following rules can be considered most important [24]:

5.2.1 Defining the problem in advance is required for which needs to be solved by simulation. Mold filling simulation is fundamental in all casting processes.

5.2.2 It is recommended to start with rough test simulation to get an indication, then generating a coarse mesh and running a solidification simulation only in order to get more clues about the gating and filling behavior.

5.2.3 The process can continue with more accurate simulation including more accurate enmeshment and mold filling simulation.

5.2.4 Considering the fluctuation of input parameters when comparing, it is important to look at several castings.

The simulation is a tool of education as well. It gives better understanding of the complex phenomena in casting. Storing the results in a systematic presentation helps in re-using this information.

5.3 SIMULATION ISSUES RELATED TO CASTING

The following issues can be introduced on how to use simulation to analyze some specific process steps which directly influence the quality of casting [24].

5.3.1 INITIAL SOLIDIFICATION SIMULATION:

Before filling simulation is carried out, it is recommended to use a rough solidification simulation to determine the hot centers in the casting as well as the modules of these hot centers and also to use this information to determine the risers' positions and sizes.

5.3.2 FILLING SIMULATION FOR GATING DESIGN:

Limiting the filling simulation to the initial time is recommended. It can be 10% of the casting to be filled, by which designing the gating system so it is full with metal as early as possible during the filling process.

5.3.3 CONTINUED FILLING SIMULATION:

The total filling process is simulated where it is important to check that the total filling time is short, and the temperature distribution in the casting after filling is uniform.

5.3.4 DETAILED SOLIDIFICATION AND FILLING SIMULATION

Depending on the objective of the simulation, several aspects can be analyzed:

a. Is the casting sound?

b. Are the positions of the risers correct?

c. Are the risers and gating too large or too small?

d. Is there a need to use more risers?

5.4 MATHEMATICAL FOUNDATION OF SIMULATION SOFTWARE MAGMASOFT®

MAGMASOFT® is a comprehensive simulation tool for the technological and quality focused production of castings. It has simulation capabilities which provide better understanding of mold filling, solidification, mechanical properties, thermal stresses and distortions. It has also built-in data base which provide complete solution for the casting design, production and quality parameters.

MAGMASOFT® simulation utilizes the equations explained in the previous section 5.4, with different boundary conditions as reflected by the mold and the core material, cast metal and their physical and thermal properties in liquid state and solid state.

The numerical modeling solution in this research was conducted by this most powerful software available. The basic mathematical and physical analysis performed by MAGMASOFT® software is simply reliable combination of theoretical calculations and experimental measurements, and utilizes the experimentally validated empirical relationships for different key properties and parameters of the mold. The core part of the casting process and the solidification analysis is the calculation, and generally the calculation related to the numerical simulation of any casting processes contains three major parts: fluid flow, solidification and stress strain analysis.

The velocity of the flow of liquid metal is related to the static pressure; hence the mechanical energy equation (Bernoulli's equation) for the cross-sectional area at the gates can be given as [25]:

$$p_1 + \frac{1}{2}\rho_1 v_1^2 + \rho_1 g h_1 = p_2 + \frac{1}{2}\rho_2 v_2^2 + \rho_2 g h_2 + \Delta p_{loss,1-2} \tag{5.1}$$

Where, p, ρ, v, g and h represent static pressure, mass density, and magnitude of the flow velocity, gravity and the elevation from reference respectively.

Furthermore, pressure losses can be described by *Darcy-Weisbach* equation [25] as follows:

$$\Delta p_{loss} = f \frac{L_{1-2}}{d} \frac{\rho v^2}{2} \tag{5.2}$$

Where $L_{1\text{-}2}$, d and f are the length of the gate between the cross-sectional areas, the diameter the friction factor respectively.

The conservation of mass can be obtained by considering a mass balance over a stationary volume through which the fluid is flowing. This is called *Eulerian* approach and can be expressed as [25]:

$$\frac{\Delta m}{\Delta t} = \sum_i \dot{m}_i \tag{5.3}$$

From the mass conservation equation, continuity equation can be simplified and given for both compressible and incompressible fluids as follows [25]:

$$\frac{\partial u_1}{\partial x_1} + \frac{\partial u_2}{\partial x_2} + \frac{\partial u_3}{\partial x_3} = 0 \tag{5.4}$$

Where u_i represents the operator velocity vector at 3-D directions i=1, 2 and 3.

For *Newtonian fluids*, using *Stokes* hypothesis [25], normal and shear components of the viscous stress tensor are given by the following equations:

$$\tau_{11} = -\mu\left[2\frac{\partial u_1}{\partial x_1} - \frac{2}{3}\left(\frac{\partial u_1}{\partial x_1} + \frac{\partial u_2}{\partial x_2} + \frac{\partial u_3}{\partial x_3}\right)\right] = -\mu\left[2\frac{\partial u_1}{\partial x_1} - \frac{2}{3}divu\right] \tag{5.5}$$

Where *div*u stand for the divergence operator applied to the velocity vector.

So, we can write the viscous stress tensor, τ, of a Newtonian fluid as follows:

$$\tau = \begin{bmatrix} \tau_{11} & \tau_{12} & \tau_{13} \\ \tau_{21} & \tau_{22} & \tau_{23} \\ \tau_{31} & \tau_{32} & \tau_{33} \end{bmatrix} = \begin{bmatrix} -\mu\left(2\frac{\partial u_1}{\partial x_1} - \frac{2}{3}divu\right) & -\mu\left(2\frac{\partial u_1}{\partial x_2} + \frac{\partial u_2}{\partial x_1}\right) & -\mu\left(2\frac{\partial u_1}{\partial x_3} + \frac{\partial u_3}{\partial x_1}\right) \\ -\mu\left(2\frac{\partial u_2}{\partial x_1} + \frac{\partial u_1}{\partial x_2}\right) & -\mu\left(2\frac{\partial u_2}{\partial x_2} - \frac{2}{3}divu\right) & -\mu\left(2\frac{\partial u_2}{\partial x_3} + \frac{\partial u_3}{\partial x_2}\right) \\ -\mu\left(\frac{\partial u_3}{\partial x_1} + \frac{\partial u_1}{\partial x_3}\right) & -\mu\left(\frac{\partial u_3}{\partial x_2} + \frac{\partial u_2}{\partial x_3}\right) & -\mu\left(2\frac{\partial u_3}{\partial x_3} - \frac{2}{3}divu\right) \end{bmatrix} \tag{5.6}$$

5.5 SIMULATION STEPS IN MAGMASOFT®

The simulation steps carried out using MAGMASOFT® are presented. These steps are repeated for every simulation after accommodating the required changes in the geometry in order to have iteratively improved results.

5.5.1 STEP 1: GEOMETRY

The first step is to load the geometry of the impeller under research with "LOAD SHEET" command available in MAGMASOFT® "PREPROCESSOR". The geometry is shown in detail drawings in Figure 4.2. In this step also you can add some parts and

components to the geometry such as risers or inlet. Then, they should be saved as one sheet.

In this step, materials of components need to be defined as in the built in material groups in MAGMASOFT®. Defining the materials of every loaded component in the STL formatted drawings is necessary for the simulation in the next steps.

5.5.2 STEP 2: ENMESHMENT

It is recommended to start with rough mesh in order to shorten the time of simulation process, however, with a high speed computer simulation can be faster with fine enmeshment.

The complete loaded geometry should be enmeshed using the "mesh generation" command in MAGMASOFT®. Since impeller geometry has thin walls at the vanes, the enmeshment was completed on the impeller and mold system with fine enmeshment using 3,000,000 units. This step can be completed by inserting the number and clicking on "generate". Figure 5.2 shows "mesh generation" window in enmeshment options in MAGMASOFT®.

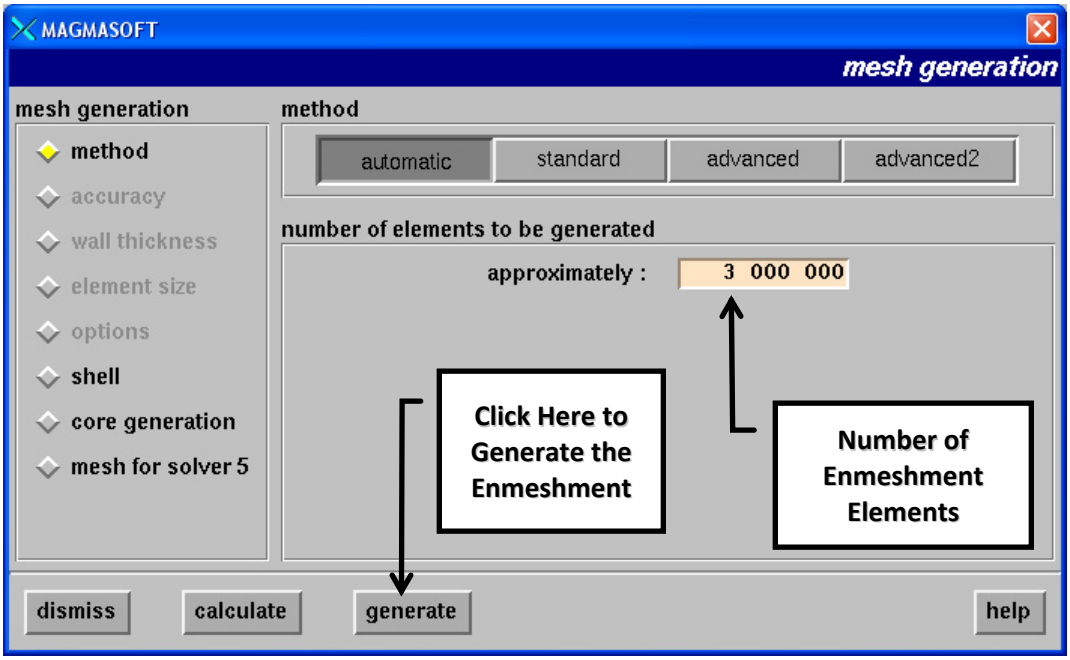

Figure 5.2 Mesh generation in MAGMASOFT®

Fine enmeshment was applied in order to keep at least three elements within the thin walls. This is recommended by the software to provide better results of simulation at thin walls.

5.5.3 STEP 3: SIMULATION

In this part of work, simulation calculations offered by the software are considered. Selecting one or two will reduce the simulation time. However, in this research, filling, solidification, stress were selected for the three simulation iterations as shown in Figure 5.3. Filling calculation should provide the filling behavior by analyzing the velocity, temperature, solidification of the molten Aluminum during the four seconds filling time as calculated from the best practices in chapter 4.

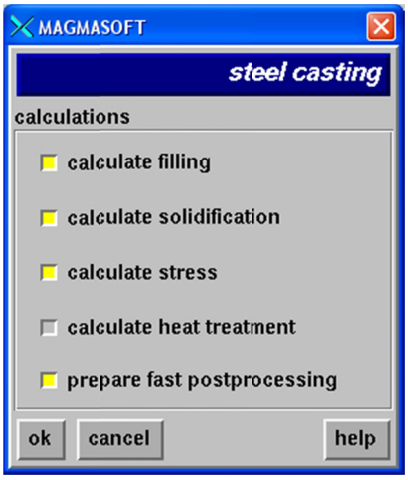

Figure 5.3 Simulation calculations selection from MAGMASOFT®

After selecting the calculations required in the study, simulation process asks for defining the materials for the material groups in the processor. The materials shown in these steps are listed according the defined materials in step 1. Selecting the material is done by clicking on the material listed, select "selecting data" and then assigning the material in MAGMASOFT® data base.

The impeller material under study is available in MAGMASOFT® database and shown as "$AlSi_6Cu_4$", and "GREEN SAND" was selected for the sand mold material as shown in Figure 5.4. MAGMASOFT® also allows creating new entries of project database. By selecting the material, parameters such as initial temperature will be automatically added from the database entries and do not have to be changed.

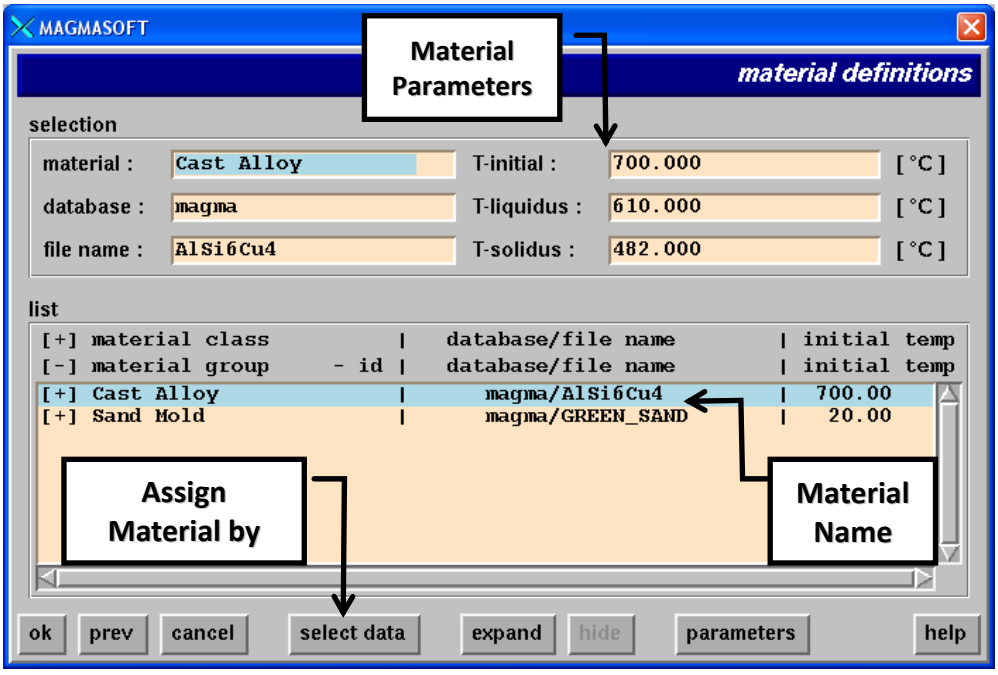

Figure 5.4 Material definition assigning window in MAGMASOFT®

After assigning the material parameters for the mold components, heat transfer definitions are also to be selected and defined. Material properties, convection and conduction designs and solvers used in simulation were based on the embedded database of MAGMASOFT®, which provides properties such as, heat transfer properties coefficients, kinematic viscosity, and density at liquid temperature, sand properties, and core materials properties.

Heat transfer coefficients (HTC) need to be applied between the cast alloy and the sand mold materials. Figure 5.5 shows that C800.0 is selected for the material $AlSi_6Cu_4$which is a constant heat transfer coefficient with a value of 800W/m^{2}K [26]. For other applications, such as steel, C1000.0 HTC with 1000 W/m^{2}K is a reasonable value for HTC between sand mold and steel.

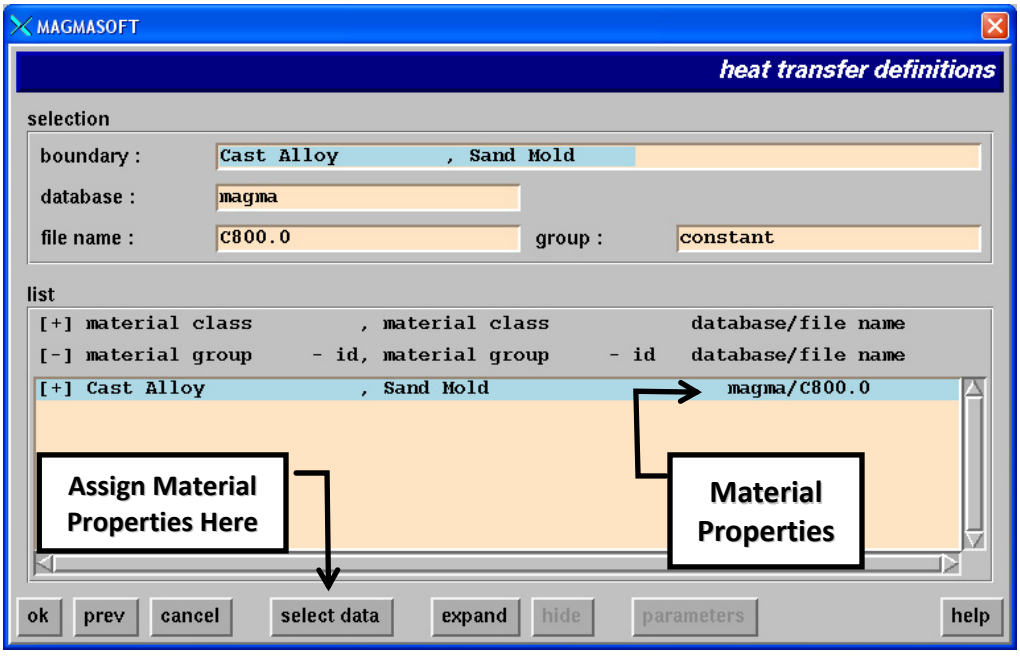

Figure 5.5 Heat transfer definitions by MAGMASOFT®

"Filling definitions" also required before simulation starts. Filling time should be defined in this stage. From geometry, direction z will define the pouring direction which is "-1" in MAGMASOFT®. This is shown in Figure 5.6.

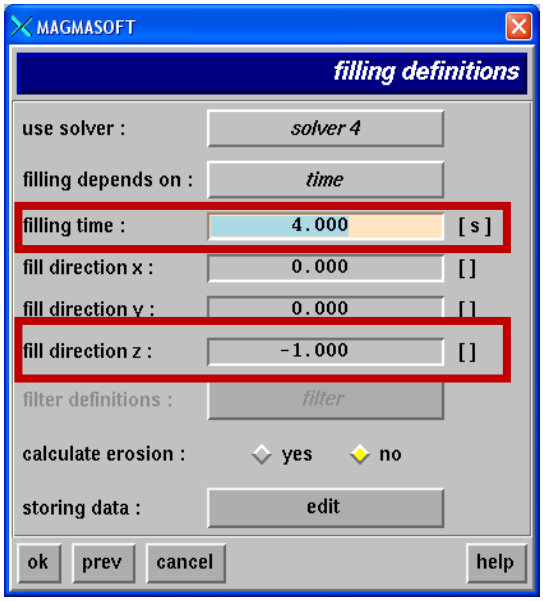

Figure 5.6 Filling definitions showing the filling time and direction

After completing the "filling definitions" window, the simulation can start. A window in MAGMASOFT® shows the initial screen of simulation, Figure 5.7. By clicking on the "start" button, simulation will start.

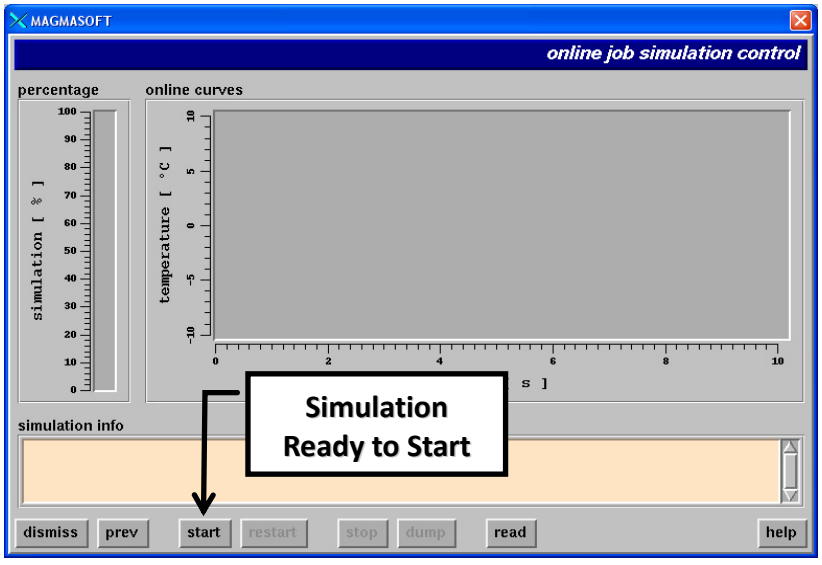

Figure 5.7 Window showing simulation ready to start.

5.5.4 STEP 4: RESULTS

"Postprocessor" command in MAGMASOFT® shows the 3D geometry with casting process analysis such as flow pattern, solidification process, temperature distribution, and velocity and pressure analysis. X-Ray settings can be activated and this allows displaying the internal of the casting and showing any thermal centers such as hot spots. X-Ray is used also to show any porosity in the casting after complete solidification. It is advantageous to choose a criterion function showing the solidification time, and randomly the points or intervals of time of the solidification process.

More results can be displayed and analyzed as shown in section 5.6 for this research.

5.6 CASTING PROCESS SIMULATION IN SEARCH OF NEAR OPTIMAL MOLD DESIGN

In order to observe the effecting parameters on casting quality, fourteen (14) control points were selected for monitoring the results during simulation. The location of these data points is shown in Figure 5.8. These control points help to get the simulation data of temperature, pressure, velocity and stress distribution during the time of filling and solidification. Fourteen data points were marked in the geometric design.

The data of pressure and velocity were collected on at runner near entry point of gate (data point 12), gate (data point 3) in cast body near gate (data point 8) and middle of casting (data point 6). The measurements of the temperature were recorded on the locations at runner (data point 12), gate (data point 3), near gate in casting (data point 8)

and middle of cast body thick section (data point 6), thin sections of cast body (data point 11) and riser (data point 5). The location of these data points is shown in Figure 5.8. The common factors in all simulation designs were the filling time as four seconds as discussed and calculated in section 4.3, two gates feeding system, rectangular runner design with 90° shape instead of circular design, and pouring temperature of the cast metal.

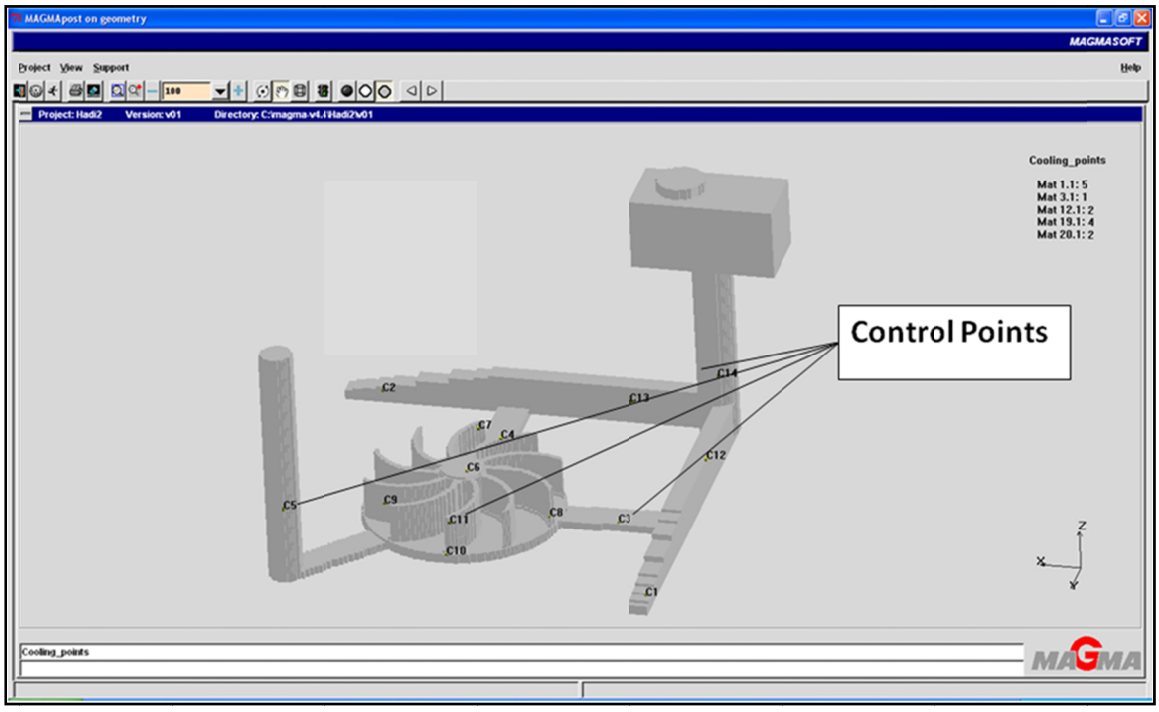

Figure 5.8 Design 1 geometry with 14 points (locations) selected for analysis.

5.6.1 DESIGN 1 SIMULATION:

The initial mold design will be considered as in the design shown in Figure 5.9. The dimensions of this initial design are calculated in section 4.3 and summarized in Table 5.1. This mold design was simulated, improved and then re-simulated in iterative manner in order to reach the near optimal design as explained below.

TABLE 5.1 Gating system dimensions of Design 1.

Design	Runner x-Sectional area mm^2	Runner Length mm	Gate x-Sectional Area mm^2	Gate Length. mm
1	900	350	147	50

The filling velocities, pressure, filling temperature, solidification temperature are the key parameters under consideration.

The effects of these factors on the casting quality were analyzed based on simulation results. The key quality features being observed were porosity, hot spot and stress distribution. On the basis of these quality features analyses, the near optimal design was finalized among various options for the real casting work.

In the first simulation, the parameters which were applied during the simulation process by MAGMASOFT® are listed in Table 5.2. The accuracy in selecting the parameters has a positive influence on the simulation results.

TABLE 5.2 Simulation parameters used in MAGMASOFT® in Simulation 1.

Selected Parameter	Description
MAGMA-Soft Simulation Info	
Module	Casting
Calculations	Filling, Solidification, Stress
Enmeshment	3,000,000 element
Material Definition	
Cast Alloy	$AlSi_6Cu_4$
Melting Point	700.00 C°
Sand Mold	Green Sand
Heat Transfer Definitions	
Cast Alloy to Sand Mold	C800.0
Simulation Options	
Sand Permeability	Yes
Particles/Control Points	Yes
Filling Definitions	
Filling Time	4 seconds

Metal flow pattern help to design the gates location. The target is to have a uniform distribution of pressure in the system and to create a condition of recommended mixed laminar/turbulent flow regime in the casting system to eliminate the air entrapment and minimize the inner mold damage. The metal flow during filling in the casting process for design 1 is simulated and analyzed. Tracer points were added to observe the flow behavior in the cavity of the mold as shown in Figure 5.10.

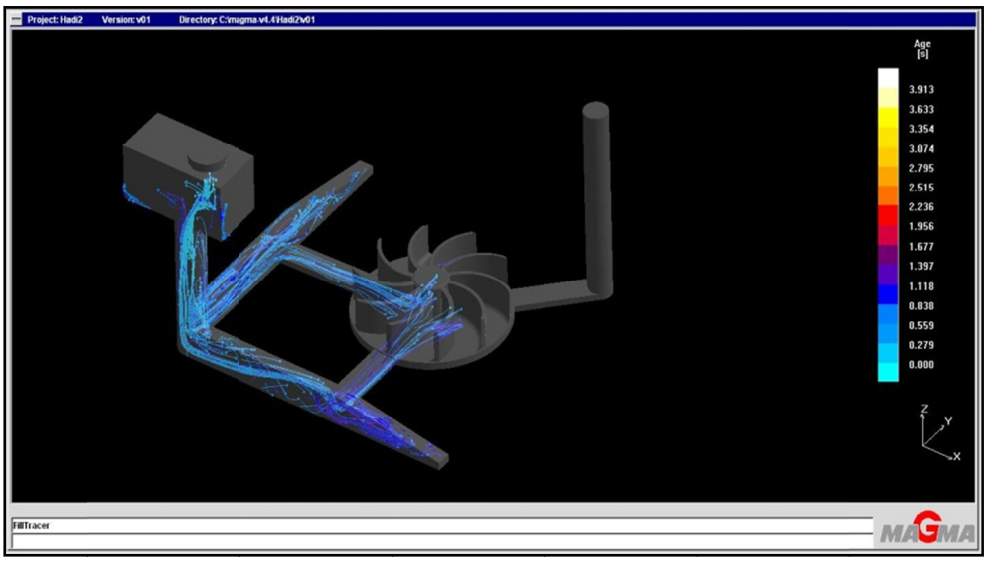

Figure 5.9 Design 1 tracer points showing the flow pattern.

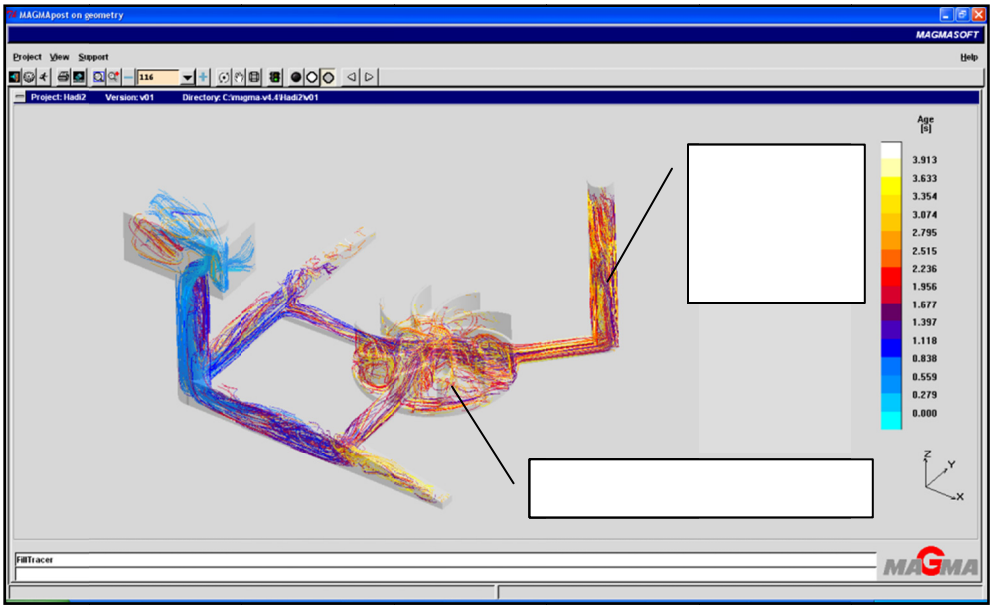

Figure 5.10 Design 1 tracer points flow during filling.

The turbulence was observed in the casting. The possible causes are the filling of riser before complete filling of casting, or the back flow of material from riser is causing

turbulence. Most significant effects due to high turbulence are air entrapment and inside mold damage.

a. Pressure Distribution in Simulation 1:

Pressure distribution during filling was one of the observation and analysis. The filling pressure at time 3.23 seconds was highly raised up to 1,436 mbar in the middle of cast body. Pressure control points located in the runners illustrated in Figure 5.11. Table 5.3 and Figure 5.12 present the pressure readings and curves of pressure along the runner. The pressure curves show a uniform filling up to the 3.27 seconds, where the highest reading of pressure was 1,130 mbar which results in the restricted flow of the metal and the turbulence. This behavior can cause the erosion of mold walls, resulting in poor surface quality and high air entrapment, shown in Figure 5.17.

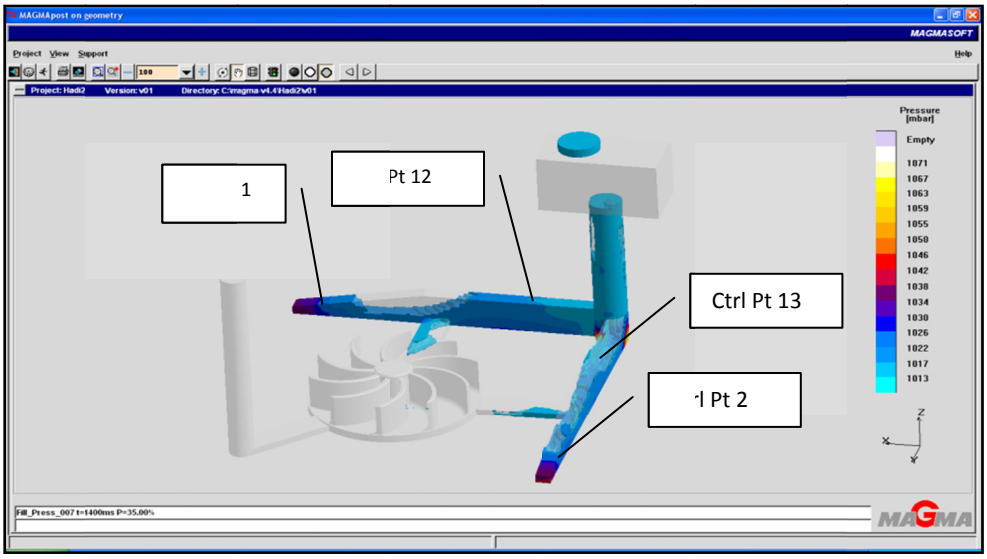

Figure 5.11 Design 1 pressure points and the flow pattern.

TABLE 5.3 Pressure readings in Design 1 simulation in the runners

Time (seconds)	Pressure (mbar)			
	Curve_1	Curve_2	Curve_12	Curve_13
0.26	1013.25	1013.25	1013.25	1013.25
0.51	1013.25	1013.25	1013.25	1013.25
0.77	1013.24	1013.24	1013.24	1013.24
1.02	1013.24	1013.24	1013.24	1013.6
1.24	1018.39	1015.65	1015.36	1017.43
1.53	1051.06	1033.22	1015.75	1019.74
1.75	1061.66	1208.3	1016.19	1114.39
2.00	1081.98	1061.67	1032.53	1046.92
2.26	1044.58	1057.83	1024.34	1045.73
2.51	1050.75	1054.2	1030.06	1042.97
2.76	1051.89	1059.24	1044.93	1054.64
3.00	1051.88	1053.48	1043.38	1047.46
3.27	1245.09	1253.9	1188.19	1190.07
3.49	1073.14	1071.7	1064.97	1066.61
3.75	1087.29	1073.29	1067.94	1064.44
4.00	0	0	0	0

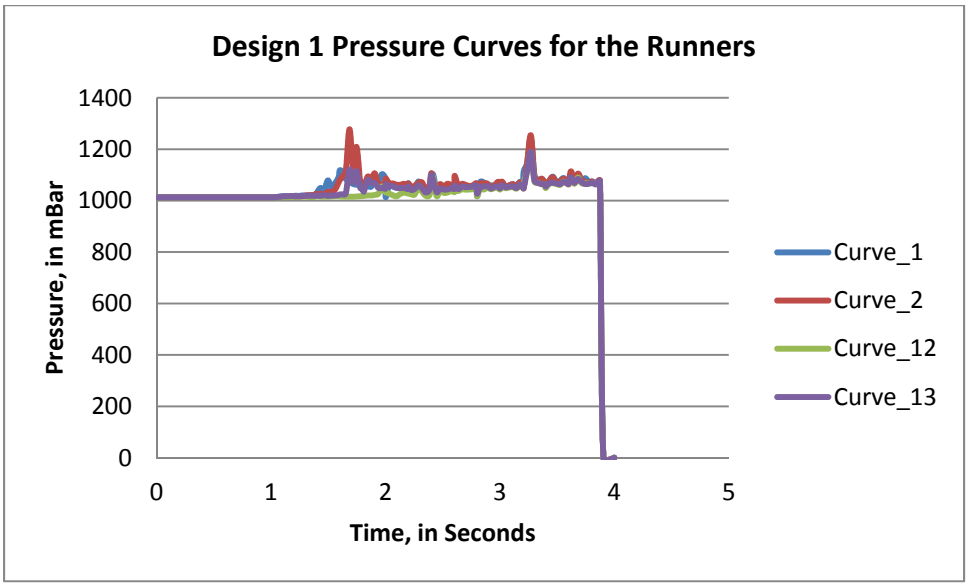

Figure 5.12 Design 1 pressure curves in the runners.

The flow pattern at the gates which represents points 4 and 5 in the pressure points location on the impeller is shown by MAGMASOFT® in Figure 5.13. The pressure points were plotted in a curve and showed uniform pressure flow. The curve peaks justify that the filling and riser filling started and back pressure occurred. The plot is shown in figure 5.14.

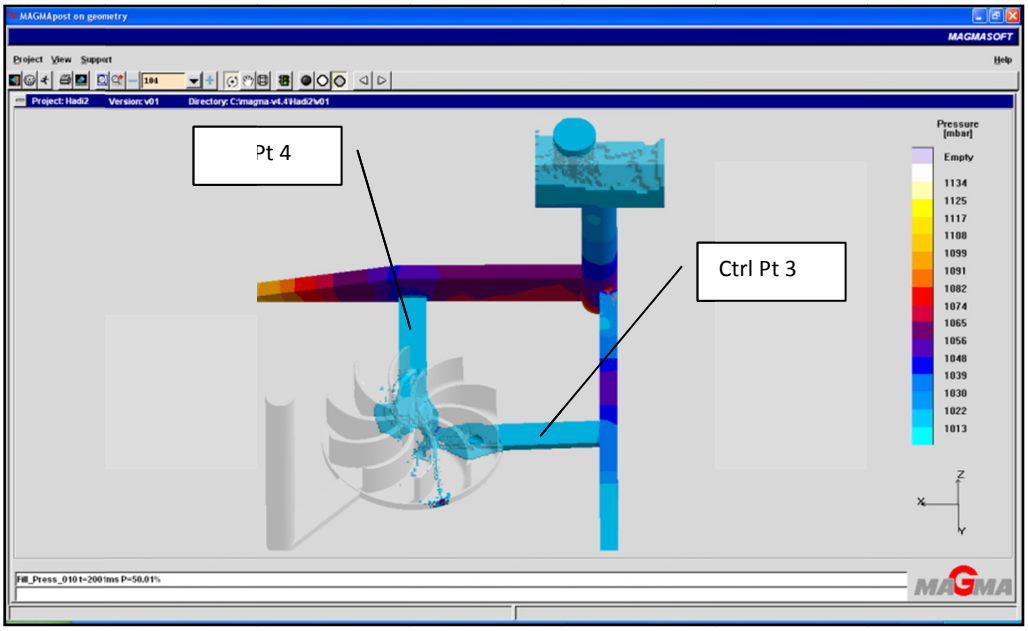

Figure 5.13 Design 1 pressure points with the flow pattern at the gates.

Table 5.4 Pressure readings in Design 1 simulation at the gates

Time (seconds)	Pressure (mbar)	
	Curve_3	Curve_4
0.26	1013.25	1013.25
0.51	1013.25	1013.25
0.77	1013.24	1013.24
1.02	1013.24	1013.24
1.24	1013.25	1013.25
1.53	1013.75	1013.74
1.75	1019.37	1233.16
2.00	1040.97	1015.97
2.26	1015.9	1014.36
2.51	1017.72	1020.66
2.76	1016.49	1015.58
3.00	1030.36	1021.74
3.27	1323.16	1336.73
3.52	1064.74	1068.87
3.78	1070.95	1069.33
4.00	0	0

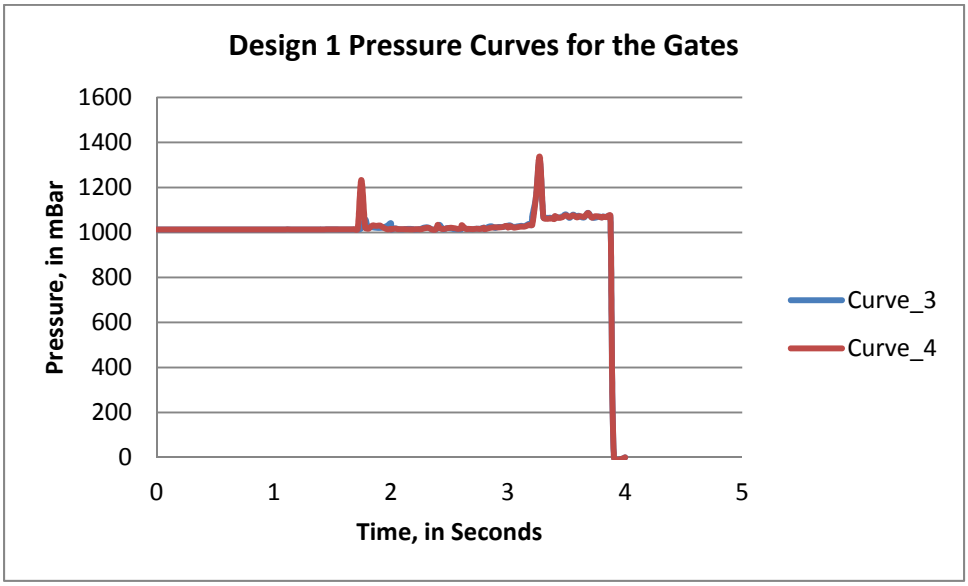

Figure 5.14 Design 1 pressure curves inthe gates.

Similarly, Figure 5.15 the pressure curves in the casting represented by points 6, 7, 8, 9, 10 and 11, show uniform pressure filling in the casting, and it shows two pressure peaks which are back pressure when riser started filling.

TABLE 5.5 Pressure readings in Design 1 simulation in the castings

Time (seconds)	Pressure (mbar)					
	Curve_6	Curve_7	Curve_8	Curve_9	Curve_10	Curve_11
0.26	1013.25	1013.25	1013.25	1013.25	1013.25	1013.25
0.51	1013.25	1013.25	1013.25	1013.25	1013.25	1013.25
0.77	1013.24	1013.25	1013.24	1013.24	1013.24	1013.24
1.02	1013.24	1013.24	1013.24	1013.24	1013.24	1013.24
1.24	1013.25	1013.25	1013.25	1013.25	1013.25	1013.25
1.50	1013.25	1013.25	1013.25	1013.25	1013.25	1013.25
1.75	1013.24	1013.24	1013.24	1013.24	1013.24	1013.24
2.00	1013.25	1013.25	1015.42	1013.25	1013.25	1013.25
2.26	1013.24	1013.24	1013.76	1013.24	1013.24	1013.24
2.51	1013.65	1013.25	1015.21	1014.22	1019.81	1015.25
2.76	1013.34	1013.25	1019.1	1016.76	1020.94	1014.57
3.00	1016.01	1013.25	1030.44	1024.93	1024.01	1015.32
3.27	1436.02	1013.25	1420.58	1459.93	1434.65	1429.55
3.49	1079.66	1013.25	1087.27	1088.05	1088.35	1080.59
3.75	1058.87	1013.25	1068.28	1070.2	1068.44	1061.91
4.00	0	0	0	0	0	0

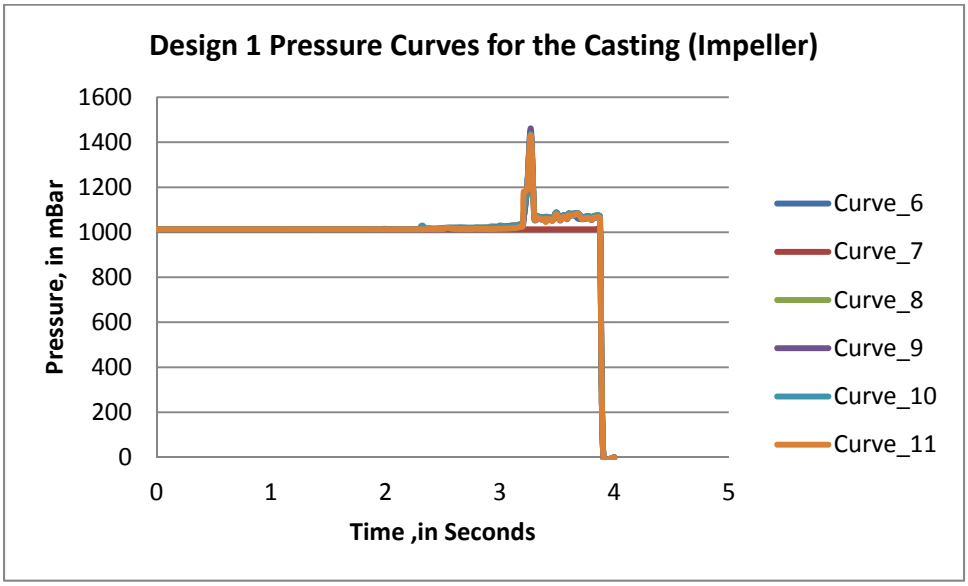

Figure 5.15 Design 1 pressure curves in the casting.

The filling pressure at time 3.23 seconds was highly raised up to 1,436 mbar in the middle of cast body as compare to pressure in runner was 1,130 mbar and in gate it was 1,323 mbar, which results in the restricted flow of the metal and the turbulence, as shown in velocity graph Figure 5.16. This behavior can cause the erosion of mold walls, resulting in poor surface quality and high air entrapment, shown in Figure 5.17.

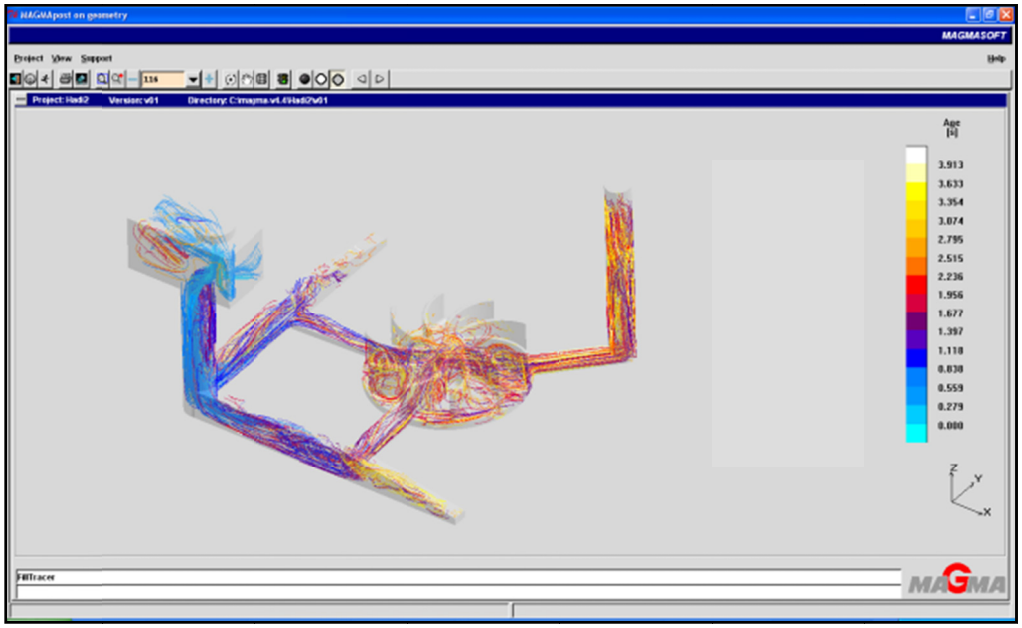

Figure 5.16 Design 1 flow turbulence in velocity by MAGMASOFT®

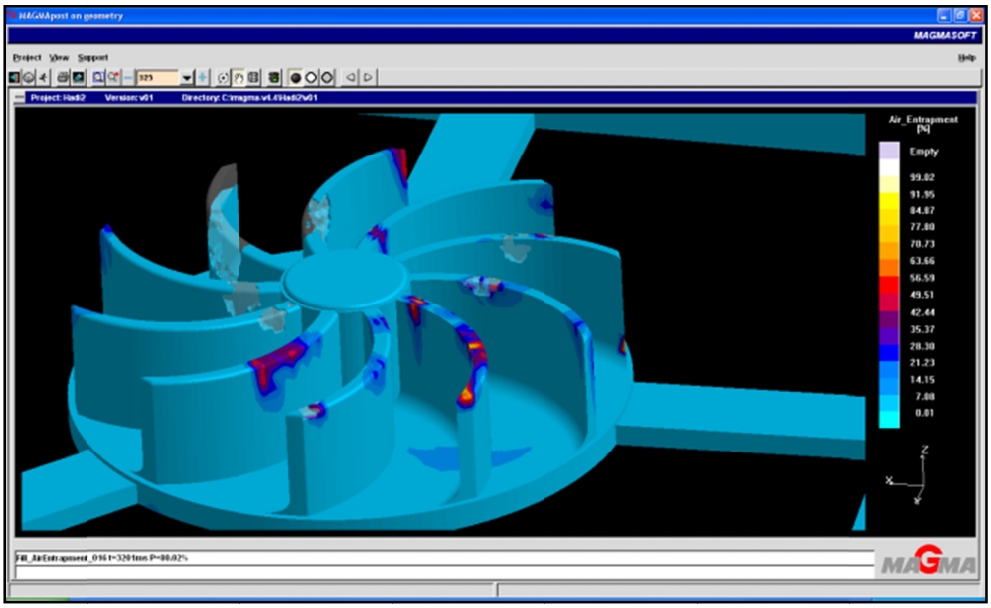

Figure 5.17 Design 1 air entrapments (X-Ray activated).

b. Velocity Distribution in Simulation 1:

The velocity control points were detected on the same locations. The filling velocity in the runners were detected and analyzed. Figure 5.18 shows the locations and the flow pattern. The velocity points values were plotted in Figure 5.19. The curves show non-uniform filling velocity at different points. However, curves 1 and 2 showed less fluctuation of velocity which justify that points 1 and 2 are located at the runner ends that stop the flow.

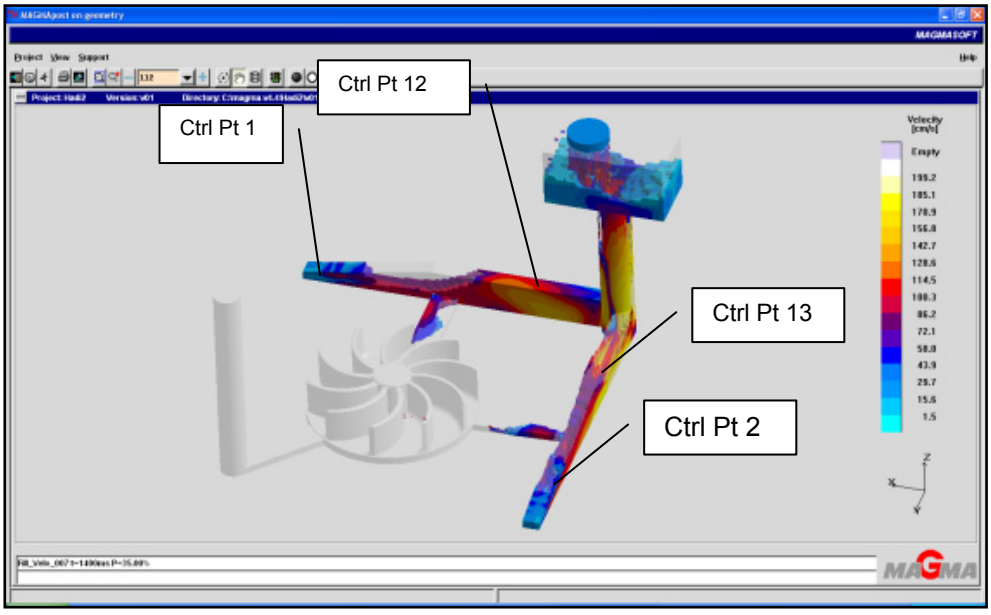

Figure 5.18 Design 1 velocity flow pattern by MAGMASOFT®

TABLE 5.6Velocity readings in Design 1 simulation at the runners

Time (seconds)	Velocity (cm/s)			
	Curve_1	Curve_2	Curve_12	Curve_13
0.26	0	0	0	0
0.51	0	0	0	0
0.77	0	0	0	0
1.00	0	0	0	45.3469
1.27	0	0	60.5801	63.421
1.52	52.2288	0	41.5726	50.7464
1.77	27.5582	15.2823	25.7566	19.8617
2.00	27.06	7.99695	9.49582	8.6565
2.24	22.869	7.11718	7.37974	15.4629
2.52	19.2205	8.62589	5.43566	25.9856
2.78	10.5539	9.77062	11.1977	49.0904
3.00	7.46542	16.2012	19.38	41.1714
3.28	11.2896	17.8189	5.35634	34.0024
3.50	9.71283	14.7642	14.3655	14.5565
3.75	4.70854	8.66634	16.9728	1.54629
4.00	0	0	0	0

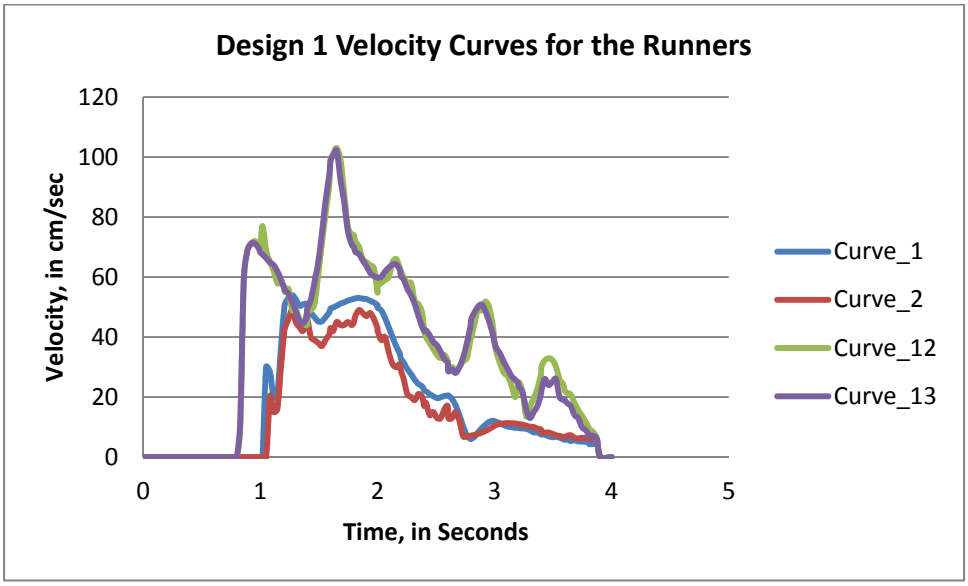

Figure 5.19 Design 1 velocity curves in the runners.

By the same method, velocity curves at the gates were analyzed. Figure 5.20 shows the velocity points at the gates. The curves of the velocity points as plotted in Figure 5.21 shows the non-uniform velocity of the molten Aluminum passing the gates to the casting during filling.

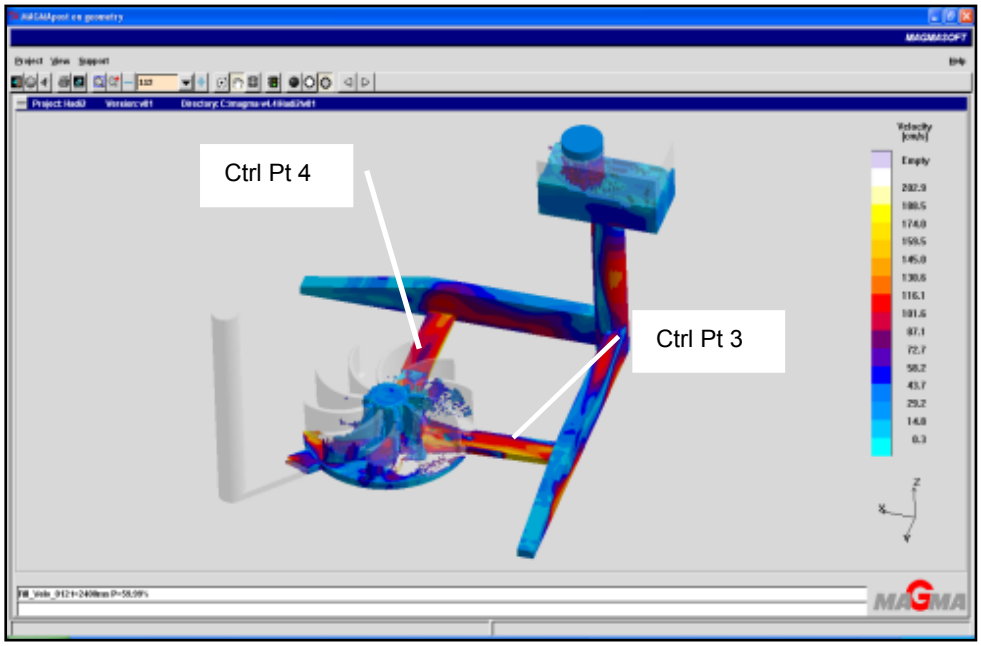

Figure 5.20 Design 1 velocity flow at the gates.

TABLE 5.7 Velocity readings in Design 1 simulation at the gates

Time (seconds)	Velocity (cm/s)	
	Curve_3	Curve_4
0.26	0	0
0.51	0	0
0.77	0	0
1.02	0	0
1.24	0	0
1.50	43.2027	46.7945
1.75	80.1319	112.212
2.00	158.683	187.18
2.26	165.037	189.129
2.51	157.376	166.832
2.76	163.205	154.137
3.00	152.134	143.771
3.27	80.6827	92.4391
3.49	51.3163	72.2148
3.78	34.3532	40.4321
4.00	0	0

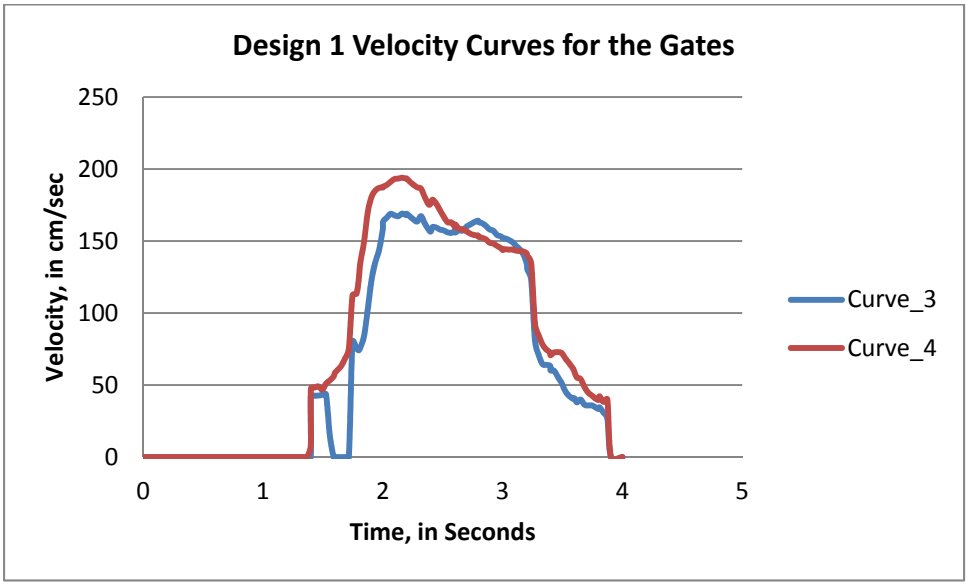

Figure 5.21 Design 1 velocity curves at the gates.

The velocity points in the casting were recorded by the software as shown in Figure 5.22, summarized in Table 5.8, and plotted in Figure 5.23.The filling velocity was highly raised up in the middle of cast body as compare to velocity in runners and in gates which results in filling the riser due to high flow of the metal and causes turbulence, as shown in velocity graph Figure 5.23. Curve 8 shows the highest value because control point 8 is located on the casting and at the gate opening to the casting. This behavior can cause the erosion of mold walls, resulting in poor surface quality and high air entrapment, shown in Figure 5.17.

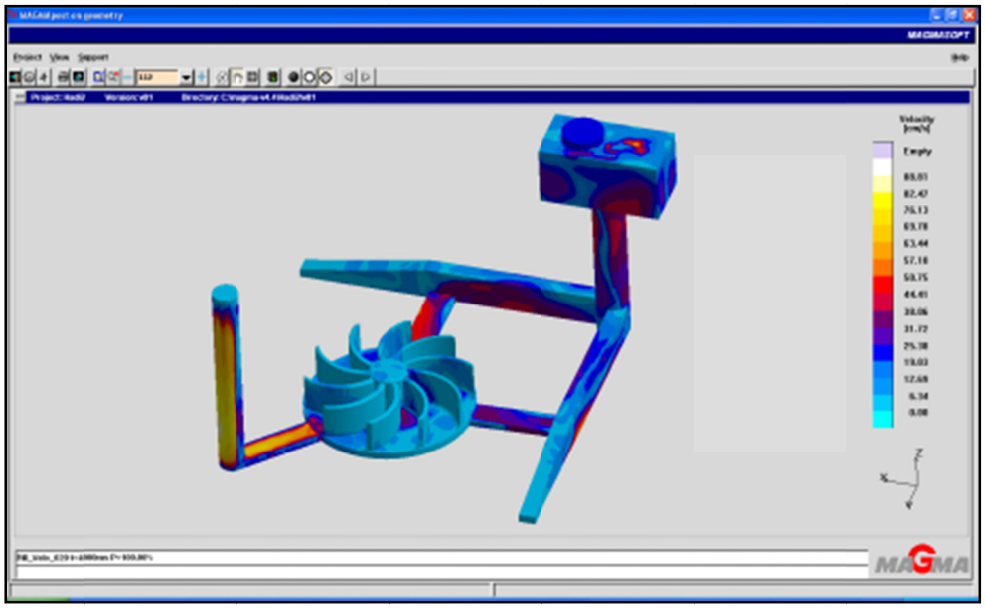

Figure 5.22 Design 1 velocity flow in the casting.

TABLE 5.8 Design 1 velocity reading simulation in the casting

Time (seconds)	Velocity (cm/s)					
	Curve_6	Curve_7	Curve_8	Curve_9	Curve_10	Curve_11
0.26	0	0	0	0	0	0
0.51	0	0	0	0	0	0
0.77	0	0	0	0	0	0
1.00	0	0	0	0	0	0
1.24	0	0	0	0	0	0
1.50	0	0	0	0	0	0
1.75	0	0	0	0	0	0
2.00	0	0	102.76	0	0	0
2.26	0	0	144.828	0	0	0
2.51	7.71743	0	134.706	0	55.6117	34.1367
2.76	13.6236	12.5478	136.592	63.0508	36.6481	1.07486
3.00	24.1099	20.6733	136.89	21.8007	19.2555	5.39205
3.27	14.2933	19.4667	103.16	20.0065	10.454	3.51562
3.49	13.7348	13.0689	39.6339	22.443	15.8281	0.845462
3.75	10.7222	8.9332	35.6099	20.9181	9.3347	0.416543
4.00	0	0	0	0	0	0

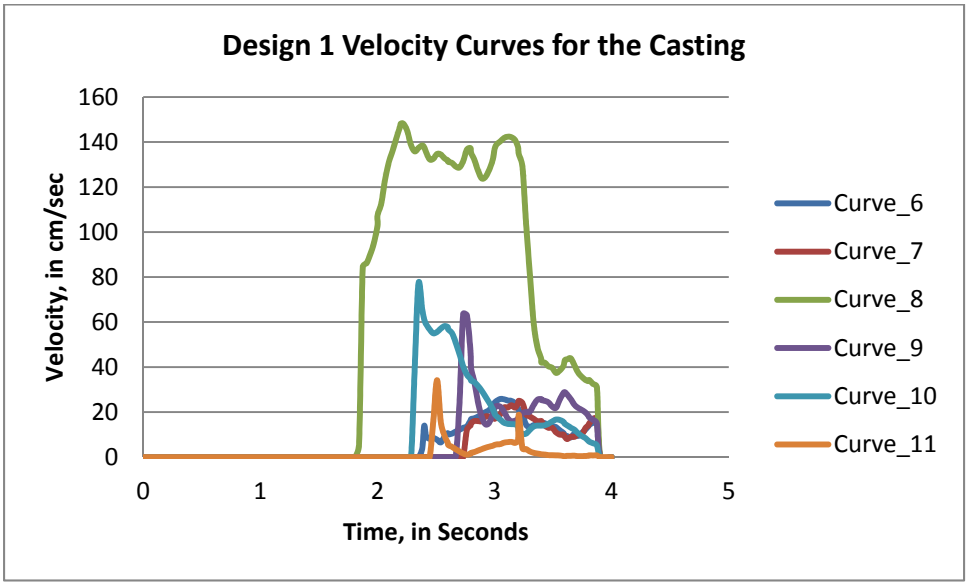

Figure 5.23 Design 1 velocity curves in the casting.

c. Temperature Distribution in Simulation 1:

Considering the cooling process and solidification, it was observed that at 8.00 seconds, solidification started as appeared in the Figure 5.24. At 275 seconds, solidification was completed as shown in Figure 5.25.

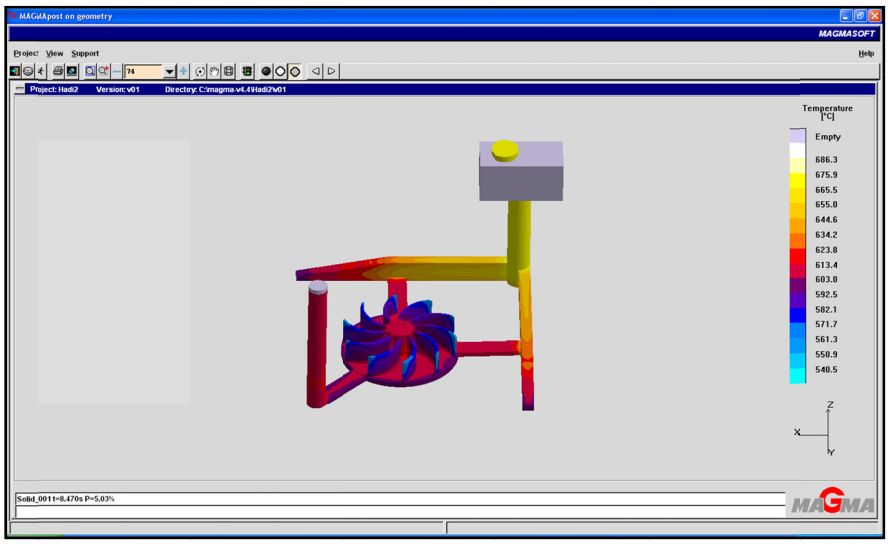

Figure 5.24 Design 1 complete filling and solidification starts.

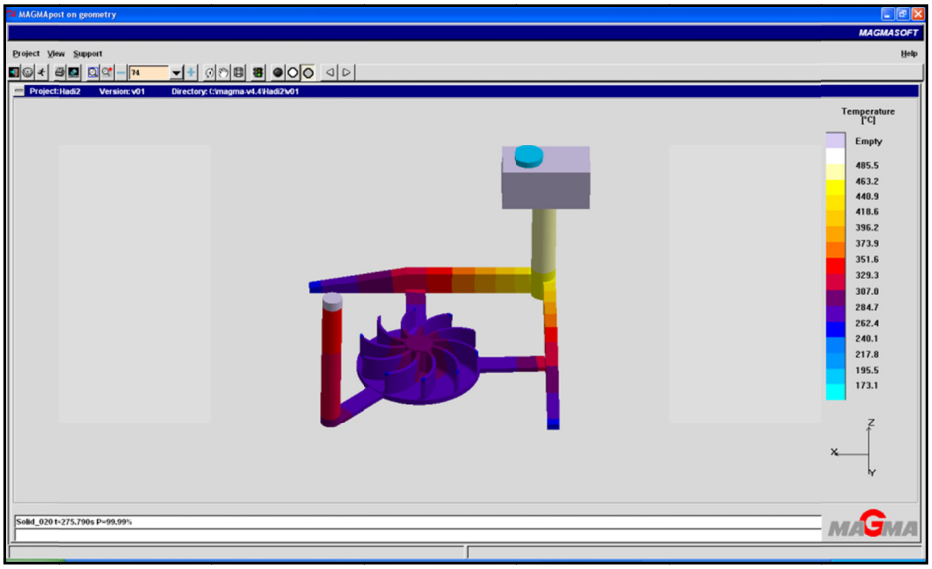

Figure 5.25 Design 1 complete solidification in the casting after 275 seconds.

The cooling rate was observed by MAGMASOFT® control points in the runners, and shows slow and uniform solidification process. Figure 5.26 shows the curves of temperature which indicate the solidification rates for the points located in the runners (points 1, 2, 12 and13). It shows that a uniform solidification rate for both runners, however, from the plot, simulation results shows faster solidification rate for point 1 and 2 more that points 12 and 13 because they are located at the runner end.

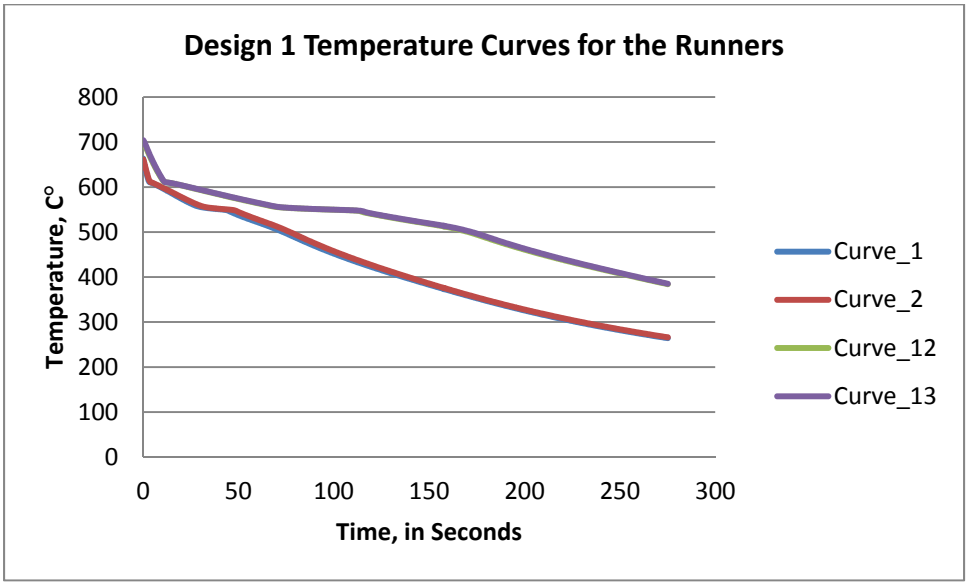

Figure 5.26 Design 1 temperature curves (solidification rate) in the runners.

By the same mean, the solidification rate was detected by the software control points at the gates. It shows slow and identical solidification in both gates as shown in Figure 5.27.

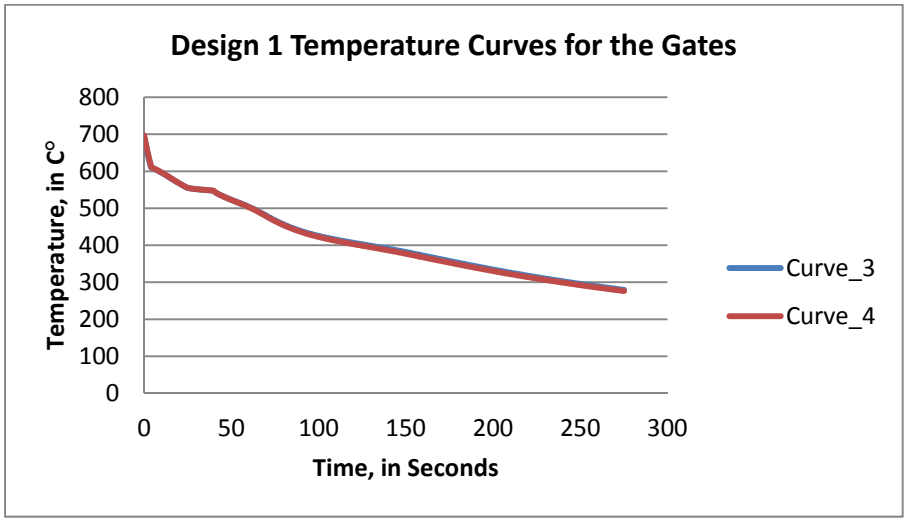

Figure 5.27 Design 1 temperature curves (solidification rate) at the gates.

The solidification process curves at different locations in the casting predicted by the MAGMASOFT® control points are shown in Figure 5.28. The curves show slower solidification in the center location such as the riser, and lower temperature gradient in the thin walls such as the body fins of the impeller.

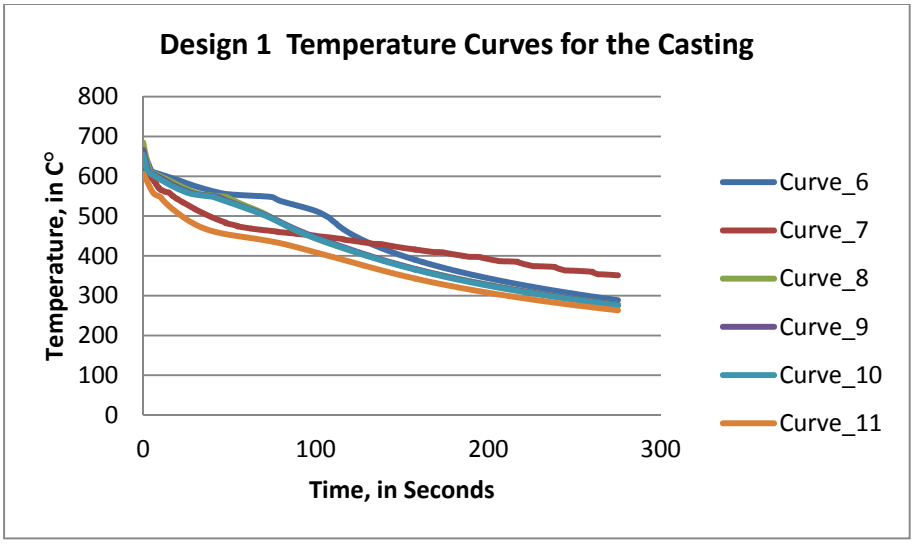

Figure 5.28 Design 1 Temperature curves in the casting (Impeller)

The solidification temperature pattern affects the shrinkage, consequently porosity, and stress distribution. The riser was attached through gate to the casting, consequently cooling rate was higher in gates, and material feeding during solidification process was restricted. This created the porosity in the middle of the cast body as shown in Figure 5.29.

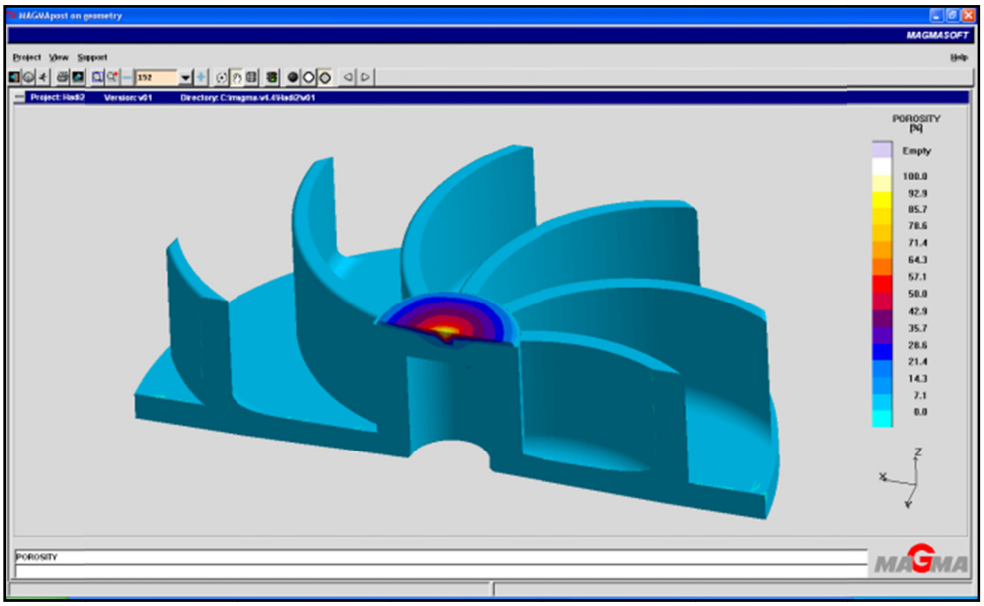

Figure 5.29 Design 1 porosity concentrations.

It is also predicted that due to the thick section in the middle of the cast body the hot spot is generated as shown in Figure 5.30 and Figure 5.31.

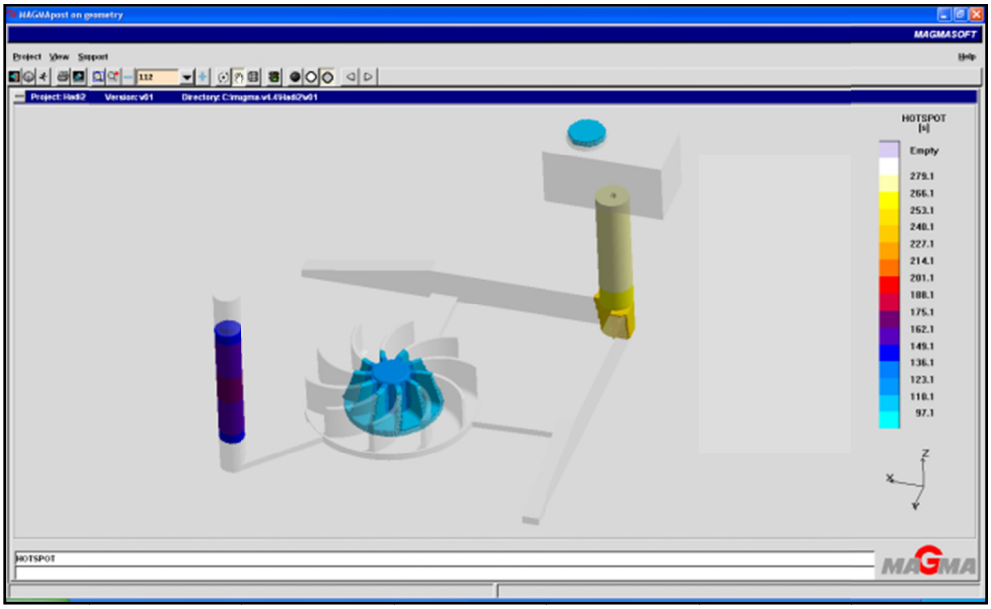

Figure 5.30 Design 1 Hot spot at the center of the casting Impeller.

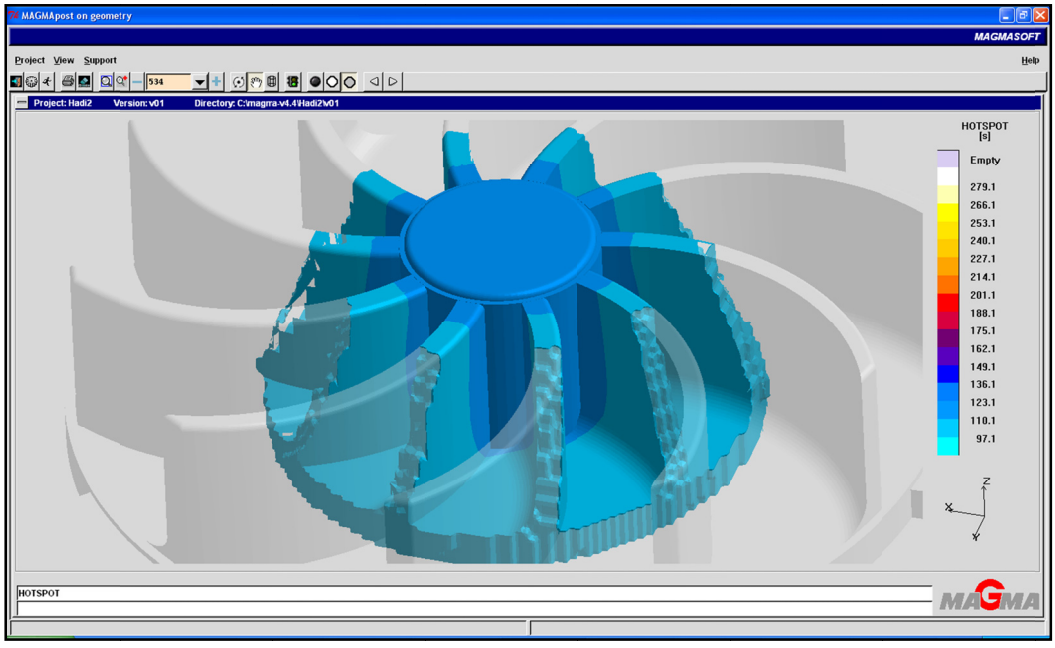

Figure 5.31 Design 1 Casting-impeller hot spots at the center – close view.

Also, as previously discussed, the filling pressure at time 3.23 seconds was highly raised up to 1,436 mbar in the middle of cast body, while the pressure in runner and gate up to 1,130 mbar and 1,323 mbar respectively. This resulted in the restricted flow of the metal and created turbulence. This behavior can cause an erosion of the mold walls subsequently, resulting in poor surface quality and high air entrapment as shown in Figure 5.32.

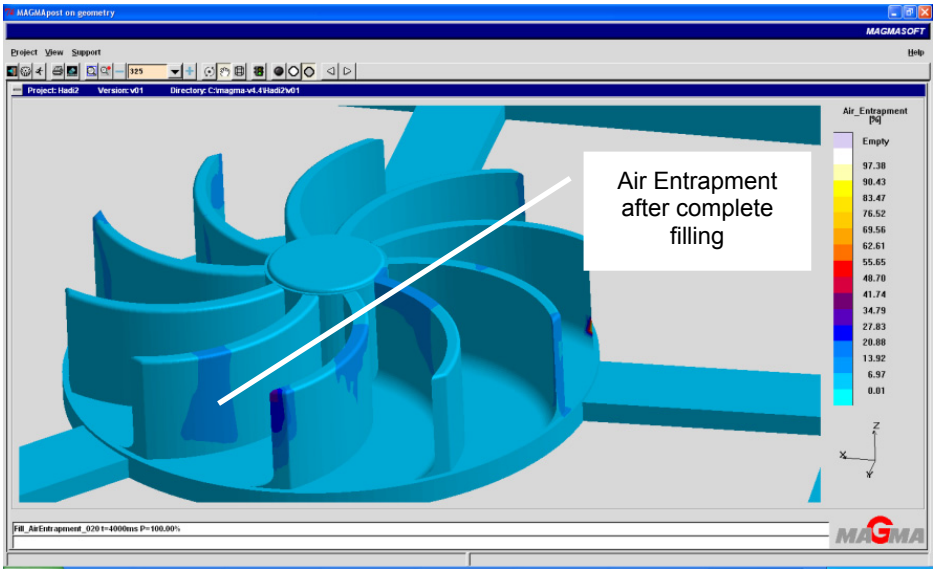

Figure 5.32 Design 1 air entrapment after complete filling (X-ray activated).

For the casting impeller, cooling rate during solidification was observed and analyzed by the control points added in MAGMASOFT®. The overall results with activation of X-ray feature by the software, the porosity in the middle of the casting was observed as shown in Figure 5.33. The reason could be predicted that the cooling rate was higher in gates and the feeder is attached through gate with casting so that material feeding during solidification process was restricted.

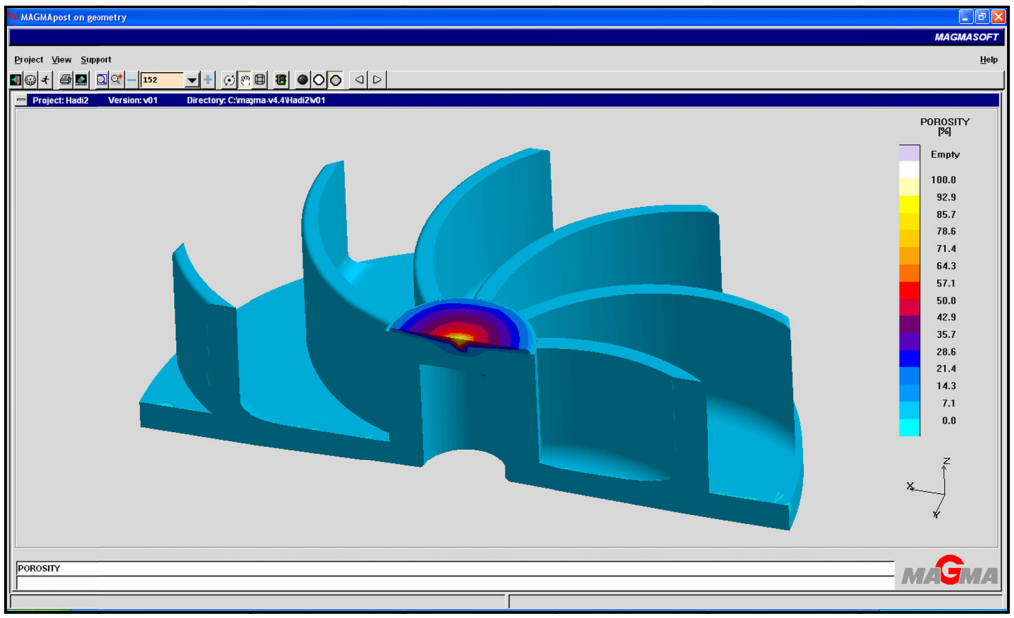

Figure 5.33 Design 1 porosity in the center of the casting.

The porosity depth at the location of the casting was also discovered by the feature of the MAGMASOFT®. Figure 5.34shows a magnified locally the porosity in the casting, it was recorded that six millimeters depth of porosity concentration in the casting center. Figure 5.35 also demonstrate the porosity zone in the center of the casting impeller from the top.

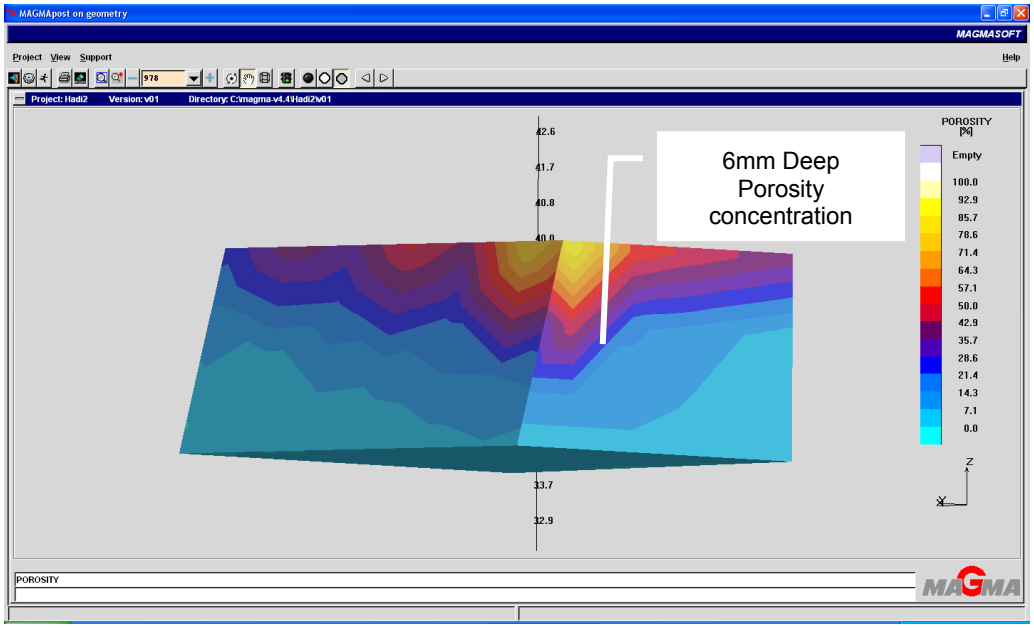

Figure 5.34 Design 1 porosity depth in the middle of the casting (X-ray activated).

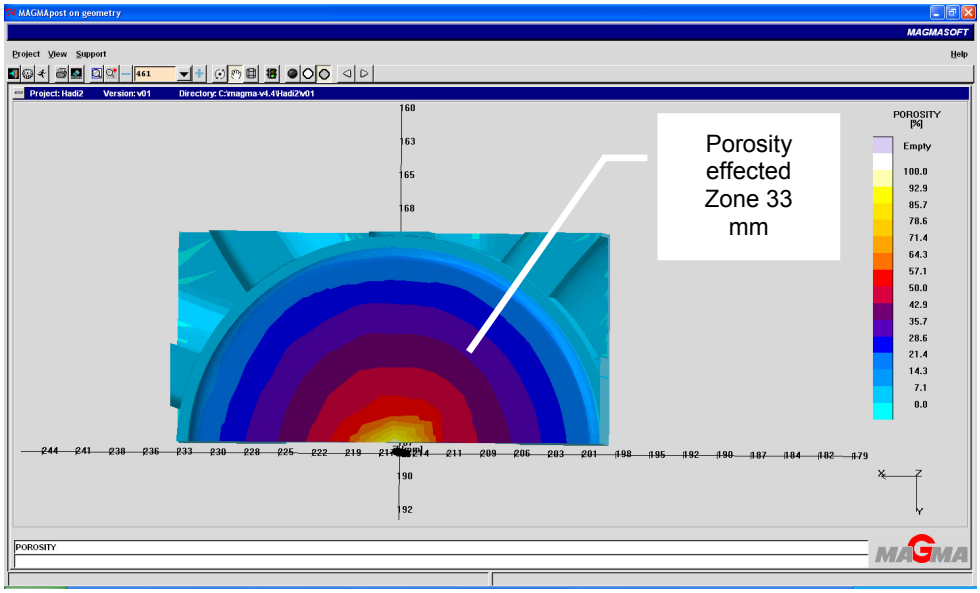

Figure 5.35 Design 1 porosity zone at the top of the core.

5.6.2 DESIGN 2 SIMULATION:

Based upon the observations on design 1 a modified design 2 was proposed. The riser location was changed and located at the top of porosity concentration area. The cast body was inverted as compare to design 1 in such a way that thin area is in drag. The gates cross-sectional areas were increased from 147 mm^2 to 220 mm^2 in order to reduce the solidification. This second mold design is shown in Figure 5.36 with control points. The gating design dimensions are mentioned in Table 5.9, and the parameters that were applied to the software in the simulation process are listed in Table 5.10.

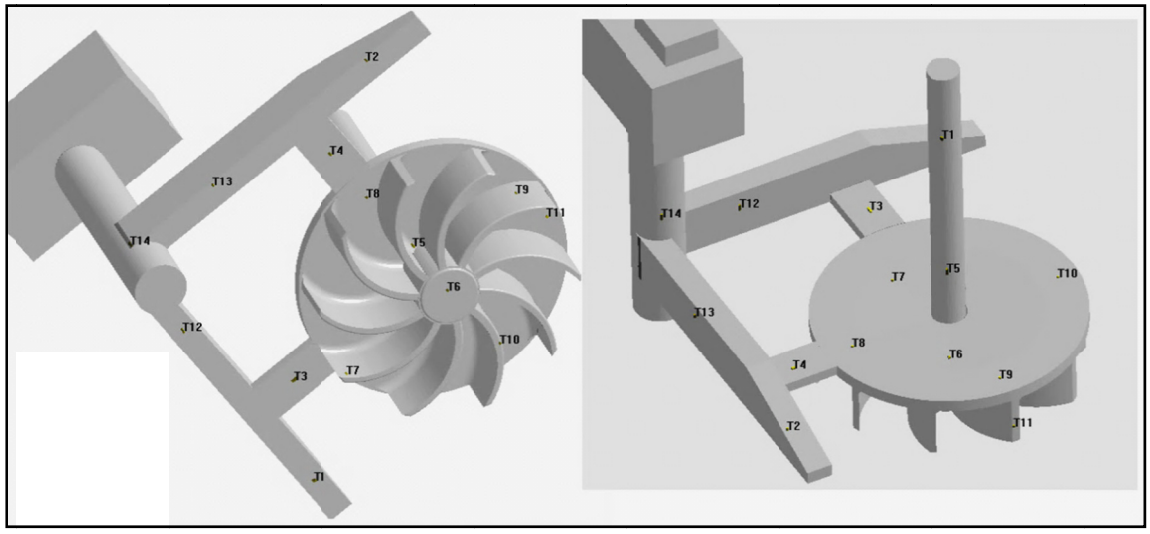

(a) (b)

Figure 5.36 Design 2 control points locations, (a) bottom view (b) oblique view.

TABLE 5.9 Gating system dimensions of Design 2

Design	Runner x-Sectional area mm^2	Runner Length mm	Gate x-Sectional Area mm^2	Gate Length. mm
2	900	300	220	50

TABLE 5.10 Simulation parameters used in MAGMASOFT® in Simulation 2.

Selected Parameter	Description
MAGMA-Soft Simulation Info	
Module	Casting
Calculations	Filling, Solidification, Stress
Enmeshment	3,000,000 element
Material Definition	
Cast Alloy	$AlSi_6Cu_4$
Melting Point	720.00 C°
Sand Mold	Green Sand
Heat Transfer Definitions	
Cast Alloy to Sand Mold	C800.0
Simulation Options	
Sand Permeability	Yes
Particles/Control Points	Yes
Filling Definitions	
Filling Time	4 seconds

Metal flow pattern help to design the gates location. The mixed laminar-turbulent flow helps to avoid the air entrapment and inner mold damage. The turbulence of the flow in design 2 during filling was observed by the tracer points in MAGMASOFT®, as shown in Figure 5.37.

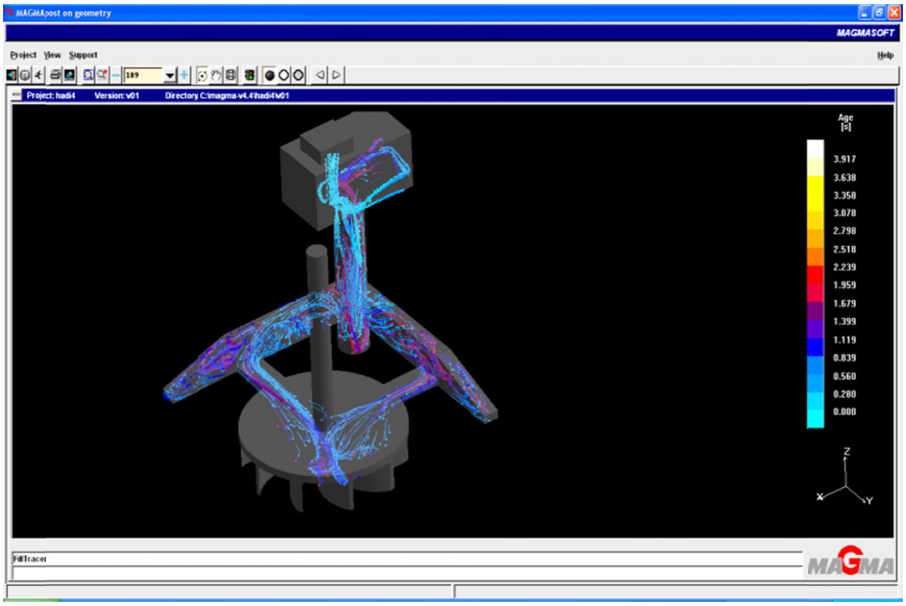

Figure 5.37 Design 2 flow pattern during filling.

In Figure 5.38, it shows that the riser filling started after complete filling of casting.

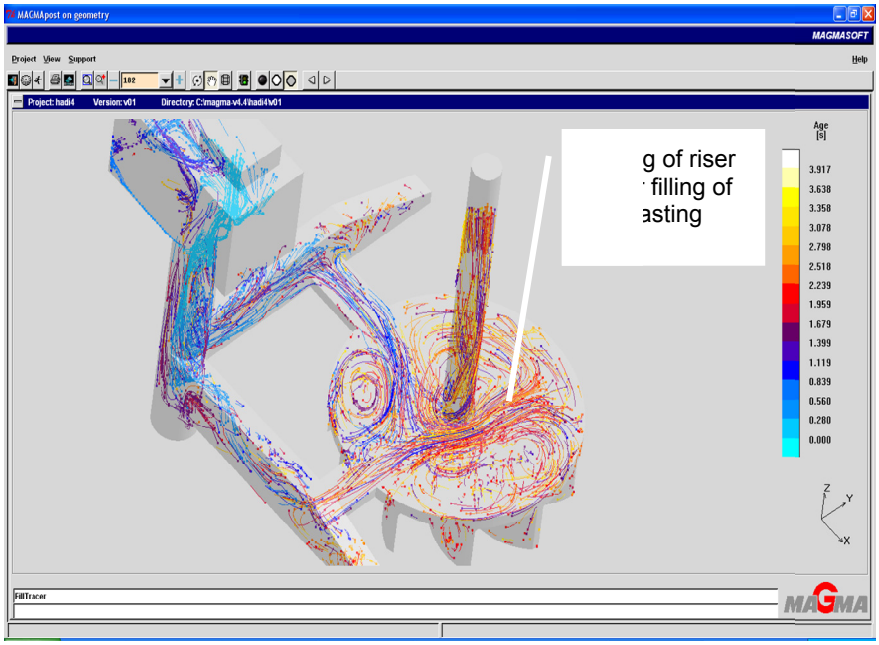

Figure 5.38 Design 2 metal flow pattern.

The control points for pressure, velocity and temperature are simulated and analyzed for runners, gates and in the casting.

a. Pressure Distribution in Simulation 2:

The measurement of filling pressure pattern in the gatings and casting predicted by the control points in simulation 2 are analyzed for the runners, gates and the castin impeller. Controls points for the the runners are 1, 2, 12 and 13. The points for the gates are 3 and 4. For the casting impeller, the control points are 5, 6, 7, 8, 9, 10, and 11.

The filling pressure measurement is collected by the software for the runners are listed in Table 5.11. The curves which represent the pressure pattern during filling in the runners are shown in Figure 5.39.The pressure curves show a peak at 3.2 seconds which could be explained the back pressure turns after filling the casting.

Moreover, the filling pressure measurement is collected by the software for the two gates are plotted in Figure 4.40. The filling pressure at time 3.52 seconds was raised up to 1,349 mbar in the middle of cast body, whereas the pressure in runner and gate were 1,180 mbar and 1,272 mbar respectively. Figure 5.41 shows the filling pattern curves of the pressure in the casting. 92 percentage of casting was filled and high pressure started to build in the feeder which results in the sound filling of the cast body and no air entrapment.

TABLE 5.11 Pressure readings in simulation 2 in the runners.

Time (Seconds)	Pressure (mbar)			
	Curve_1	Curve_2	Curve_12	Curve_13
0.23	1013.25	1013.25	1013.25	1013.25
0.51	1013.25	1013.25	1013.25	1013.25
0.77	1013.25	1013.25	1013.25	1013.25
1.00	1013.24	1013.24	1013.24	1013.79
1.24	1013.25	1013.25	1017.01	1025.74
1.52	1023.15	1024.77	1024.4	1026.95
1.74	1046.83	1045.54	1033.07	1032.17
2.00	1033.06	1023.7	1029.05	1033.2
2.24	1034.06	1039.54	1041.11	1046.72
2.49	1036.34	1033.03	1030.67	1029.08
2.74	1034.99	1039.65	1033.28	1037.59
3.00	1043.27	1047.65	1043.27	1038.96
3.25	1063.71	1065.26	1057.06	1060.44
3.50	1059.12	1063.88	1056.28	1059.63
3.75	1075.93	1067.13	1060.98	1061.11
4.00	0	0	0	0

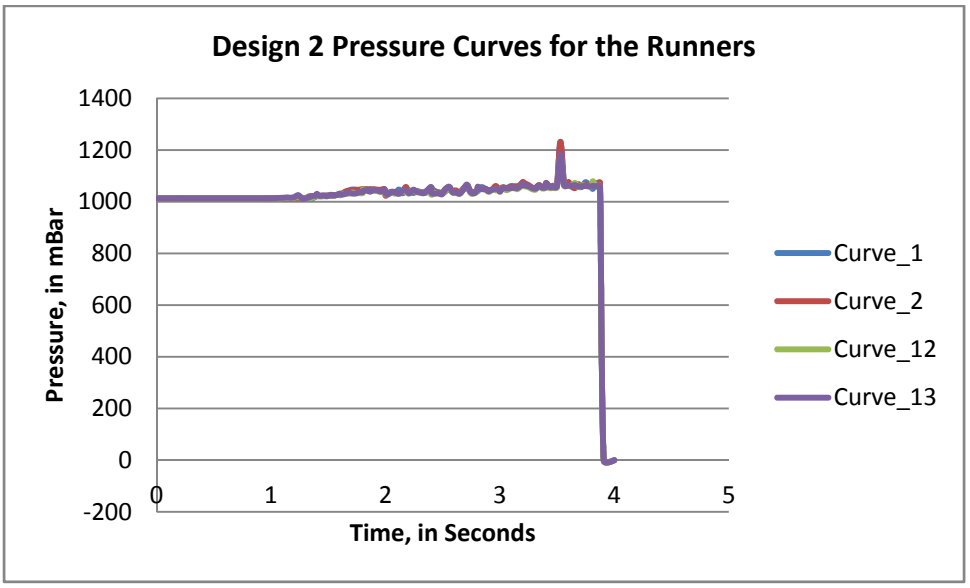

Figure 5.39 Design 2 pressure curves in the runners .

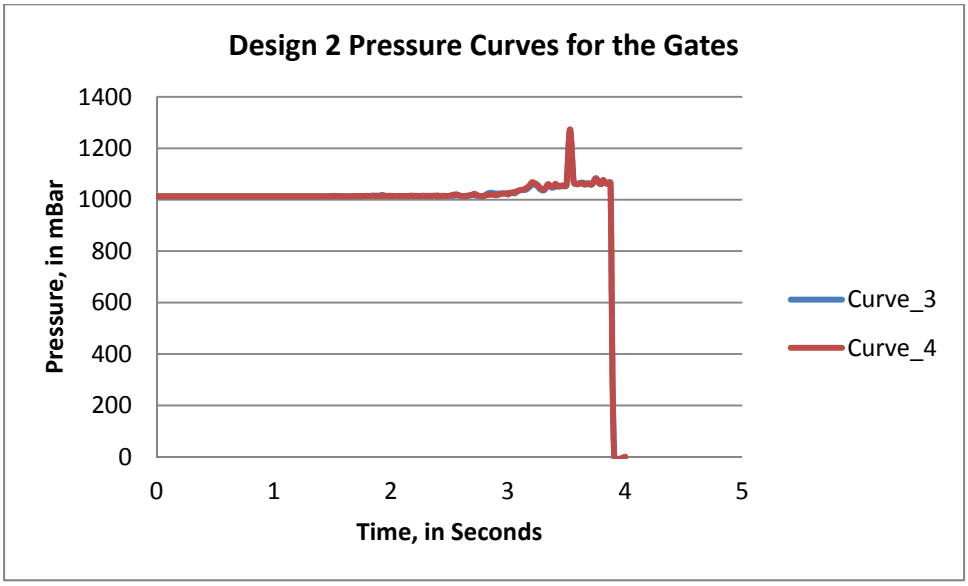

Figure 5.40 Design 2 pressure curves in the gates.

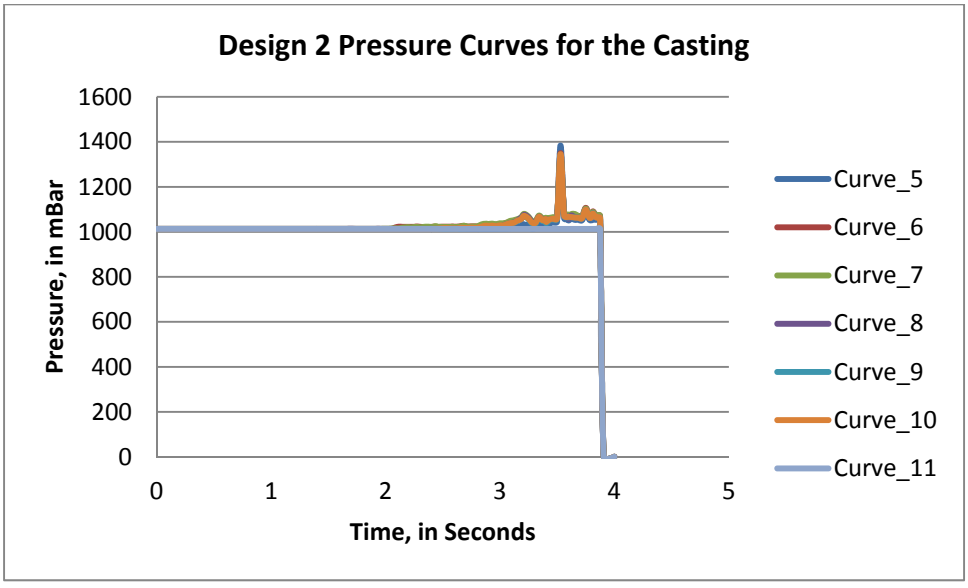

Figure 5.41 Design 2 pressure curves in the casting (Impeller).

b. Velocity Distribution in Simulation 2:

The velocity pattern was predicted by the control points located in the runners, gates and the casting. The velocity graphs predicted the turbulence which is the behavior that can affect the mold wall erosion and consequently will produce poor surface quality. The flow can be observed by the tracer points of the simulation software shown in Figure 5.42.

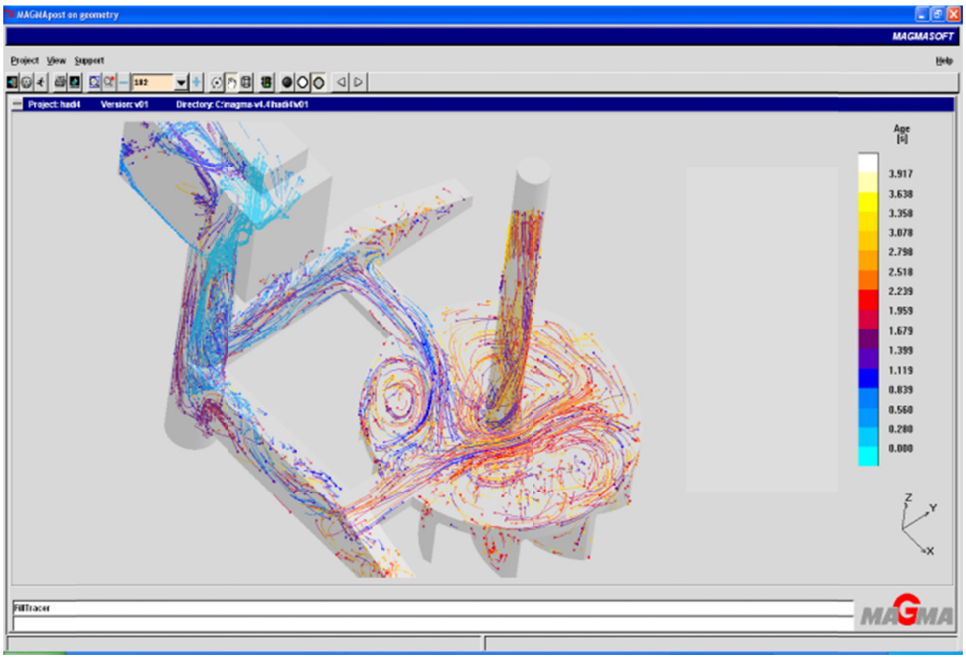

Figure 5.42 Design 2 metal flow pattern – tracer points.

Figure 5.43 shows the velocity pattern curves behavior of the runners (points 1, 2, 12 and 13) which indicates the turbulence in the flow.

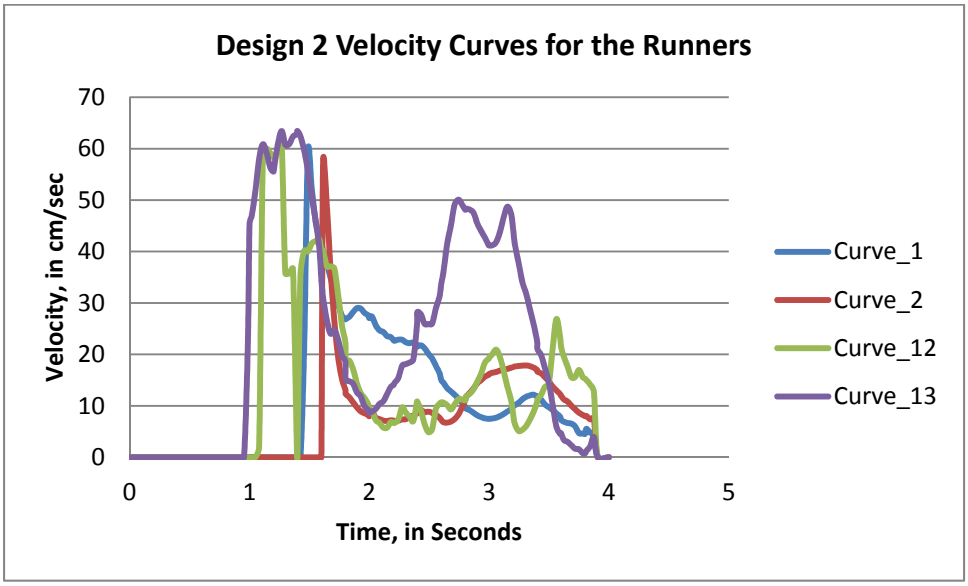

Figure 5.43 Design 2 Velocity curves in the runners.

The velocity graphs of the control points in the gates predicted the high turbulence in the flow, which is shown in velocity graphs Figure 5.44.

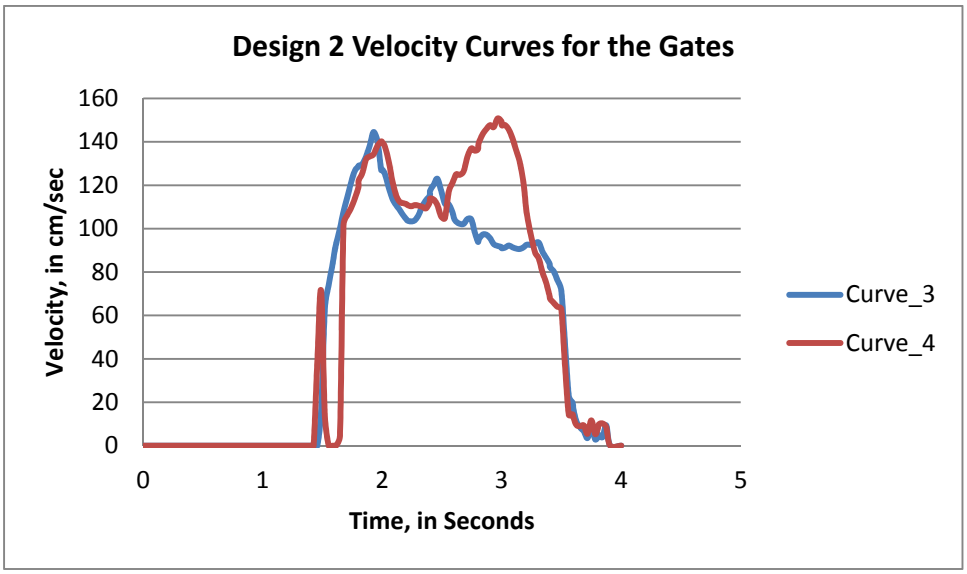

Figure 5.44 Design 2 Velocity curves in the gates.

The filling velocity profile in the casting presents different behavior of turbulence. Figure 5.45 shows the curves of the control points in different location in the castings. The more turbulence in the flow, the more air entrapment in the casting as predicted by the software with X-ray feature activated in Figure 5.46.

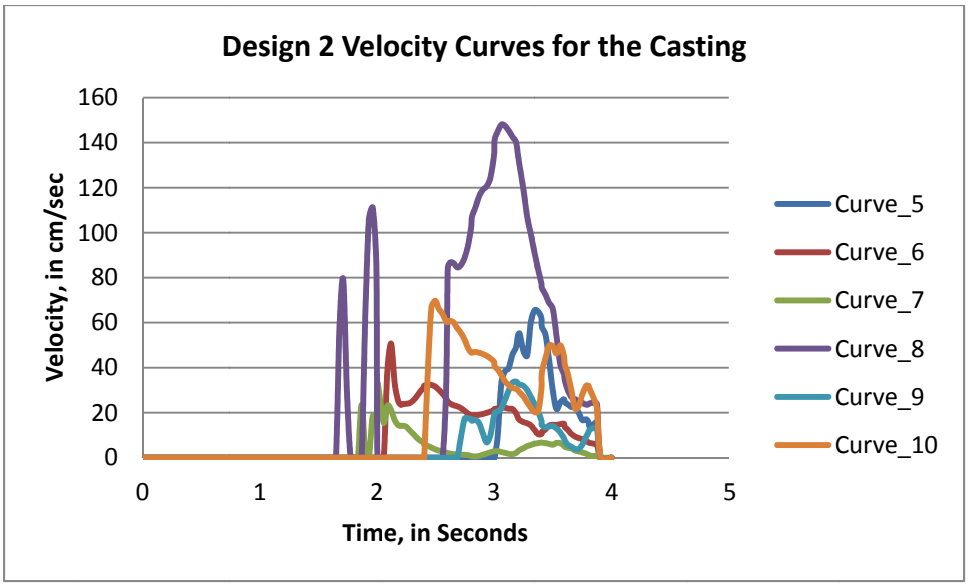

Figure 5.45 Design 2 velocity curves in the casting (Impeller).

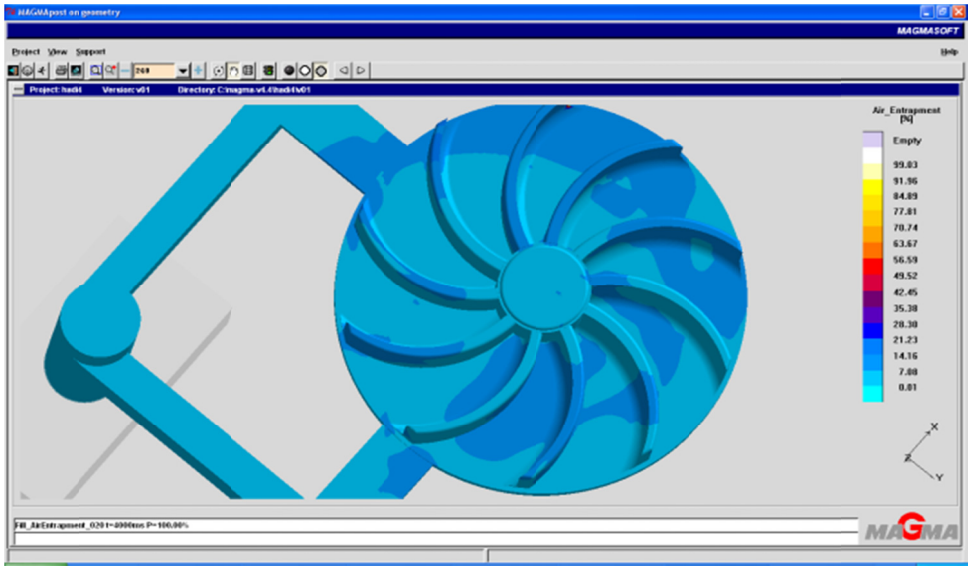

Figure 5.46 Design 2 air entrapment from simulation 2.

c. Temperature Distribution in Simulation 2:

It was predicted by MAGMASOFT® that the solidification started within eight seconds after complete four seconds filling time, and 266 seconds required completing the solidification. Figure 5.47 shows the solidification in 266 seconds after complete filling.

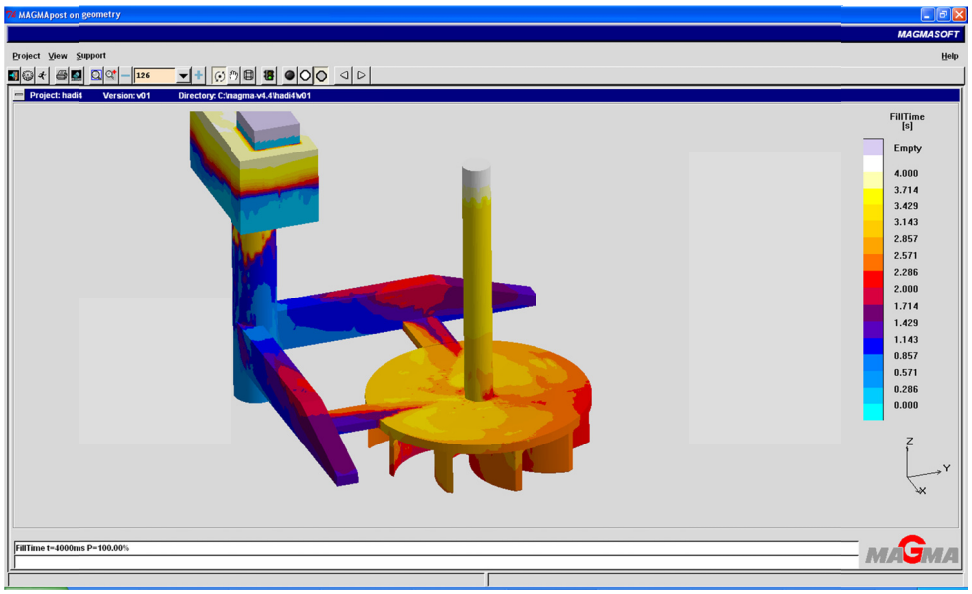

Figure 5.47 Design 2 solidification process completed in 266 seconds.

Similarly, the solidification process was predicted by the software in the runners, gates and the casting. Solidification rate in the runners can be shown in Figure 5.48. The solidification rate in the gates was also predicted by the software control points 3 and 4 and shown in Figure 5.49.

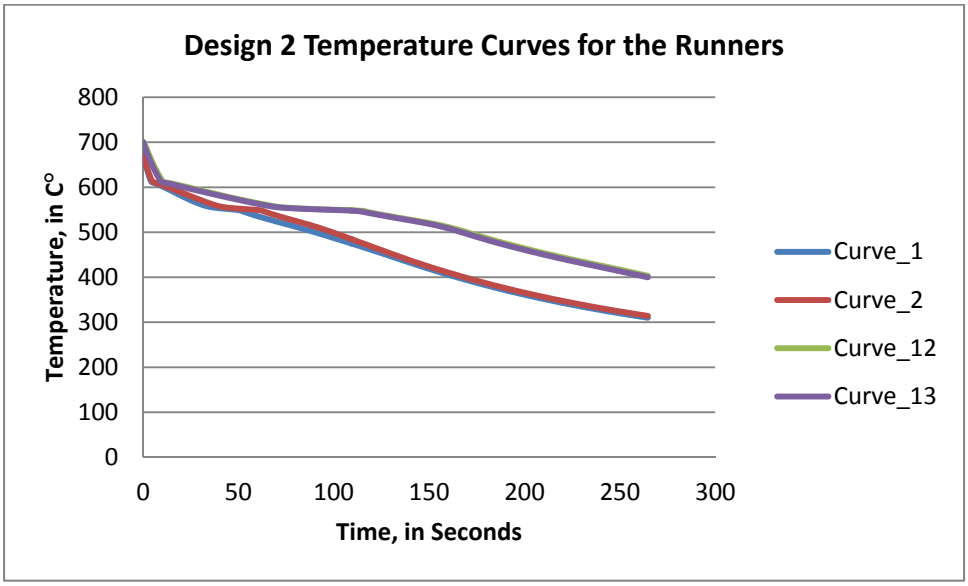

Figure 5.48 Design 2 temperature curves (solidification rate) in the runners.

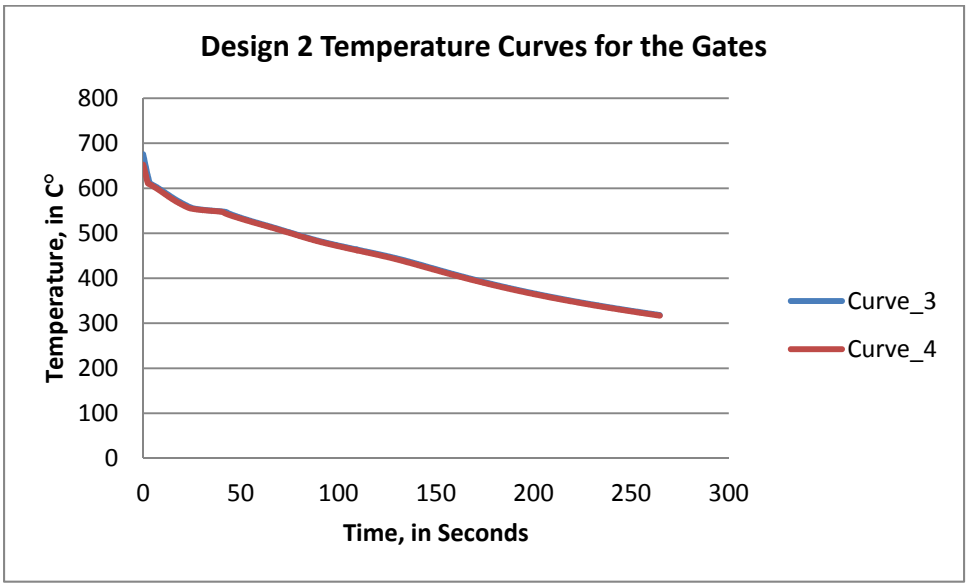

Figure 5.49 Design 2 temperature curves (solidification rate) in the gates.

It was observed that the solidification rate curves in the casting showed uniform rates at the symetrical locations. Curves 5 and 6 locations are in the casting body next to the

gates, and presented slower cooling rate than 7, 8, 9 and 10 which presents the locations at the edges and on the vanes. The plotted pattern behavior is shown in Figure 5.50. The riser and center of the casting have the same cooling rate and slower than the main casting body, which help to eliminate the porosity as shown in Figure 5.51.

It is also predicted by MAGMASOFT® that due to the direct attachment of riser to the middle of casting section, significant reduction of the hot spot, as shown in Figure 5.52.

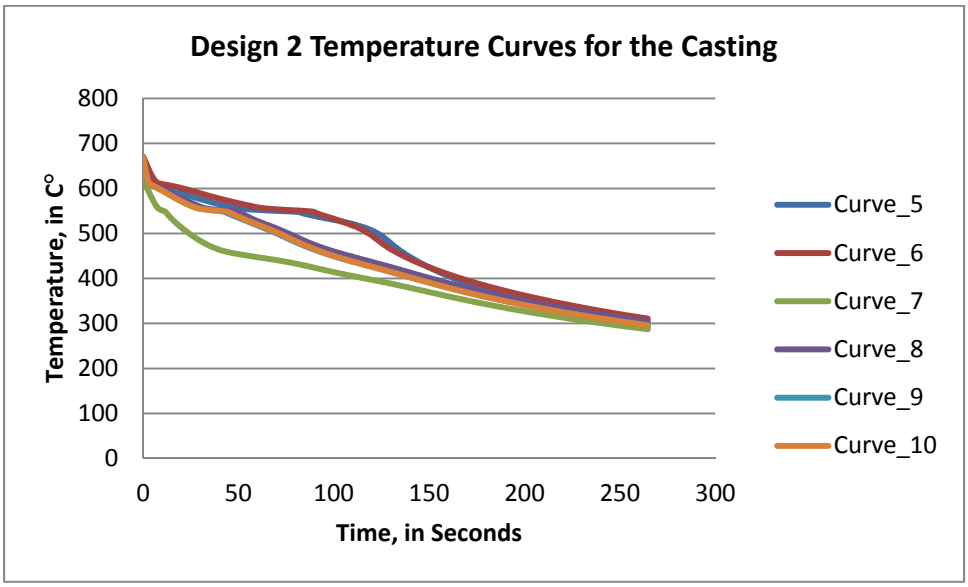

Figure 5.50 Design 2 solidification rate curves in the casting.

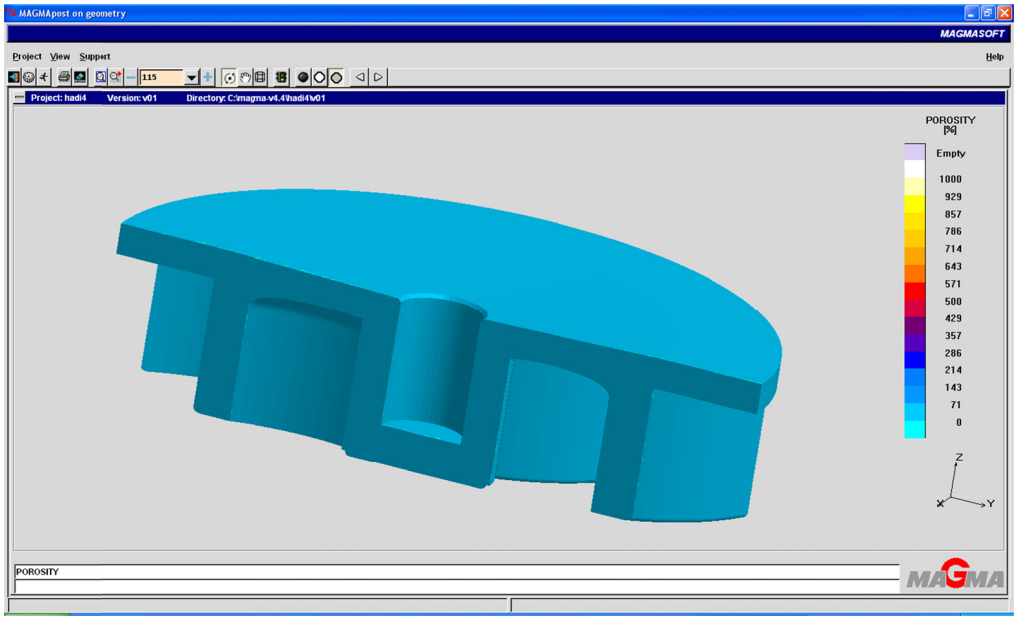

Figure 5.51 Design 2 porosity free in simulation 2 (X-Ray activated).

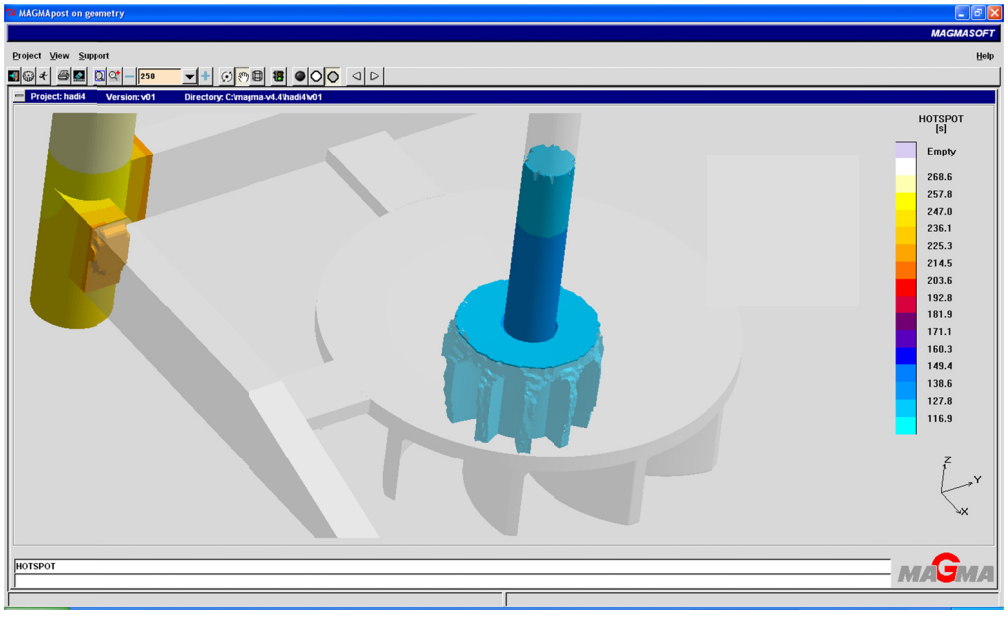

Figure 5.52 Design 2 hot spot in the center of the casting (X-Ray activated).

The stress distribution is shown in Figure 5.53. An evenly distributed stress was predicted. This is a one of key factor indicating sound and good quality of casting and shows the improvements in the design.

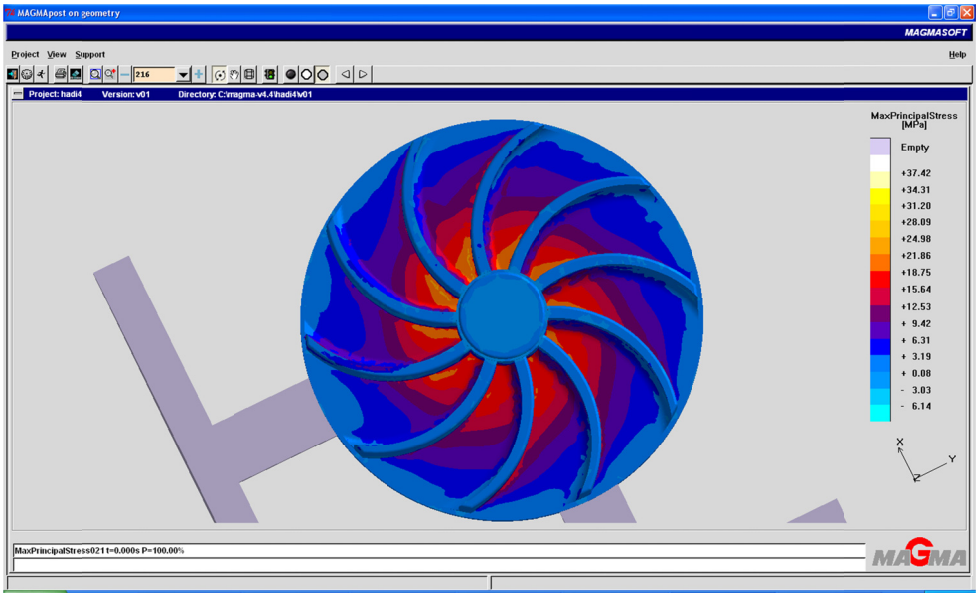

Figure 5.53 Design 2 stress distribution in simulation 2.

5.6.3 DESIGN 3 SIMULATION

The third design (Design 3) for simulation analysis is shown in Figure 5.54. This design is an improved version of Design 2. The main objective was to increase the yield by reducing the volume of gating design. The runners' cross-sectional area was reduced from 900 mm^2 to 690 mm^2, and the runners' length from 300 mm to 200 mm. The gates lengths were also reduced significantly from 50 mm to 20 mm. The design modification was done by the recommendations of JICA standards [20]. Design 3 detail dimensions are listed in Table 5.12.

The simulation results are showing the effect of the size reduction of gating. The parameters under consideration were remained same and predicted data was collected on same locations as per Design 1 and 2. The simulation parameters and conditions are also listed in Table 5.13.

TABLE 5.12 Gating system dimensions of Design 3.

Design	Runner x-Sectional area mm^2	Runner Length mm	Gate x-Sectional Area mm^2	Gate Length. mm
3	690	200	220	20

TABLE 5.13: Simulation parameters used in MAGMASOFT® in Simulation 3.

Selected Parameter	Description
MAGMA-Soft Simulation Info	
Module	Casting
Calculations	Filling, Solidification, Stress
Enmeshment	3,000,000 element
Material Definition	
Cast Alloy	$AlSi_6Cu_4$
Melting Point	700.00 C°
Sand Mold	Green Sand
Heat Transfer Definitions	
Cast Alloy to Sand Mold	C800.0
Simulation Options	
Sand Permeability	Yes
Particles/Control Points	Yes
Filling Definitions	
Filling Time	4 seconds

Design 3 was simulated for analysis with respect to the Pressure, Velocity and Solidification pattern in different locations in the gating and the casting by the control points as shown in Figure 5.54.

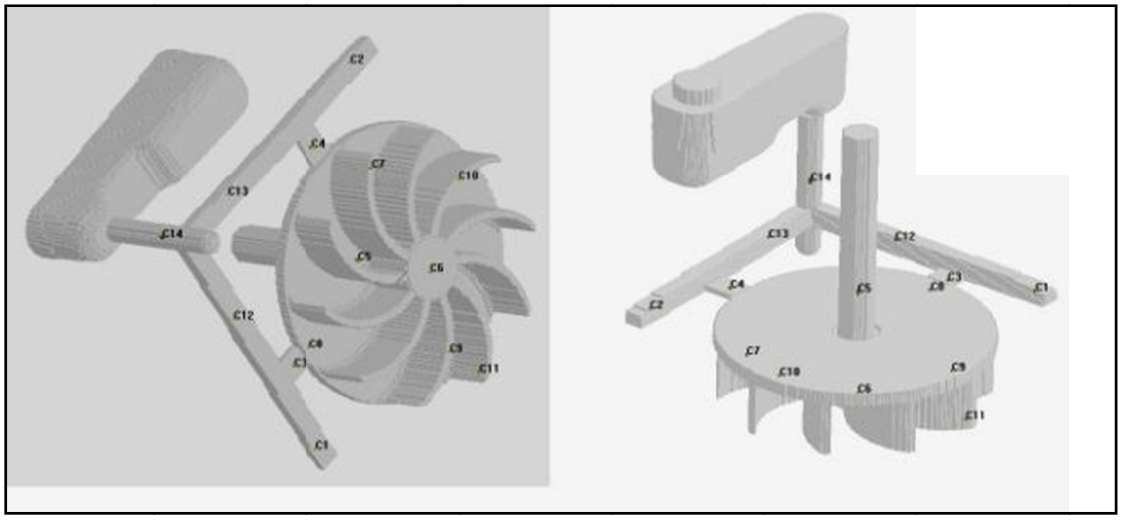

Figure 5.54 Design 3 geometry and control points.

a. Pressure Distribution in Simulation 3:

The measurement of filling pressure curves are given in Figure 5.55 and 5.56 for both runners (points 1, 2, 12, and 13) and gates (points 3 and 4). The filling pressure in runner and gates remained high during complete filling cycle as compare to cast body. The higher and gradual increase in pressure as compare to previously studied designs in runner and gate indicated the pressurized system.

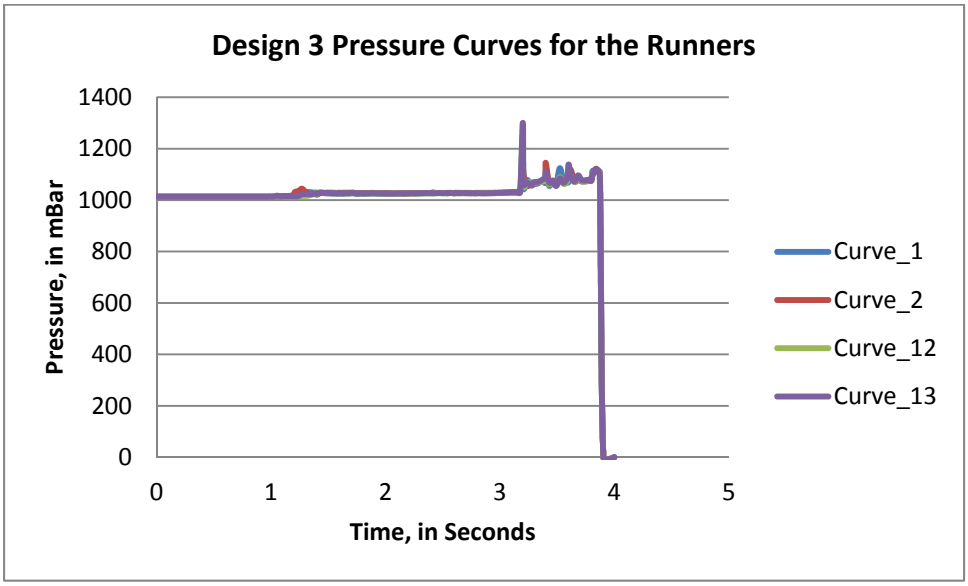

Figure 5.55 Design 3 pressure curves in the runners.

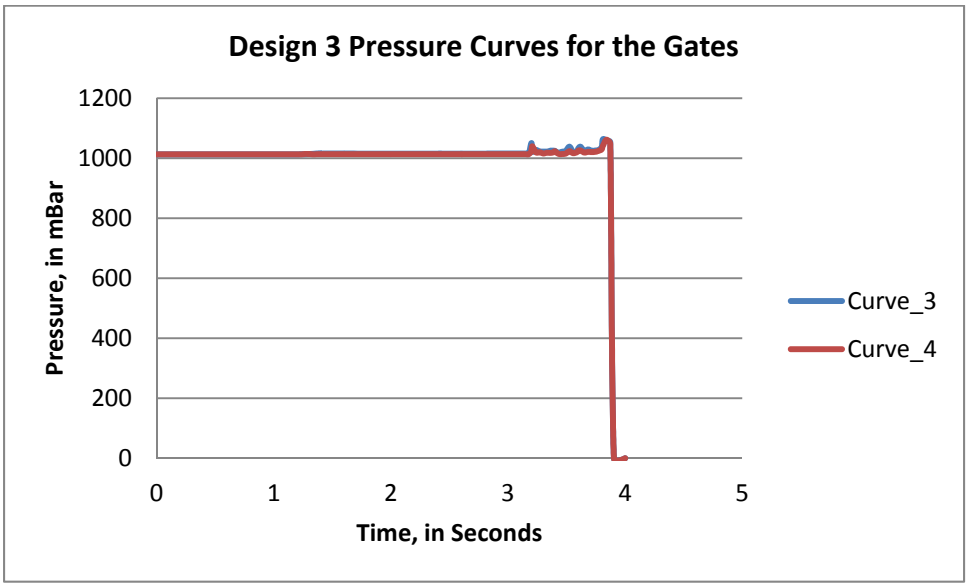

Figure 5.56 Design 3 pressure curves in the gates.

The filling pressure pattern in the casting is also plotted in Figure 5.57. It represents a very smooth and uniform filling pattern of pressure inside the casting.

The uniform distribution of pressure in the system also provides a recommended mixed laminar/turbulent flow in the casting system as illustrated in Figure 5.57. Consequently it eliminates the possibility of mold wall erosion and better surface quality and elimination of porosity and hot spots as shown in Figure 5.58. However, due to the short and pressurized gating system design, air entrapment occurred in design 3, as shown in Figure 5.59.

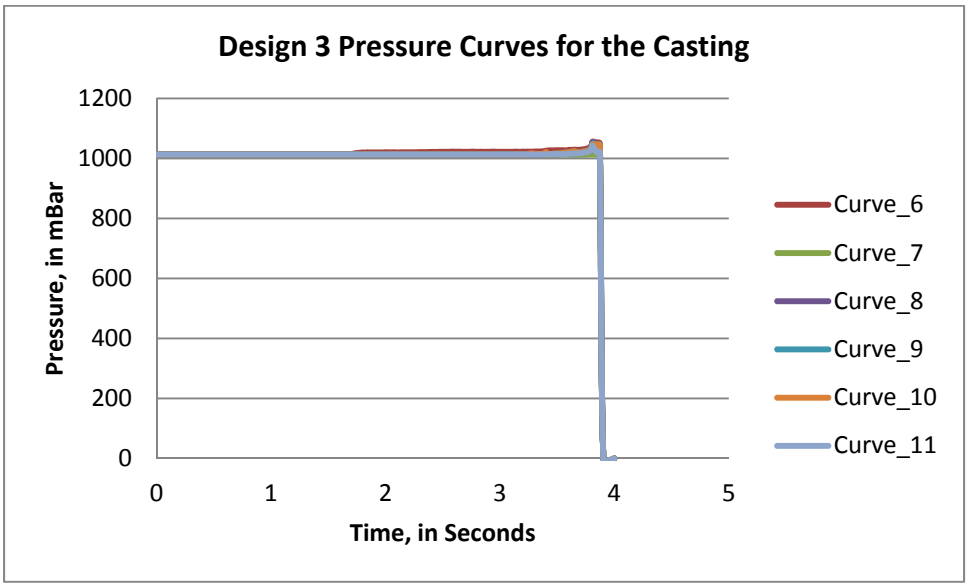

Figure 5.57 Design 3 pressure curves in the casting.

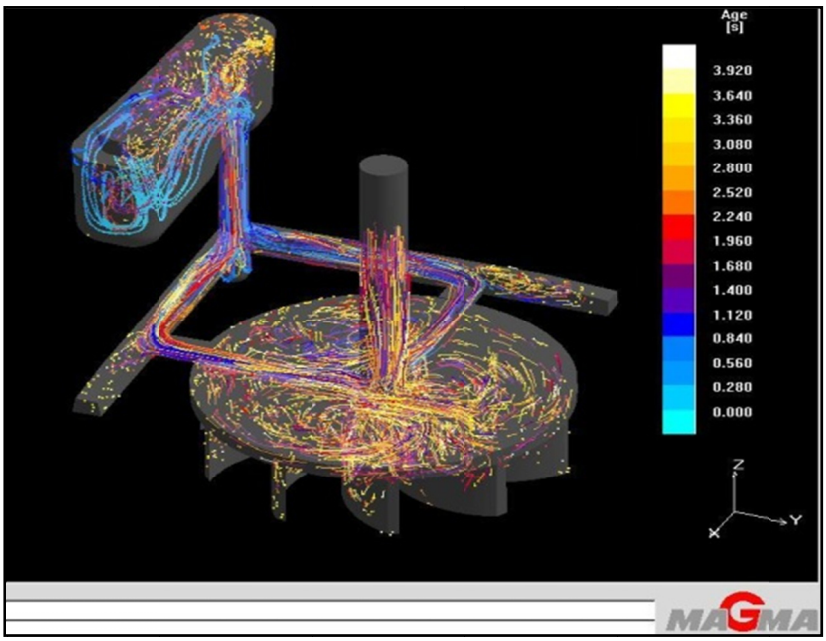

Figure 5.58 Design 3 metal flow pattern – tracer points.

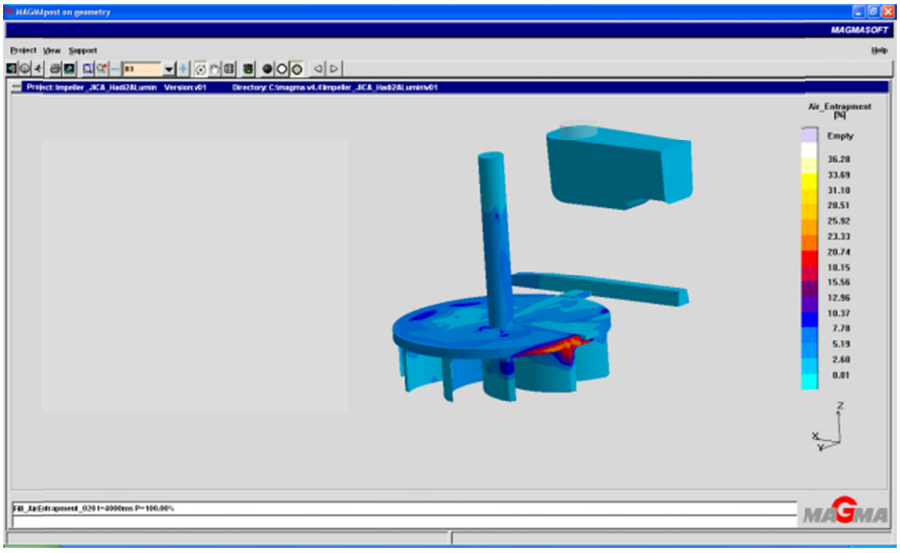

Figure 5.59 Design 3 air entrapment (X-Ray activated).

b. Velocity Distribution in Simulation 3:

The velocity pattern for design 3 was predicted by the control points located in the runners, gates and the casting. The velocity graphs predicted the mixed laminar-turbulence flow which reduce the affect the mold wall erosion and consequently will produce better surface quality. Figure 5.60, the velocity curves of the points in the runners shows relative variation in velocity at the runners due to changes in pressure. However, the flow in the gates is more uniform and mixed of laminar-turbulent.

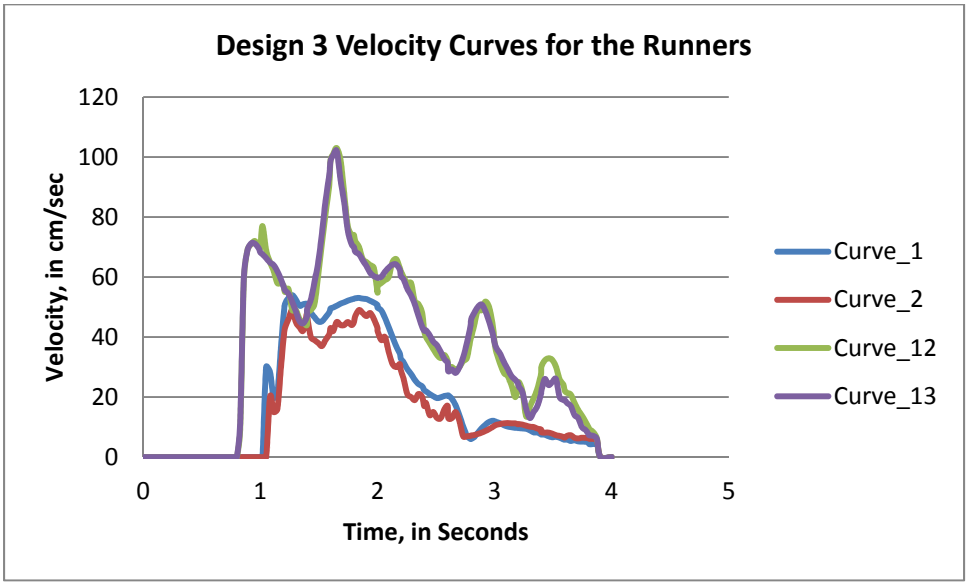

Figure 5.60 Design 3 velocity curves in the runners.

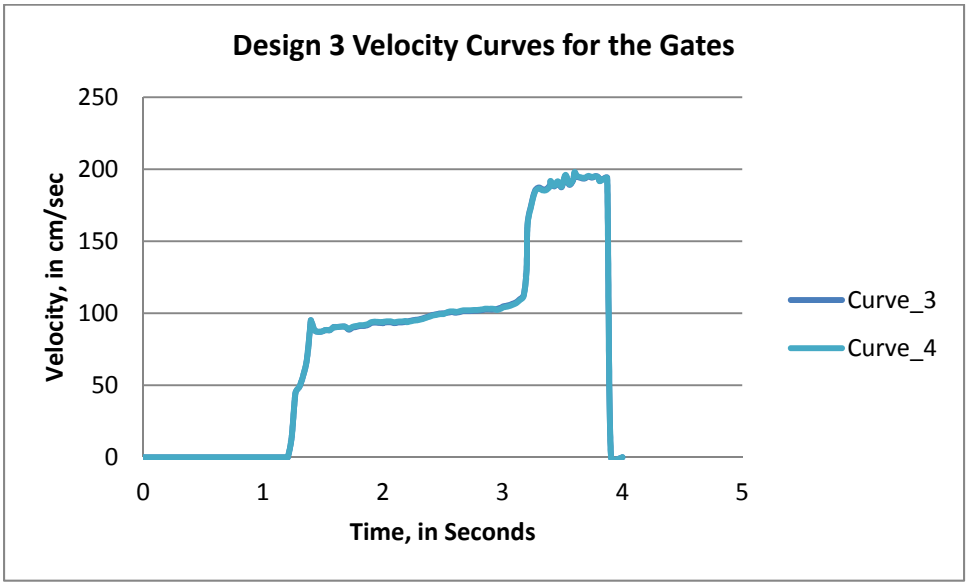

Figure 5.61 Design 3velocity curves in the gates.

In the casting, Figure 5.62 demonstrates the velocity curves which show modest variation in the flow, however, it is steady flow in the casting. Tracer points in Figure 5.58 confirm the velocity curves.

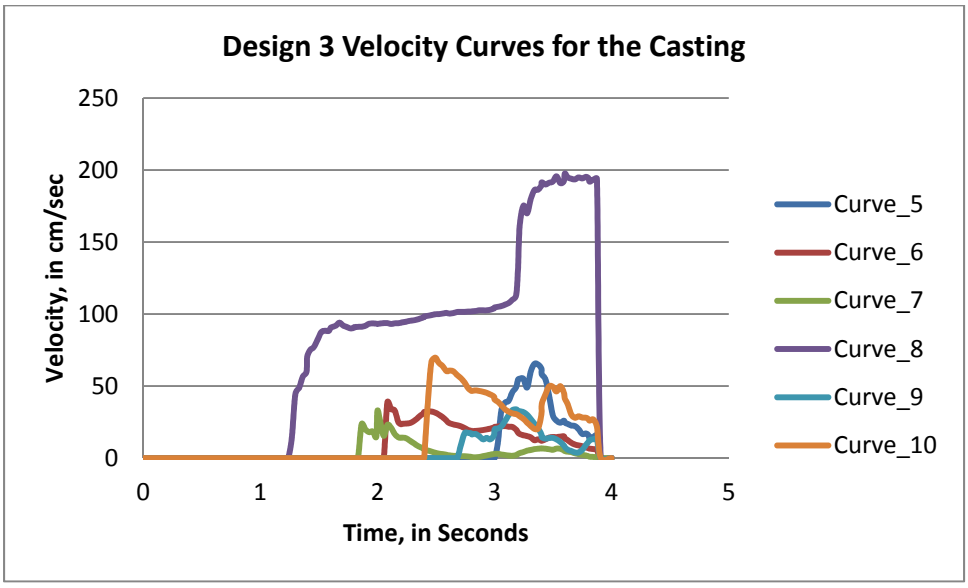

Figure 5.62 Design 3 velocity curves in the casting.

c. Temperature Distribution in Simulation 3:

A sequential pattern of cooling was predicted. The cooling rate in feeder and middle of casting is slower than the whole casting. The curves of the temperature behavior in runner, gate and casting of the solidification rate are shown in one plot in Figure 5.63. It demonstrates a steady solidification process and uniform cooling rate. The resultant effect is a sound and porosity free casting as shown in Figure 5.64, and elimination of hot spot as predicted by MAGMASOFT® as shown in Figure 5.65.

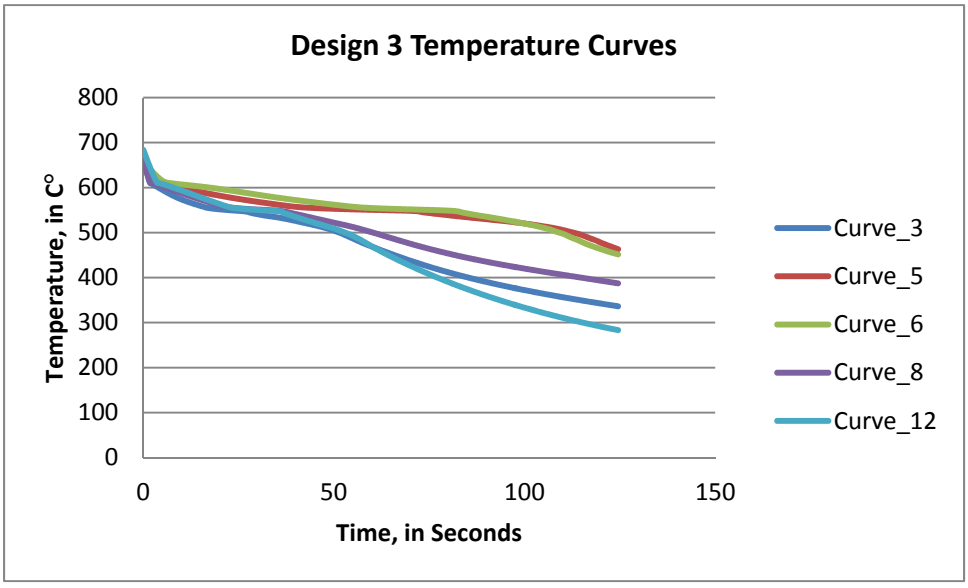

Figure 5.63 Design 3 temperature curves (solidification rate).

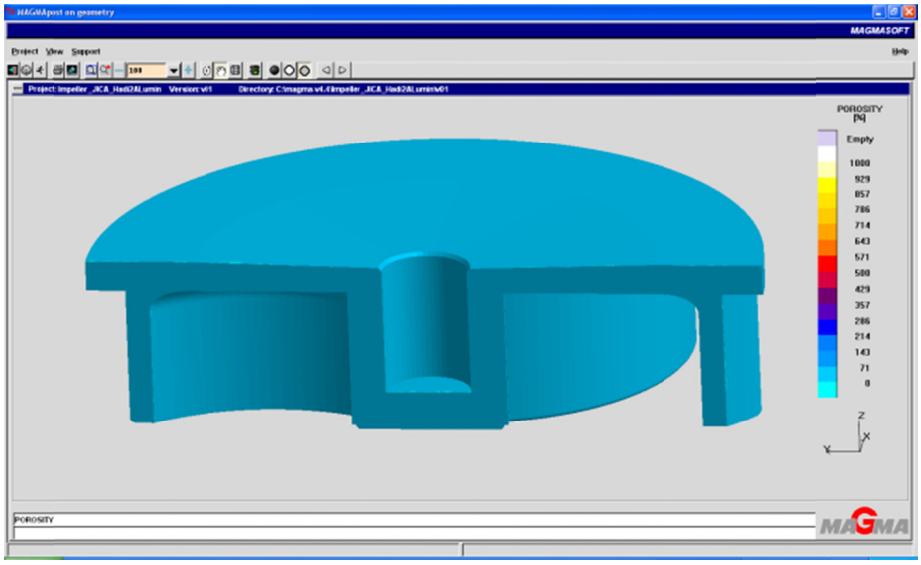

Figure 5.64 Design 3 porosity free casting – X-ray activated.

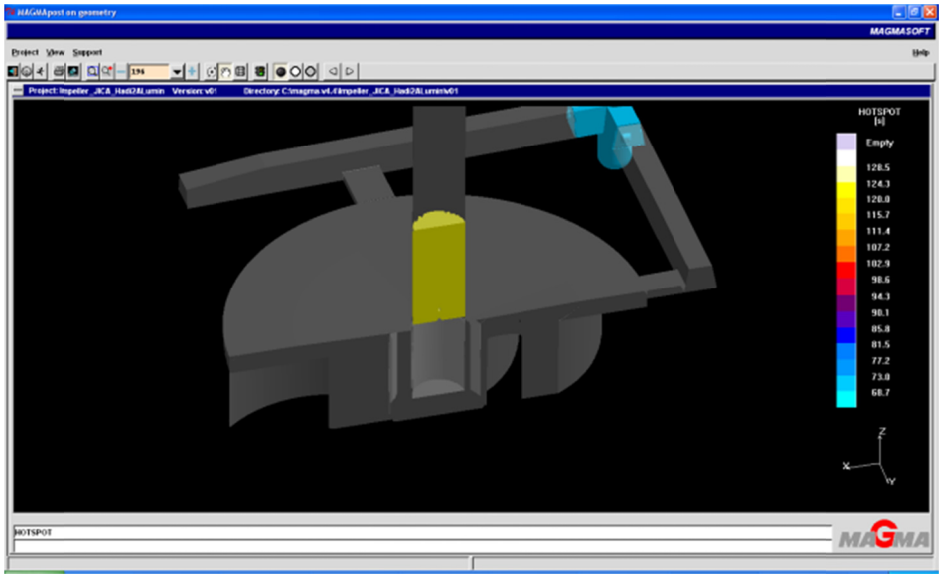

Figure 5.65 Design 3 hot spot (X-Ray activated).

Furthermore, evenly distributed stress was predicted, which indicates crack free, sound quality casting of Design 3. Stress distribution of the casting is shown in Figure 5.66.

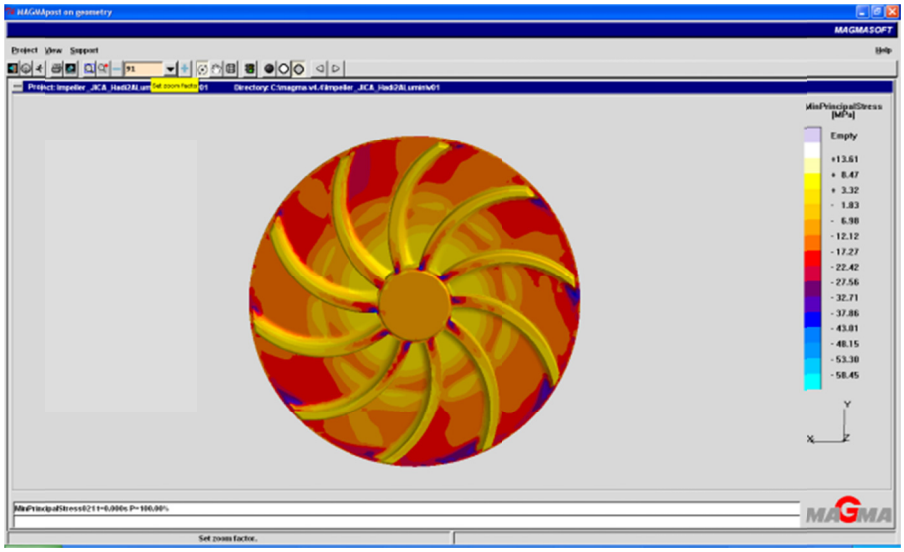

Figure 5.66 Design 3 stress distribution predicted by MAGMASOFT®

5.7 NEAR OPTIMAL DESIGN

On the basis of the predicted results, three simulated designs were compared to select the relatively best design. Due to air entrapment, porosity, hot spot and unevenly distributed stress, the Design 1 was not considered to be a near optimal design because of the flow behavior as in the Figures 5.9 and 5.10, and due to some quality issues in the product such as porosity as in the Figure 5.30 and the hot spot as shown in Figure 5.31. Due to much closer results and defect free casting predictions of Design 2 and 3, both designs were compared thoroughly and Design 3 was selected for the final casting on two bases: filling conditions and solidification pattern.

5.7.1 FILLING CONDITIONS

Comparing filling pressure, in design 2 and 3, high pressure in casting was predicted in Design 2 during filling at 95 percentage of filling as in Figure 5.41, while in Design 3, a continuous high pressure was maintained first in the runner then gates and then casting Figures 5.55, 5.56 and 5.57which indicates the pressurized gating system. As a result of these pressure variations, in Design 2 the high turbulence in filling velocity was predicted where as in Design 3, it presents smooth pattern which indicates a recommended mixed laminar/turbulent flow regime of the casting which is more suitable for mold integrity and reducing the air entrapment and porosity in the casting as shown in Design 3 simulation results.

5.7.2 SOLIDIFICATION PATTERN

The solidification patterns were compared for three results. It was obvious and predicted the higher cooling rate in thin wall sections as compared to thick sections. In design 1 the feeder was not connected near the heat concentrated areas. The connecting gate x-section was very smaller than the feeder so that the feeding gate solidified before the feeder and main cast body, and metal flow during solidification stopped, consequently, it resulted in the porosity and uneven stress distribution in casting. Whereas, Design 2 and 3, feeder is directly attached with the thick and low cooling rate sections. The porosity was completely eliminated, and an even stress distribution was predicted, which will result in minimal residual stresses.

As a conclusion of the discussion in this chapter, it is observed that design 2 and 3 are better than design 1. Both Design 2 and 3 are comparable to each other in many casting features, however, Design 3 has an added advantage that it gives higher yield by reducing the material used in gating system which leads to lower cost and greater productivity. Hence, Design 3 has been selected as the near optimal design. It is important to emphasize that more simulations may further improve the design; however, since the Design 3 satisfies the quality requirements we can safely terminate the iterative process of simulation by selecting this as final design ready for further experimental pattern making in Chapter 6 and metallurgical and hardness studies reported in Chapter 7.

CHAPTER 6

RAPID PROTOTYPING TECHNOLOGY AND PATTERN MAKING

Rapid Prototyping or tooling (also called Desk-top manufacturing or free-form fabrication) is a family of processes by which a solid physical model of a part is made directly from a three dimensional CAD drawing involving a time span that is much shorter than that for traditional prototype manufacturing. Prototype in this case is the pattern for casting process. In this chapter, the use of Rapid Prototyping techniques to produce a master pattern/or pattern are discussed and its advantages and limitations are presented.

6.1 MAKING OF PATTERN

Pattern (a replica of the object to be cast) is used to prepare the mold cavity in the sand mixture into which molten metal is poured during the casting process. The pattern may be made of wood, plastic or metal. Also, molds may be made of a combination of materials in order to reduce the patterns wear in critical regions [4]. Pattern makers learn their skills through apprenticeships and trade schools over many years of experience. Although an engineer may help to design the pattern, it is usually a patternmaker who executes the design.

6.1.1 METHOD OF PATTERN MAKING

Patterns can be designed with a variety of features for specific application and economic requirements [4].

The following is a brief description of different types of pattern design according to its use:

a. One-Piece pattern: generally used for simple and basic shape of castings with low quantity of production. They are typically made of wood and could be expensive.
b. Split patterns: they are two piece patterns and made so that each part forms a portion of the cavity for the casting. It is widely used for complicated shapes.
c. Match-plate patterns: they are a common type of mounted pattern in which two piece patterns are constructed by securing each half of one or more split pattern to the opposite sides of a single plate. The gating system can be mounted on the drag side of the pattern.

6.1.2 PATTERN MATERIALS

Because patterns are repeatedly used to make molds, the strength and durability of the pattern material selected must reflect the number of castings expected to be produced. It can be made of wood, metal, resins, or plastic. The selection of a pattern material depends on the size and shape of the casting, dimensional accuracy and the quantity of casting required as well as the molding process to be used. Also, patterns are usually coated with a parting agent to facilitate their removal from the molds [4].

6.1.3 MASTER PATTERN

Master pattern is the name given to a pattern having a double contraction or shrinkage allowance. The castings made from the master pattern are used by the patternmaker in making duplicate patterns that will have only a single contraction or shrinkage allowance for the particular metal required of the final casting. An allowance is made not only for the shrinkage of the metal pattern, but also, a second allowance is added for the shrinkage of the casting produced from the metal pattern [4].

The different types of material that can be used in the construction of master patterns are numerous. These types include wood, plaster, aluminum, brass, bronze, plexi-glass, ren-shape, and more. As comparatively few castings are made from a master pattern, the cost of the materials is held to a minimum so that the pattern can be made as economically as possible. Therefore, for the general purposes of lower cost and of speed in the manufacture of a master pattern, poplar is the most logical material to use.

In this research, rather than using a master pattern, we have designed and manufactured the pattern of the impeller directly using FDM process.

6.2 RAPID PROTOTYPING TECHNOLOGY

Developed in the 1980's, Rapid Prototyping (R.P.) is an important advance in manufacturing operations by which a solid physical model of a part is made directly from a three-dimensional CAD drawing. The process of prototyping involves additive manufacturing which build parts in layers. Rapid Prototyping can also be done by

subtractive process using computer-controlled high speed machining. The additive manufacturing inherently involves integrated computer-driven hardware and software [5]. The sand casting process is apparently simple; however, the production of the sand molds and cast metal parts depends upon the complexity of the shape and the experience of the designer. The fabrication of the pattern, and development of the sand mold cavity, and its integration with other mold elements such as gates, runners, sprue and riser, can be time consuming. The application of RP technology to the sand casting process can reduce the pattern and mold development time to expedite the receipt of prototype or production sand cast parts [27].

When used for pattern production, RP technology has a potential to reduce the lead time from weeks to days while offering cost savings. Since many RP processes are automated, unattended processes, they can benefit sand casting foundries by increasing overall efficiency and productivity while reducing the labor costs. An additional benefit when using RP technology for sand casting patterns is that there is no change in tool design, the tool making process or the casting process. The benefits are delivered by simply replacing machining with RP technology while retaining standard design practices and manufacturing procedures. In this research, we used FDM technology as an RP process to facilitate the pattern production.

6.2.1 FUSED DEPOSITION MODELING TECHNOLOGY:

Fused deposition modeling (FDM) is an additive manufacturing technology commonly used for modeling, prototyping, and production applications. The technology was

developed by S. Scott Crump in the late 1980s and was commercialized in 1990. Furthermore, FDM is the largest used process and constitutes 37 percentage of all rapid prototyping systems used worldwide [5].

The FDM system builds a prototype by depositing melted plastic. A plastic filament is unwound from a spool and is delivered to an extrusion head. The extrusion head contains the nozzle for delivery of the melted plastic, heating elements, and incorporates mechanisms which allow the flow of the melted plastic to be turned on and off. The nozzle is mounted in the head which can travel in horizontal XY plane. As the nozzle is moved over the table driven by the required geometry, it deposits a thin bead of extruded plastic to form each layer. The plastic hardens immediately after being extruded from the nozzle and bonds to the layer below. The entire system is contained within a chamber that is held at a certain temperature [29].

FDM, developed and manufactured by *Stratasys*, is available in a number of systems. These include the FDM *Maxum*, FDM *Titan*, FDM *Vantage* and *Prodigy Plus*. FDM offers functional prototypes with ABS, *Sulfone*, Polycarbonate and other materials. 90 percentage of FDM prototypes are produced by ABS material [30].

6.2.2 MACHINE/EQUIPMENT USED IN THE RESEARCH:

FDM Titan™ by STRATASYS

The FDM *Titan*™ from *Stratasys* was used in this research and it is shown in Figure 6.1. It has a build envelop size of 406 mm, 355 mm, and 406 mm in length, width and height respectively. ABS, PC and PPSF material can be used for the model generation. Layer

thickness ranges from 0.127 mm to 0.33 mm for ABS material. *Stratasys* has established "*Insight*" software to import the STL file and preprocessing of the model. It generates non intersecting planer slices, support structure and material extrusion path [31].

Figure 6.1 FDM Titan™ by STRATASYS.

Titan™ reported the achievable accuracy of ±0.127 mm up to 5 inches and for models greater than 5inches is ±0.0015mm per mm. The study carried out (Grimm & Associates, 2003) has reported that the maximum dimensional deviation of FDM *Titan*™ is 3.2 mm and average deviation from nominal data is 0.47mm.The surface finish is 475 µin on the top surfaces, 425 µin on side walls and 575 µin on bottom surfaces. The making process

of the impeller inside the FDM *Titan*™ chamber can be shown in Figure 6.2. This technology is being used to develop the functional prototypes and pattern manufacturing [30].

6.2.3 METHODOLOGY OF MAKING THE PATTERN BY FDM

In the Fused-Deposition Modeling (FDM) process, a gantry-robot controlled extruder head moves in two principal directions over a table. The table can be raised and lowered as needed. A thermoplastic filament is extruded through the small orifice of a heated die. The initial layer is placed on a foam foundation by extruding the filament at a constant rate while the extruder head follows a pre-determined path. When the first layer is completed, the table is lowered so that subsequent layers can be superimposed.

In the FDM process, the extruded layers thickness is determined by the extruder die diameter. The diameter is typically in the range of 0.33 mm to 0.12 mm. The thickness represents the best achievable dimensional tolerance in the vertical direction. The overall dimensional tolerances may be compromised unless care is taken in applying the required finishing operations [5].

The material of the pattern used in this research and made by the FDM is ABS (*acrylonitrile-butadiene-styrene*). It is strong, durable industrial-grade ABS plastic in a wide variety of colors. Its strength is 60 percentage to 80 percentage that of injection molded ABS plastic. [31]

The impeller was made according to the process described in sections 6.2.3 and 6.2.4, and the process is described in the flow diagram in Figure 6.2.The resulted part is shown in Figure 6.3.

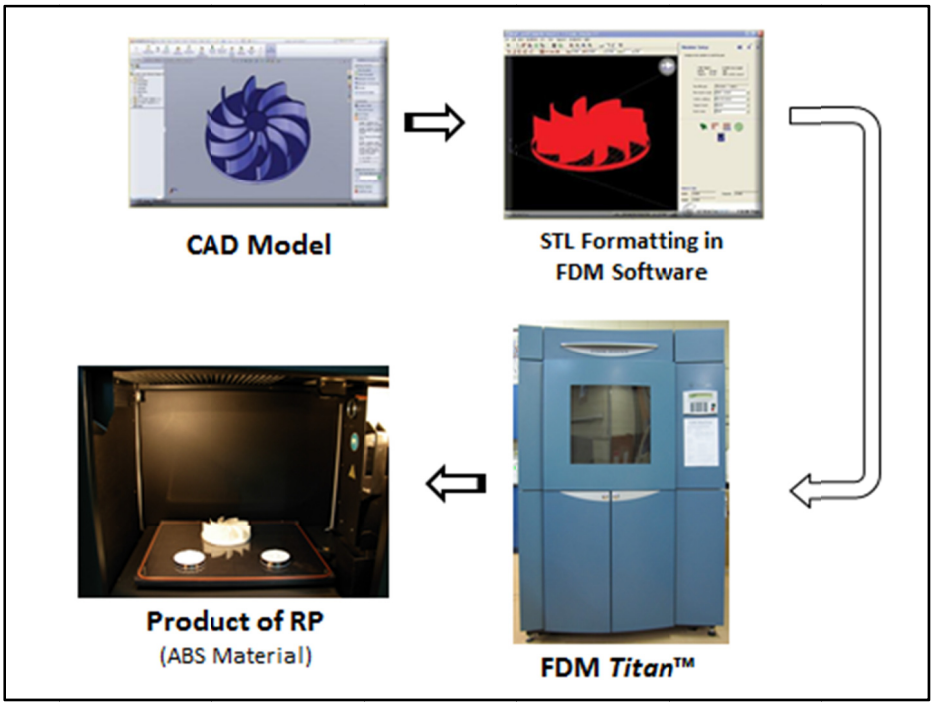

Figure 6.2 Process of making the impeller by FDM *Titan*™

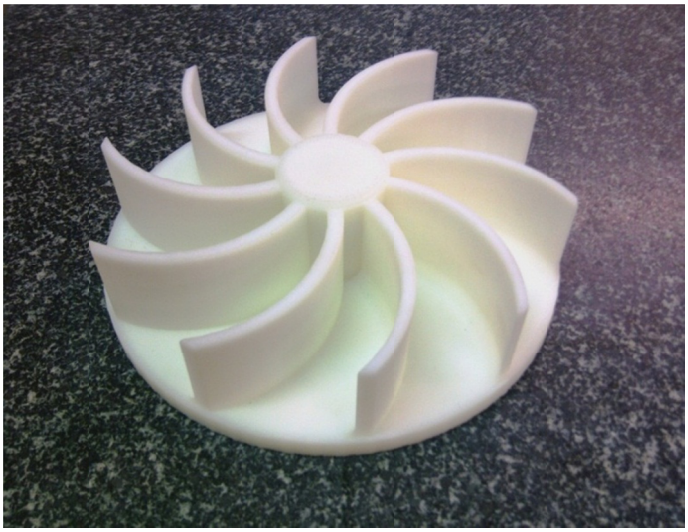

Figure 6.3 Impeller made by FDM Titan™ with ABS material.

6.3 ADVANTAGES AND BENEFITS

The importance and economic impact of rapid prototyping can be evaluated as follows:

a. The conceptual product design is viewed in its integrity and from different angles on a monitor through a three dimensional CAD system.
b. A prototype from various nonmetallic and metallic materials is manufactured and studied thoroughly from functional, technical, and esthetic aspects.
c. Prototyping is accomplished in a much shorter time and at a lower cost than by traditional methods.

Two factors can be presented to explain the advantages of using Rapid Prototyping and FDM in making the pattern for the casting:

6.3.1 QUALITY

The quality of the pattern used in sand casting is very important. It has an effect on the quality of the mold which consequently affects the physical quality of casting product. The quality of the pattern prepared and used in this research can be determined by three following measures:

a. *Surface Finish*: The surface roughness resulting due to staircase effect in the rapid prototyped parts is one of the major areas of studies for realizing pattern improvements and acceptance [32]. It can be improved up to order of 0.3 μm with 87 percentage confidence level, with proper orientation of the part being built [33]. Table 6.1 shows a

summary of the average of three surface finish readings conducted on the impeller ABS material produced using FDM.

More information about the surface finish/roughness test and results of the produced pattern of the impeller are shown in the appendix B1.1.The test was conducted by using *Mitutoyo* Surface Analyzer to confirm the required surface finish for ABS material.

b. *Strength*: The strength of the ABS material produced by FDM is competitive. Its tensile strength is about 22 MPa, as per ASTM# D638, and the ultimate tensile strength is 40 MPa.

Table 6.2 shows the mechanical properties of the ABS material. It has been shown that the strength of ABS material used in Rapid Prototyping is suitable in different applications and FDM technology has the potential to lower development costs and improve the competitive advantage [31]. More material information is also shown in Appendix B1.2.

6.3.2 TIME

Number of studies presented information showing that R.P. technology and pattern making by FDM has an advantage of speed, tolerance and quantities produced [34].

The time that FDM (or any other rapid tooling machine) takes to produce a three dimensional geometrical model is counted by hours, whereas preparing a master pattern by wood or any other material requires days and special skills to make it which is the current practice in foundry industries.

TABLE 6.1 Surface finish test of ABS material using *Mitutoyo* surface analyzer.

Test Description	Roughness Profile			Cut off Length		M-speed
	R_a (µm)	R_z (µm)	R_q (µm)	λ_c (mm)	λ_s (µm)	(mm/sec)
Surface 1 Location	14.13	60.59	16.53			
Surface 2 Location	16.33	66.78	19.16	0.8	2.5	0.5
Surface 3 Location	16.69	74.75	19.82			
Average Reading	15.72	67.37	18.50	0.8	2.5	0.5

TABLE 6.2 Pattern ABS material properties (*STARTASYS*®, Startasys GmbH Germany)

Property	Unit	Range	*ASTM#*
Tensile Strength	(MPa)	22	*D638*
Tensile Modulus	(Ma)	1,627	*D638*
Heat Deflection	(°C)	96	*D648*
Density	(g/cm^3)	1.05	
Elongation (at break)	%	>10	

CHAPTER 7

EXPERIMENTAL VALIDATION OF OPTIMIZED DESIGN

In this chapter, results from the actual casting of the tested impeller is shown and discussed. The final system design resulted after simulation was selected and mold was prepared. The sample collected after complete solidification of the cast part (impeller) was tested physically and its microstructure was observed.

7.1 EXPERIMENTAL CASTING PROCESS

The ABS pattern of the impeller was made by using FDM technology in KFUPM Reverse Engineering and RP lab was coated for easy release from sand mold. The ABS impeller pattern is shown in Figure 6.3. The gating system was prepared from wood. Green sand was used in making the mold in KFUPM manufacturing lab. The complete mold making process steps in KFUPM manufacturing lab are explained as follows [35]:
The pattern made by FDM was coated by a release agent to ease the removal from the mold as shown in Figure 7.1.

Figure 7.1 Pattern made by FDM with ABS Material (Coated with release agent).

Results of the system after last simulation showed the most optimized mold design for which the actual mold was prepared and casting process was done at KFUPM Mechanical Workshop facilities. Various steps are explained illustrated in the images below.

The mold was prepared by adding the sand in the drag on the pattern as shown in Fig 7.2. The drag view before removing the pattern is shown in Figure 7.3. After removing the pattern of the impeller, the technician ensures that the gating is unbroken for optimum flow as shown in Figure 7.4. Final view of the drag showing the impeller and gating cavity is shown in Figure 7.5. Then, the cope was prepared and applied on the drag by adding green sand as shown in Figure 7.6 and Figure 7.7. And then, the final shape of the mold is ready for casting as shown in Figure 7.8.

Figure 7.2 Mold preparations by adding green sand to the drag.

Figure 7.3 View of the drag before removing the pattern.

Figure 7.4 Fixing mold cavity of the drag.

Figure 7.5 Final view of the drag showing the impeller and gating cavity.

Figure 7.6 Applying the cope on the drag and adding green sand.

Figure 7.7 Final steps of closing the mold.

Figure 7.8 Final shape of the mold.

The casting process was also completed in the manufacturing workshop in KFUPM. The process was started by setting up the furnace and ladle in the lab, as shown in Figure 7.9 and Figure 7.10. The Aluminum alloy was melted in the furnace until the pyrometer registered the molten metal temperature as 720 °C (Figure 7.11) as the pouring temperature set in MAGMASOFT® simulations. Then pouring of molten Aluminum was performed in four seconds as input parameter calculated during designing stage (section 5.4), and the process is shown in Figure 7.12 and 7.13. The mold was left for 180 minutes to complete solidification and cooling to the room temperature. After that, the mold was shake and broken, and then the casting part (impeller) was removed for inspection as shown in Figure 7.14.

Figure 7.9 Furnace preparations and Aluminum melting.

Figure 7.10 Furnace heating up and Aluminum temperature increases.

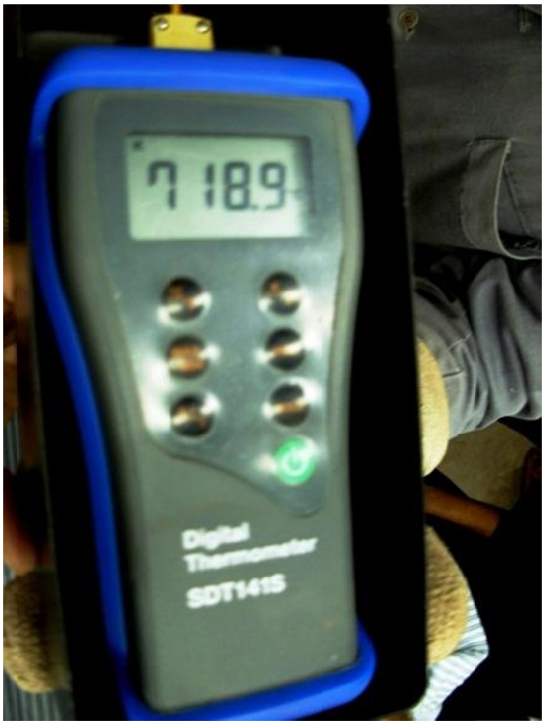

Figure 7.11 Melting and pouring temperature of Aluminum ($AlSi_6Cu_4$).

Figure 7.12 Molten Aluminum in the ladle before pouring into the mold.

Figure 7.13 Mold after complete filling.

Figure 7.14 Mold opening and casting removal.

7.2 QUALITY EVALUATION

The casting impeller of the optimum design generated from the simulation was taken for quality check. The quality check involved a physical check, hardness and microstructure studies. Then, it was supported with the surface finish measurement, and observation of any shrinkage or vanes defects. For the microstructure, certain locations were selected to check the internal structure of the part to correlate it with the cooling rate at that location.

7.2.1 VISUAL INSPECTION BEFORE MACHINING

The part was removed after complete solidification and was examined for any external defects. That includes any visible shrinkage, external porosity with surface finish or vanes defects. [36] The examination resulted in defect free part as of external check is concerned. Figure 7.15 shows the complete part before any treatment or machining.

Figure 7.15 Complete part removed after casting.

7.2.2 PHYSICAL CHECK AFTER MACHINING

The part after removal from the sand was prepared for cleaning and machining. The casting impeller after machining is show in figures 7.16. The high quality casting shows no thin wall shrinkage at the impeller vanes [37], as closely shown in Figure 7.17, and eliminated porosity at the center of the casting as shown in Figure 7.18.

Figure 7.16 The impeller after machining showing no physical defect– Top View.

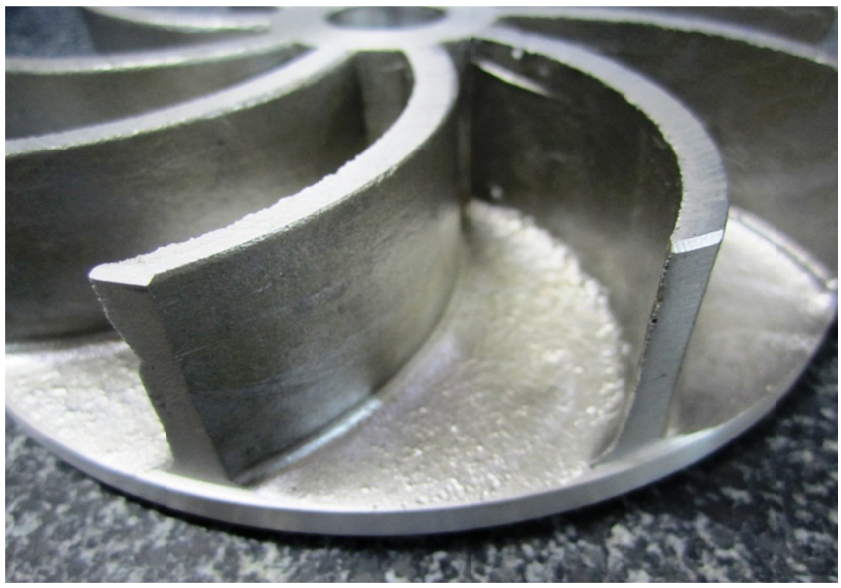

Figure 7.17 The impeller after machining showing no physical defect– Vanes.

Figure 7.18 The impeller after machining showing no physical defect–Core.

7.3 MICROSTRUCTURE ANALYSIS

The impeller and its components (including the gating) were tested and analyzed by conducting SEM and Hardness testing. The purpose of this task is to validate the results of the microstructure with the results collected by the simulation tool in Chapter 5.

7.3.1 METALLURGICAL ANALYSIS OBJECTIVES.

Cooling rate during the solidification process affects the hardness and grain formation in casting. Faster cooling rate causes the small dendroid structure and high hardness.

The objectives of the metallurgical analysis can be summarized as follows:

a. The validation of simulation results of cooling rate with the observed microstructure in the casting.
b. Elimination of the porosity in the casting.
c. The observation of cracks generated due to stresses.

7.3.2 CASTING IMPELLER SAMPLES PREPARATION FOR TESTING

Figure 7.19 and 7.20 shows the impeller as a set of sliced 12 parts prior to testing. The samples were numbered according to their location shown in Figure 7.21. The samples were prepared and tested at KFUPM Material Science Lab facilities.

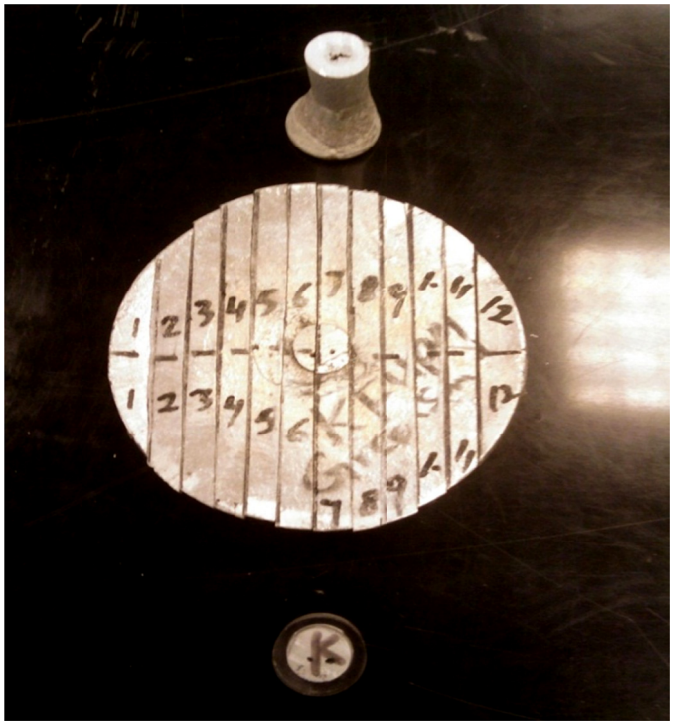

Figure 7.19 Impeller cut into 12 parts for quality testing preparation.

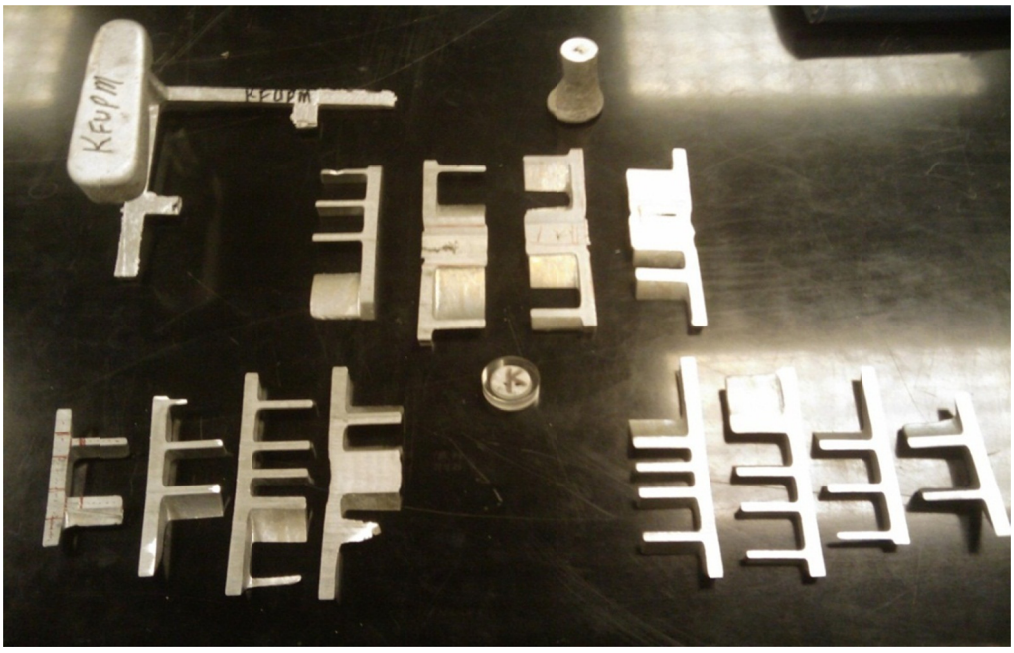

Figure 7.20 Complete casting cut and prepared for quality test.

For the analytical purpose, locations on the gates and runner were selected for microstructure testing. Figure 7.22 shows the arrangement where samples are collected by numbers and Figure 7.22 shows the prepared samples for Hardness testing by *Vicker*.

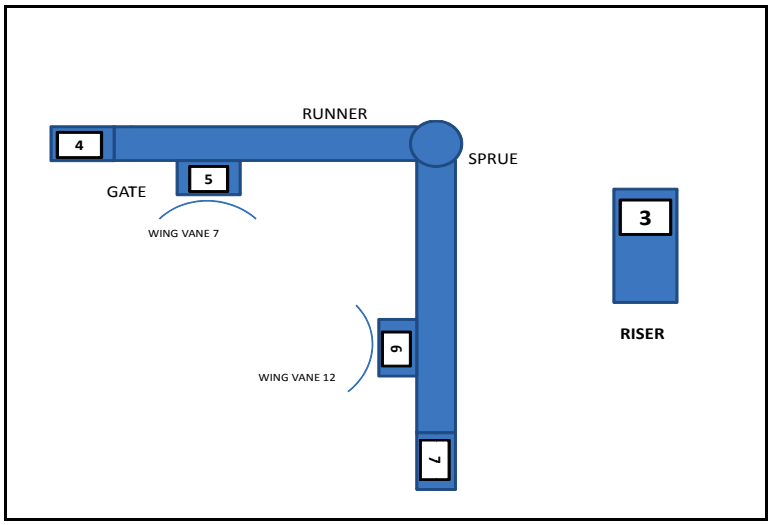

Figure 7.21 Arrangements of Gating and Collected Samples Indicated by Numbers.

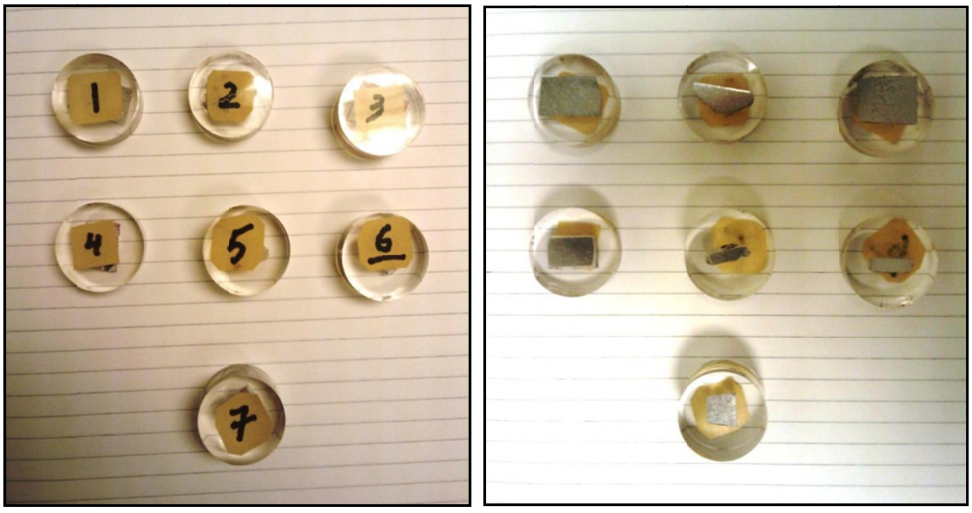

Figure 7.22 Samples prepared for microstructure and hardness testing by *Vicker*.

The samples shown in Figure 7.22 were prepared in the material sciences lab as follows before the optical microscopy was used:

a. Samples were cut from the selected locations on the casting impeller.
b. Mounting by using *Lucite* powder under 4,000 psi pressure and 200 °C temperature.
c. Grinding with *Emery* papers 240, 320, 400 and 600 respectively.
d. Polishing with Al_2O_3 powder/water solution and *Micro-cloth* polishing cloth.
e. Etching with 2% hydro fluoric acid.

7.3.3 MICROSTRUCTURE TESTING RESULTS:

The microstructure testing used to support the simulation and casting results. Table 7.1 shows the samples selected from the gating system and their respective microstructure. From Table 7.1, the grain sizes were studies by the microstructure scanning. The average size of grains of each sample was calculated and compared with the solidification rate as listed in Table 7.2. Solidification rate was predicted by MAGMASOFT®, simulation results as reported in Figure 5.63, which considers the solidification when the molten metal transform to the *solidus* (T_S) phase. It shows that cooling rate during the solidification process affects grain formation in casting. Faster cooling rate causes the small grain structure [19].

TABLE 7.1 Microstructure scanning of selected samples from gates, runners and riser

Sample #	Location	Microstructure Scan (Grains)
3	Riser	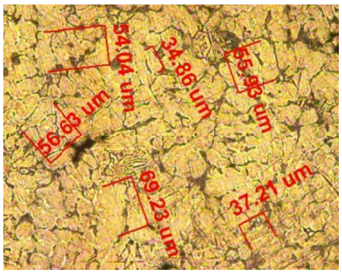
4	Runner 1	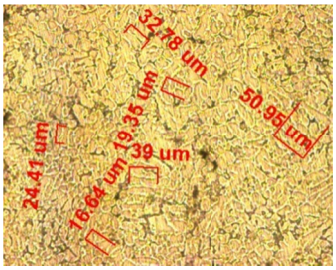
5	Gate 1	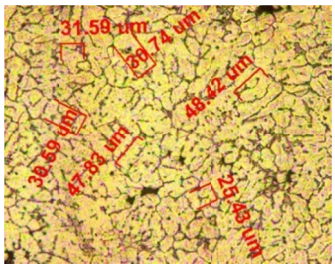
6	Gate 2	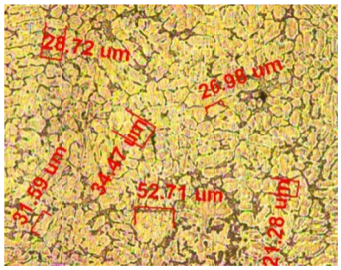
7	Runner 2	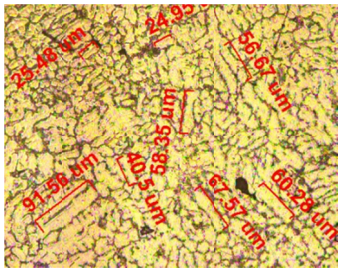

TABLE 7.2 Grains size compared with solidification rate for gating system

Sample #	Location	Average Grain Size (μm)	Solidification Rate $\Delta T/\Delta t$ °C/second
3	Riser	50	3.74
4	Runner 1	41	4.21
7	Runner 2	44	3.90
5	Gate 1	34	4.40
6	Gate 2	32	4.49

Now, we present the results of microstructure for the samples collected from the casting impeller. Figure 7.23 shows the locations of those five selected samples. Five locations were identified to represent different position of solidification and flow behavior within the casting after complete solidification.

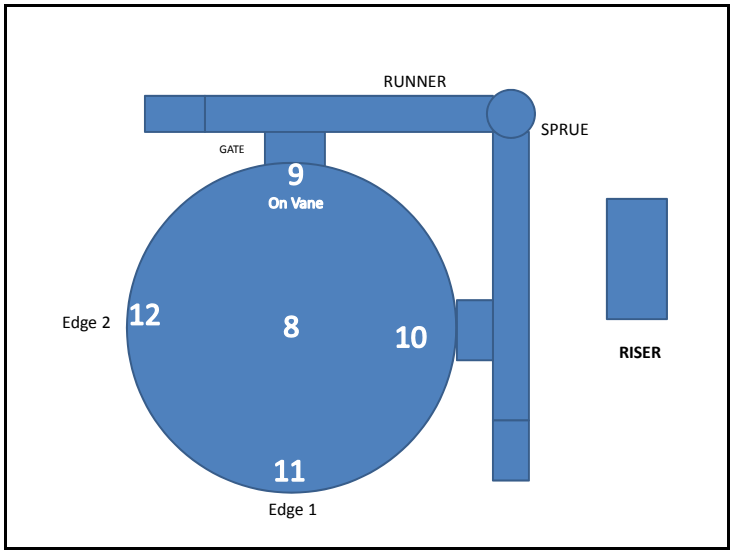

Figure 7.23 Sketch showing location of samples collected from the casting (Impeller).

Temperature curves of the solidification was predicted by MAGMASOFT® and simulation results reported in Figure 5.63, which considers the solidification when the molten metal transform to the *solidus* (T_S) phase. Figure 7.24 presents the temperature curves of the samples 8, 9, 10, 11 and 12. These temperatures are obtained by MAGMASOFT® simulation in section 5.6.3. It shows the complete solidification time of each location when the curve reaches the solidus temperature. In order to show the solidification rate for the selected control points located at the sample numbers, Figure 7.25 shows the linear correlation between the simulated results and the validation experiment on the same locations and from the linear fitted lines both solidification time, and solidification rates are estimated and reported in Table 7.4 and Table 7.5 . These tables show that cooling rate during the solidification process affects grain formation in casting. Faster cooling rate causes the small grain structure.

Table 7.3 shows the microstructure of each sample of the casting with grains measurements. Table 7.4 shows the average grain sizes compared with solidification rate for casting (points 8, 9, 10, 11 and 12). Grains structure was observed that faster cooling rate generated the smaller grains compared to slower cooling areas where larger grains were observed [19].

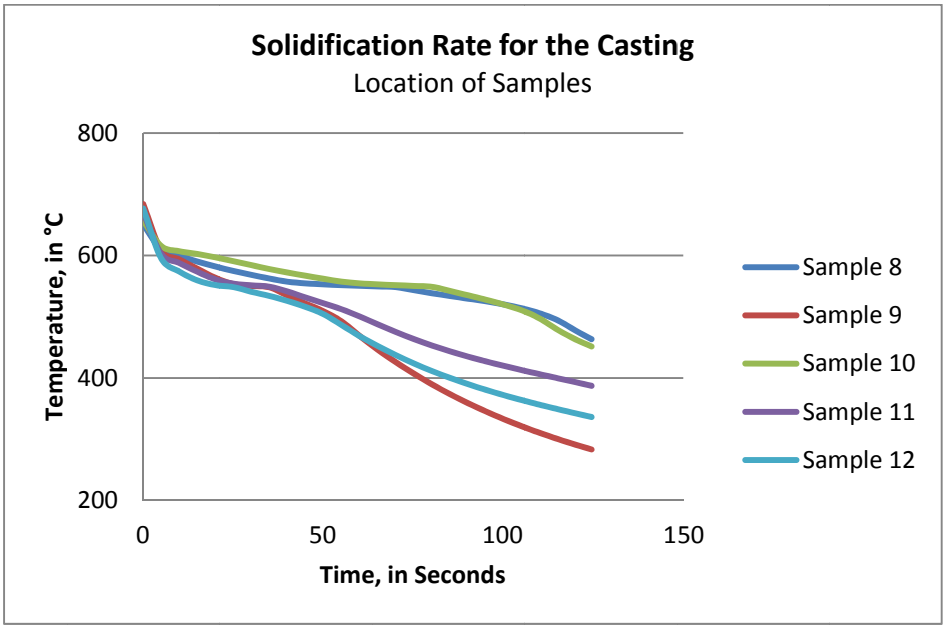

Figure 7.24 Solidification rate of the casting impeller showing location of control points.

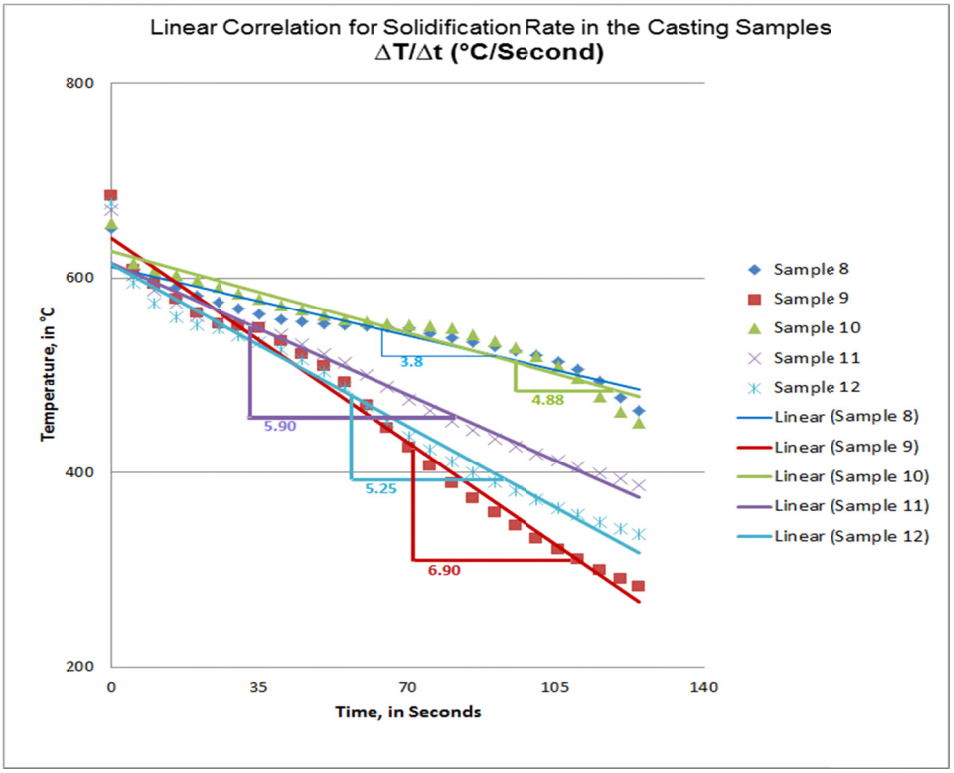

Figure 7.25 Linear correlation for solidification rate in the casting (Slope calculation).

TABLE 7.3 Microstructure scanning of selected samples from casting (Impeller)

Sample #	Location	Microstructure Scan (Grains)
8	Center/Core	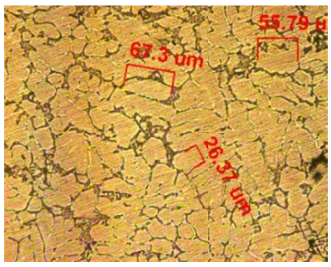
9	Vane	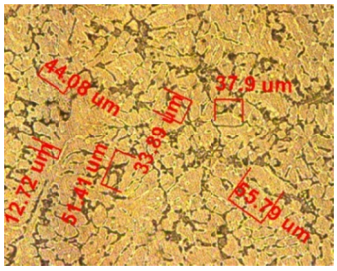
10	Impeller Base	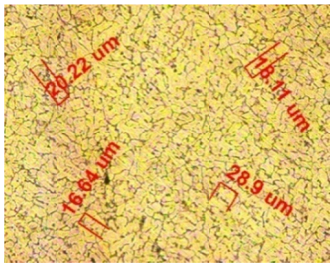
11	Impeller Base Edge 1	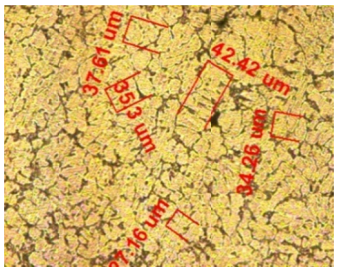
12	Impeller Base Edge 2	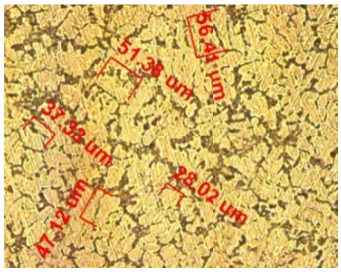

TABLE 7.4 Grain sizes compared with solidification rate for casting

Sample #	Location	Average Grain Size (μm)	Solidification Rate $\Delta T/\Delta t$ °C/second
8	Center (Core)	56	3.8
9	On the Vane	25	6.9
10	Impeller Base	28	4.88
11	Impeller Base Edge 1	38	5.9
12	Impeller Base Edge 2	37	5.25

7.3.3 HARDNESS TEST ON SAMPLES

The hardness testing using *Vicker* was conducted on the same samples collected and presented in Table 7.5. It was also conducted in Material Sciences lab at KFUPM. The instrument used for this test is *Micro hardness* tester by *Buehler* USA.

These readings show the samples of both gating system and the casting impeller. Comparing the hardness values of samples 8, 9, 10, 11 and 12 located in the casting with the solidification time collected by MAGMASOFT® (Temperature curves in Chapter 5), it is observed that the faster cooling rate develops higher hardness in those locations, likewise are the other samples in the gating system. For example, the highest solidification time occurs in the center of the casting (sample 8 location) which is 124 seconds as presented in Table 7.4 shows the lowest hardness value of 62 HV. Whereas, the location of sample 9 which is on the vane of the impeller (thin wall area) shows the fastest solidification rate of 58 seconds and shows the highest value of hardness of 86 HV.

TABLE 7.5 Values of hardness by *Vicker*–100g load testing, with solidification time, rate and average grain sizes of the samples.

	Sample #	**Location**	**Solidification Time** (from Chapter 5) (*Second*)	**Solidification Rate** ΔT/Δt °C/second	**Average Reading** (HV)	**Average Grains Size** (μm)
Gating System	3	Riser	124	3.74	59	50
	4	Runner 1	92	4.21	73	41
	5	Gate 1	94	3.90	73	44
	6	Gate 2	65	4.40	71	34
	7	Runner 2	63	4.49	82.5	32
Casting	8	Center/Core	124	3.8	62	56
	9	Vane	58	6.90	86	25
	10	Impeller Base	76	4.88	76.5	28
	11	Impeller Base Edge 1	64	5.90	80	38
	12	Impeller Base Edge 2	64	5.25	79	37

The plot in Figure 7.26 shows the relation between solidification time and solidification rate simulated by MAGMASOFT® and the hardness measurement collected after the experiment in samples 8, 9, 10, 11 and 12 located in the casting. From the data plot, it

shows the inverse relationship between the solidification and the hardness. For example, sample 8 location which is in the core of the casting shows the longest solidification time (124 seconds) and lowest hardness (62 HV). Whereas, on the vane of the impeller (sample 9) shows the fastest solidification time (58 seconds) and the highest hardness (86 HV).

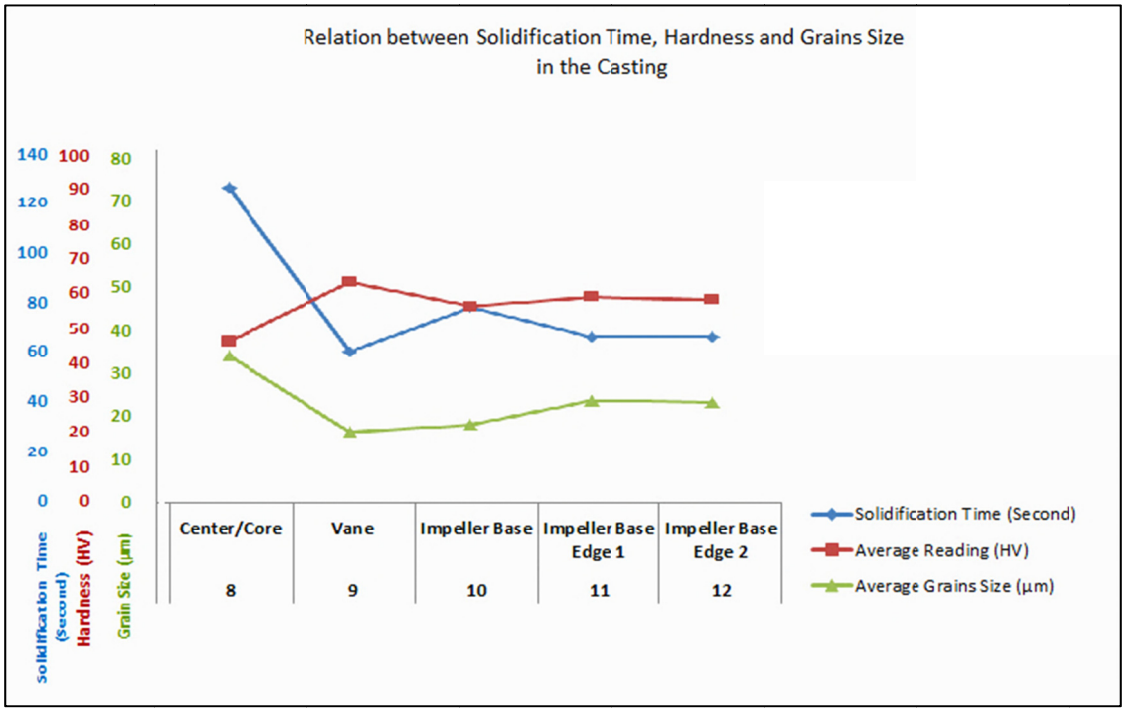

Figure 7.26 The relation between hardness, solidification and grain size in the casting (Impeller)

For practically propose our major interest in the resulting properties of casting, the designed mold in this work has produced casting (impeller) of sound quality and acceptable hardness profile within a range of 62 to 86 HV.

CONCLUSION

This research proposed a strategy to develop near optimal mold in short time. The procedure is built on the following:

a. First designing an initial mold by using relevant metal casting theory, analysis and calculations.
b. Then, refining the design using industrial practices or standards, such as JICA.
c. Then, further analyzing and improving the design sequentially by conducting a series of MAGMASOFT® simulations. Each iteration of the sequence of simulations is based upon improving a spectrum of casting process quality aspects.
d. Finally, stopping the process of improvement when a defect free product is simulated, with a high casting yield.

The methodology was illustrated using an impeller as a cast product, which is a typical type of value added part which local casting industries often produce. The above steps were illustrated by designing a virtual mold, using the best practices in the casting industry, and further analysis and streamlining of the mold was done by using MAGMASOFT®. On the basis of the predicted results, eventually three simulated designs were compared to select a near optimal design. By studying the results, and following the targets to have no or minimum air entrapment, porosity and hot spots, the last simulated mold design (Design 3) was considered to be a near optimal design as it simulates a defect free casting with a relatively higher yield.

The near optimal design showed the existence of high pressure which was maintained first in the gating system and then in the casting cavity, which indicates a situation of pressurized gating system. It has shown a uniform pattern of cooling rate gradient, and smooth pattern of velocity with minimum turbulence which is in line with the recommended mixed laminar/turbulent flow regime resulting in a casting mold which eliminates the air entrapment and erosion of the mold.

The near optimal design according to the simulation results and analysis was selected for experimental validation. The mold design was implemented by actually preparing the pattern, the pattern was made using modern additive manufacturing process, FDM, which is a time compress technology and reduces the lead time to get the pattern. The pattern was integrated with the designed gating system, and the corresponding sand mold was prepared. Separately Aluminum alloy was melted in a gas furnace and the liquid metal was poured in the mold. The resulting impeller was first visually examined and then according to a plan various samples were cut from this impeller to determine grain size, hardness and other metallurgical results at different locations. The results were mapped with the effect of factors such as filling time, filling pressure, filling velocity and cooling rate reported from simulation. The result shows a casting of sound and acceptable quality with no additional quality issues such as porosity, cracks or shrinkage, as none of them were observed in the produced casting impeller. A complete agreement between the grain structure and predicted cooling rate from the simulation was observed. Faster cooling rate at thin sections were reported and correspondingly fine grains structure and high hardness was observed.

The thesis work highlighted the effectiveness of simulation to reach a near optimal design of mold minimizing the costly hit and trial conventional mold design and development practices in the foundry industry. Benefits of using numerical simulation and rapid prototyping technique in casting as illustrated by the work done in this thesis can be summarized as follows:

a. Conventional costly foundry's practice of tedious hit and trial method to get the optimum design of a pattern, gating system and mold can be improved and the development time for the mold is substantially reduced by utilizing simulation tools in design improvement.
b. Design optimization of the gating system facilitates the smooth filling of the mold without air entrapment, and other material flow hindrance.
c. Simulations fairly accurately predicts the key factors affecting the cast product quality such as filling pressure, velocity, cooling rate, hot spots and inside porosity. These predicted results can be helpful for the optimal gating location and sizing, and location of feeder, air vents and chills.
d. The pressure and velocity information can be utilized to get the flow regime in good practice design Reynolds number 'Re' (2000 <Re< 20000) to avoid the air entrapment and mold wall damage.
e. The effect of design on parameters such as temperature gradient, filling pattern, cooling rate, solidification and defects such as air entrapment, hot spot and porosity can be studied.

APPENDIX

A1.1

Impeller –Pattern and Gating Detail Drawings – Final Design

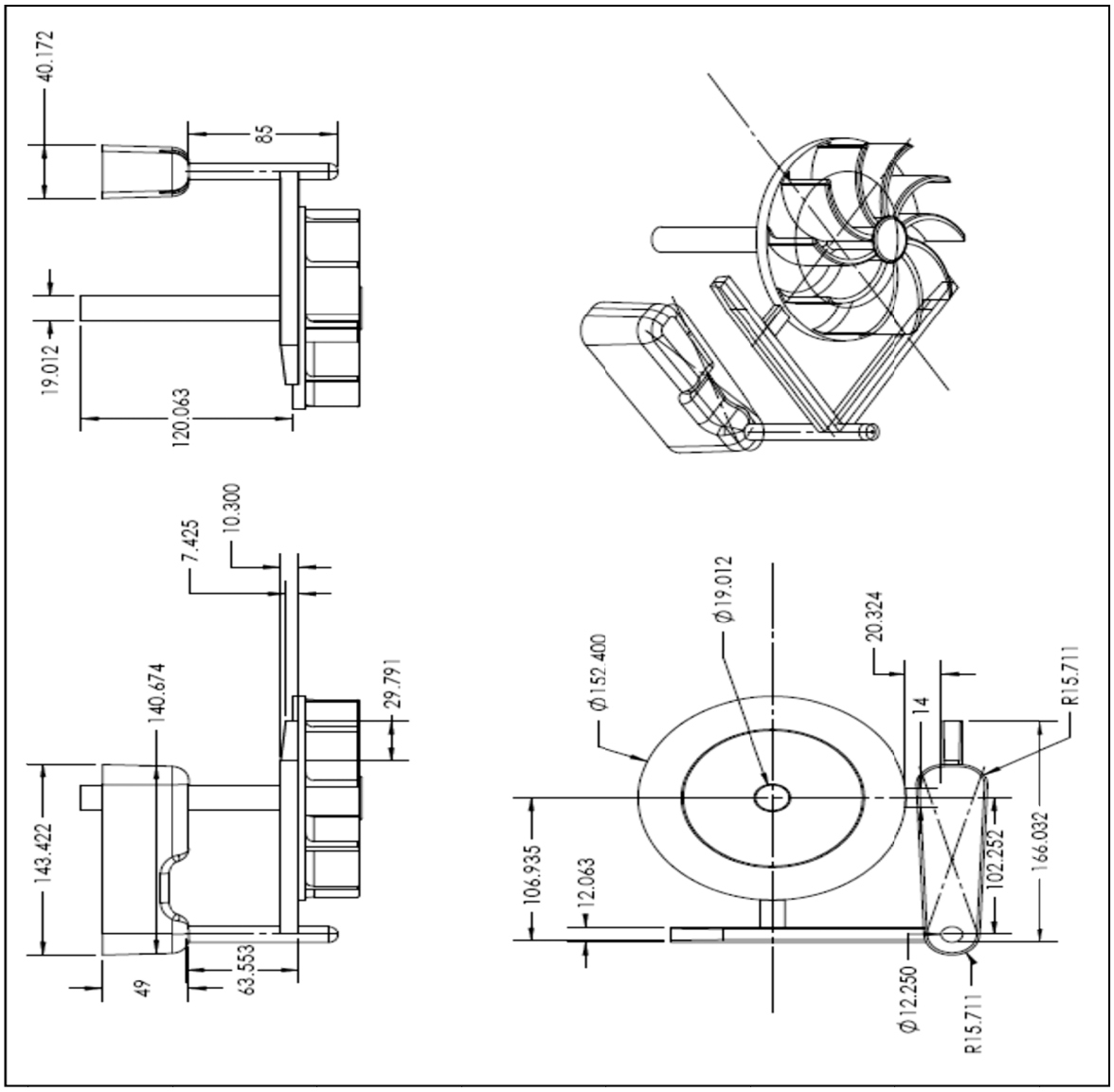

A1.2

Impeller –Pattern and Gating Detail Drawings – Final Design

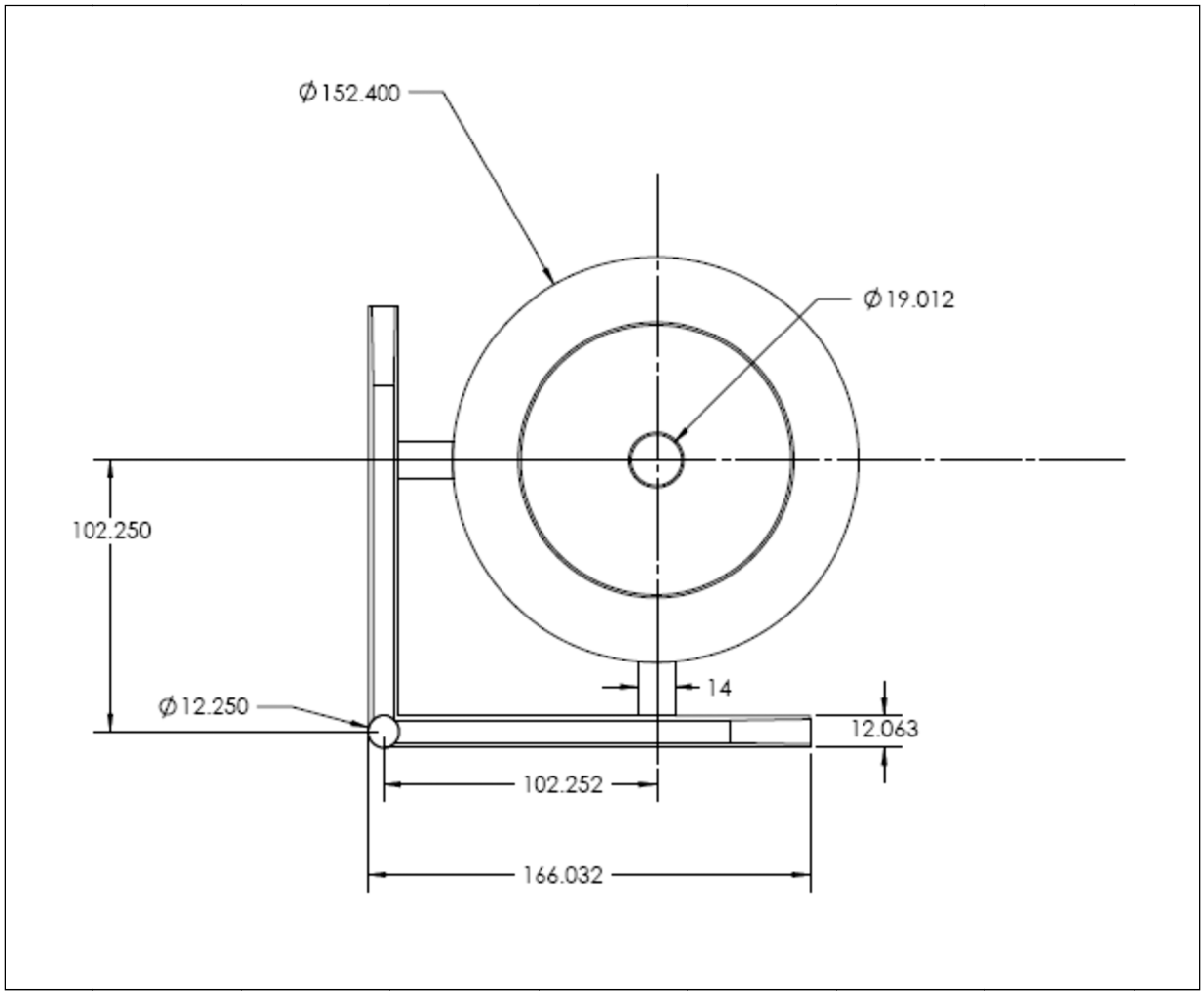

B1.1

Impeller –Pattern ABS Material Surface Finish Testing by *Mitutoyo* Surface Analyzer

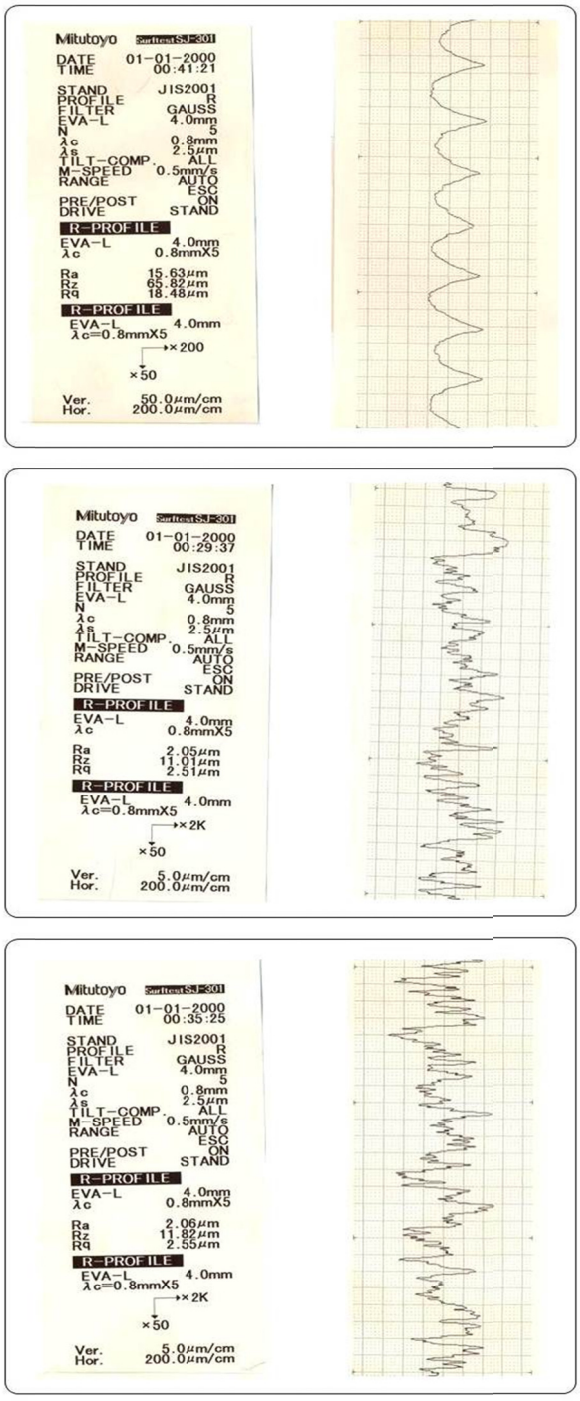

B1.2

Pattern ABS Material Properties by FDM (STARTASYS®, Startasys, GmbH Germany)
www.startasys.com

Data Detail	Description
FDM Material	ABS (Acrylonitrile-Butadiene-Styrene) FDM uses thermoplastics including ABS which matches those of the intended production material. ABS prototype has up to 80% of the strength of injection molded ABS meaning that it is extremely suitable for functional application.
Lead Time	4-5 days
Software	FDM Titan uses *Insight*™ software to import STL files which automatically slices the file, generates the necessary support structures and material extrusion path.

ABS Material Properties:

Property	Unit	Range	ASTM#
Tensile Strength	MPa	22	D638
Tensile Modulus	MPa	1,627	D638
ABS Flexural Strength	MPa	41	D790
ABS Flexural Strength	MPa	1,834	D790
ABS Heat Deflection	°C	96	D648
ABS Density	g/cm^3	1.05	
ABS Elongation (at break)	%	>10	

Nomenclature

f :	Friction Factor in Flow	…….	unitless
G:	Thermal Gradient	…….	°C/m
g:	Gravity	…….	m/sec^2
Q:	Flow Rate	…….	m^3/hour
Re:	Reynold's Number	…….	unitless
T_L:	Liquidus phase line	…….	°C
T_S:	Solidus phase line	…….	°C
v:	velocity	…….	m/sec
ρ:	density	…….	kg/m^3
$R_{a,\,z,\,q}$:	Roughness Profile (Surface Analysis)	…….	µm
$\lambda_{c.s}$:	Cut-off Length	…….	µm

REFERENCES

[1] Ammen C. W. (1979). *The Complete Handbook of Sand Casting*. TAB Books Inc.

[2] Venkatesan, Gopinath, V. and Rajadurai, A. (2004). Simulation of casting solidification and its grain structure prediction using FEM. *Journal of Materials Processing Technology*.

[3] Casting Design Handbook. (1962). Metals Park, Ohio: American Society for Metals,

[4] Kalpakjian, S. (1995). *Manufacturing Engineering and Technology*. Addison-Wesley Publishing Co.

[5] Kalpakjian S. and Schmid, S. (2008). *Manufacturing Processes for Engineering Materials*.Printice Hall.

[6] Senthilkumara, B., Ponnambalamb, S. G. and Jawahar, C. N. (2008). Process factor optimization for controlling pull-down defects in iron castings.*Journal of Materials Processing Technology*.

[7] Fu-Yuan, H., Jolly M. and Campbell, J. (2009). A Multiple-gate runner system for gravity casting.*Journal of Materials Processing Technology*.

[8] Guo-fa, M., Xiang-yu, L., Kuang-fei, W. and Heng-zhi, F. (2009). Application of numerical simulation technique to casting process of valve block.*Journal of Iron and Steel Research International.*

[9] Hong-Jun, H., Ming-Bo, W., Jing, L. W. and Kang, C. (2006). Application of the software ProCAST in the casting of solidification simulation.CailiaoKexueyuGongyi/*Material Science and Technology*.

[10] Zhang, L., Luoxing L. and Zhu, B. (2009). Simulation study on the LPDC process for thin-walled Aluminum alloy casting. *Materials and Manufacturing Processes*.

[11] Ferguson, D., Chen, W., Bonesteel, T. and Vosburgh, J. (2009). A look at physical simulation of metallurgical processes, past, present and future. *Materials Science and Engineering*.

[12] Vijayaram, T.R., Sulaiman, S., Hamouda, A.M.S. and Ahmad, M.H.M. (2006). Numerical simulation of casting solidification in permanent metallic molds. *Journal of Materials Processing Technology*.

[13] Venkatesan, A., Gopinath, V. M. and Rajadurai, A. (2004). Simulation of casting solidification and its grain structure prediction using FEM. *Journal of Materials Processing Technology*.

[14] Cheah, C. M., Chua, C. K., Lee, C. W., Feng, C. and Totong, K. (2004). *Rapid prototyping and tooling techniques: a review of applications for rapid investment casting*. Springer-Verlag London Limited: International Advance Manufacturing Technology.

[15] Dunne, P., Soe, S. P., Byrne, G., Venus, A. and Wheatley, A. R. (2004). Some demands on rapid prototypes used as master patterns in rapid tooling for injection molding. *Journal of Materials Processing Technology*.

[16] Wu, M., Tinschert, J., Augthun, M., Wagner, I., Schaedlich-Stubenrauch, J., Sahm, P. R. and Spiekermann, H. (2001). Application of laser measuring, numerical simulation and rapid prototyping to Titanium dental castings. *Dental Materials*.

[17] Hu, B. H., Tong, K. K., Niu, X. P. and Pinwill, I. (2000). Design and optimization of runner and gating systems for the die casting of thin-walled magnesium telecommunication parts through numerical simulation. *Journal of Materials Processing Technology*

[18] Fu-Yuan, Jolly, M. and Campbell, J. (2009). A multiple-gate runner system for gravity casting. *Journal of Materials Processing Technology*.

[19] Talamantes-silva, M. A., Rodriguez, A., Talamantes-silva, J., Valtierra, S. and Colas, R. (2008). Effect of solidification rate and heat treating on the microstructure and tensile behavior of an Aluminum-Copper alloy. *The Minerals, Metals & Materials Society and ASM International* (DOI: 10.1007/s11663-008-9204-0).

[20] JICA Standards and Best Practices (1995). Nogoya International Training Center. Japan International Cooperation Agency.

[21] Kaufman, J. Gilbert (2009). Aluminum Alloy Database, Knovel.

[22] The Essentials of Gating and Risering System Design (2000). SORELMETAL®, Rio Tinto Iron & Titanium Inc. Montreal: Canada.

[23] Casting Design Handbook (1962). American Society for Metals, Ohio: Metals Park.

[24] MAGMASOFT® 4.4 Manual, "Part One", MAGMA Giessereitechnologie GmbH, 2005.

[25] Hattel, J. (2005). *Fundamentals of Numerical Modeling of Casting Processes*.PolytekniskForlag, Narayana Press.

[26] MAGMA Giessereitechnologie GmbH, MAGMASOFT® Computer Program. Germany: MAGMA Giessereitechnologie GmbH.

[27] Onuh, S. and Yusuf, Y. (1999). Rapid Prototyping Technology: Applications and benefits for rapid product development. *Journal of Intelligent Manufacturing*.

[28] Bernard, A., Delplace, J., Perry, N. and Gabriel, S. (2003). Integration of CAD and rapid manufacturing for sand casting optimization. *Rapid Prototyping Journal*, 9(5).

[29] Tong, K., Joshi, S. and Amine, E. (2008). Error Compensation for Fused Deposition Modeling (FDM) Machine by Correcting Slice Files. *Rapid Prototyping Journal*.

[30] Grimm T.A. Grimm & Associates, April 2003 Volume 11 Issue 2. http://www.fortus.com/uploadedFiles/North_America/Resources/White_Papers/Files_-_White_Papers/WPGrimm.pdf

[31] FDM TITAN Data sheet.http://www.fortus.com/uploadedFiles/North_America/Products/FDM_Products/Titan07.pdf

[32] Zarubina (2005). Studying the effect of the rapid prototyping method on the dimensional precision of pattern making. LitejnoeProizvodstvo.

[33] Pandey, P., Reddy, N. and Dhande, S. (2003). Improvement of surface finish by staircase machining in fused deposition modeling. *Journal of Materials Processing Technology*.

[34] Spielman, R. (2009). Rapid Prototypes + Mold making = Profits. Gardner Publications, Inc, www.gardnerweb.com.

[35] Iqbal, H., Sheikh, A.K., Al-Yousef, A.H. and Younas, M. (2011). Mold Design Optimization for Sand Casting of Complex Geometries Using Advance Simulation Tools", Dept. of Mechanical Engineering, King Fahd University of Petroleum and Minerals.

[36] Gunasegarama, D., Farnsworth D. and Nguyen, T. (2009). Identification of critical factors affecting shrinkage porosity in permanent mold casting using numerical simulations based on design of experiments. *Journal of materials processing technology*.

[37] Li, L. and Zhang, B. (2009). Simulation Study on the LPDC Process for Thin-Walled Aluminum Alloy Casting. *Materials and Manufacturing Processes* 24(12).

[38] Selby, K. (2006). Casting simulation: a must, not a maybe, for optimum casting design. Inst. of British Foundryman 88(2).

VITA

Abdul-Hadi Al-Yousef was born in Riyadh, Saudi Arabia, and his nationality is Saudi. Currently he lives in Al-Khobar, Eastern Province of Saudi Arabia, and his permanent address is listed below. In August 2003, he received the degree of Bachelor of Engineering Sciences in Mechanical Engineering from King Fahd University of Petroleum and Minerals in Dhahran, Saudi Arabia.

Permanent Address: P. O. Box 4918
Al-Khobar 31952
Telephone: 00966-505-887407
e-mail: alyousef@altuwairqi.com